

Alma Mater Studiorum – Università di Bologna

DOTTORATO DI RICERCA IN  
INGEGNERIA CHIMICA DELL'AMBIENTE E DELLA  
SICUREZZA

Ciclo XXV

**Settore Concorsuale di afferenza:** 09/D2

**Settore Scientifico disciplinare:** IND-ING/24

CONFRONTO TRA SUPPORTI CROMATOGRAFICI DI AFFINITÀ  
PER SEPARAZIONE DI PROTEINE

**Presentata da:** JOUCIANE DE SOUSA SILVA

**Coordinatore Dottorato**

Prof.ssa Serena Bandini

**Relatore**

Prof. Ing. Giulio Cesare Sarti

**Correlatore**

Dott. Ing. Cristiana Boi

**Esame finale anno 2013**



Even mistaken hypotheses and theories are of use in leading to discoveries. This remark is true in all the sciences. The alchemists founded chemistry by pursuing chimerical problems and theories which are false. In physical science, which is more advanced than biology, we might still cite men of science who make great discoveries by relying on false theories. It seems, indeed, a necessary weakness of our mind to be able to reach truth only across a multitude of errors and obstacles.

Claude Bernard



# Contents

|   |           |
|---|-----------|
| <b>Introduction</b> .....                               | <b>1</b>  |
| <b>Chapter 1 – Affinity Chromatography</b> .....        | <b>4</b>  |
| 1.1. Introduction to Chromatography.....                | 4         |
| 1.2 Affinity chromatography .....                       | 6         |
| 1.2.1 Chromatographic supports.....                     | 9         |
| 1.2.2 Advantages and limitations of adsorbers.....      | 12        |
| 1.3. Langmuir model .....                               | 14        |
| <b>Chapter 2 – Materials and methods</b> .....          | <b>17</b> |
| 2.1. Introduction.....                                  | 17        |
| 2.2 Ligand .....  | 19        |
| 2.3. Chromatographic supports.....                      | 22        |
| 2.3.1. Resin.....                                       | 22        |
| 2.3.2. Membrane.....                                    | 23        |
| 2.3.2.1. Regenerated cellulose membranes .....          | 24        |
| 2.3.2.2. Membrane Sartobind® Epoxy.....                 | 25        |
| 2.3.2.3. Membrane Sartobind® Aldehyde.....              | 26        |
| 2.3.3. Monoliths.....                                   | 23        |
| 2.4. Analytical methods.....                            | 26        |
| 2.4.1. Protein concentration determination methods..... | 29        |
| 2.4.1.1. UV adsorption.....                             | 29        |
| 2.4.1.2. BCA assay.....                                 | 31        |

|   |           |
|---|-----------|
| 2.4.1.3. Electrophoresis .....  | 32        |
| 2.4.1.3.1. Experimental procedure .....                                   | 34        |
| 2.4.1.4. HPLC .....   | 36        |
| 2.4.2. Chromatographic apparatus .....                                    | 38        |
| 2.4.2.1. Qualitative description of chromatographic cycles .....          | 43        |
| 2.4.3. Elaboration of experimental data.....                              | 45        |
| 2.5. Buffers and protein .....  | 38        |
| <br>  |           |
| <b>Chapter 3 – Affinity Membranes .....</b>                               | <b>49</b> |
| 3.1. Ligand immobilization.....   | 49        |
| 3.1.1. SartoE membranes .....   | 49        |
| 3.1.2. SartoA membranes .....   | 52        |
| 3.1.3. RC membranes .....   | 54        |
| 3.2. Ligand density .....   | 54        |
| 3.3. Ligand leakage .....   | 55        |
| 3.4. Results and discussion .....   | 55        |
| 3.4.1. Efficiency evaluation of the membrane modification procedure ..... | 55        |
| 3.5. Characterization of the modified membranes with batch tests .....    | 60        |
| 3.5.1. Experimental results .....   | 61        |
| 3.5.1.1. Elution step.....  | 64        |
| 3.5.2 Dynamic experiments .....   | 67        |
| <br>  |           |
| <b>Chapter 4 – Affinity Monoliths.....</b>                                | <b>78</b> |
| 4.1. CB immobilization on CIM disks .....                                 | 78        |

|   |            |
|---|------------|
| 4.2. CB-monoliths characterization through the separation of pure BSA solution in batch system..... | 83         |
| 4.3. Dynamic experiments.....   | 84         |
| 4.4. Results and discussion .....   | 86         |
| 4.4.1. Ligand immobilization .....  | 86         |
| 4.4.2. Batch tests .....  | 86         |
| 4.4.3. Dynamic experiments.....   | 89         |
| <b>Chapter 5 – Comparison of the affinity supports .....</b>  | <b>94</b>  |
| 5.1. Introduction.....  | 94         |
| 5.2. Dynamic binding capacity .....   | 94         |
| 5.2.1 Dynamic experiments with BSA solutions loaded until saturation .....                          | 95         |
| 5.2.2. Dynamic experiments with BSA solutions loaded until 10% breakthrough .....                   | 101        |
| 5.3. Productivity.....  | 106        |
| 5.4. Tests with bovine serum .....  | 109        |
| <b>Conclusions.....</b>   | <b>113</b> |
| <b>References .....</b>   | <b>116</b> |
| <b>Appendix I .....</b>   | <b>125</b> |
| <b>Appendix II.....</b>   | <b>129</b> |

# Introduction

Chromatography is the most widely used technique for high-resolution separation and analysis of proteins [1]. In chromatographic processes a solute mixture is introduced into a column containing a selective adsorbent, called stationary phase; the separation results from a different solute partition between the mobile phase and the fixed bed. This technique is very useful for the purification of delicate compounds, e.g. pharmaceuticals, because it is usually performed at milder conditions than separation processes typically used by chemical industry. In particular, affinity separation allows to obtain high purity products using an economic process, for this reason the research of new stationary phases and techniques is stimulated.

Many different types of chromatographic techniques are used in biotechnology, due to several possible interaction mechanisms (such as electrostatic, hydrophobic, and others) that occur between proteins and stationary phases. This thesis focuses on affinity chromatography, this technique is based on specific reversible complexes formation between the molecules to purified and the ligand bound on a suitable insoluble support.

Chromatographic processes are traditionally performed using columns packed with porous resins; these media have a high binding capacity, because of the high specific surface area due to the network of intraparticle pores present in the beads. However, these supports have several limitations, including the dependence on intra-particle diffusion, a slow mass transfer mechanism, for the transport of solute molecules to the binding sites within the pores and high pressure drop through the packed bed [1]. These limitations can be overcome by using chromatographic supports like membranes or monoliths [2]. In chromatography processes with these supports the transport of solutes through binding sites takes place mainly by convection, thus the process time is



reduced. The pressure drop is also significantly lower than with packed beds. The main disadvantage of these media is their low binding capacity, since the specific surface area is much lower than that of resins [1].

In recent years, supports were modified in different ways and various ligands were tested. Dye-ligands, as triazine dyes, are considered important alternatives to natural ligands. These dyes are able to bind most types of proteins, they interact with the active sites of proteins by mimicking the structure of the substrates, cofactors or binding agents for those proteins [3].

Several reactive dyes, particularly Cibacron Blue F3GA, are used as affinity ligand for protein purification. Most of them consist of a chromophore linked to a reactive group. The interaction between the dye ligand and proteins can be realized by combination of electrostatic, hydrophobic and hydrogen bonds. Cibacron Blue F3GA is a triazine dye that interacts specifically and reversibly with albumin [4].

The aim of this study is to prepare dye-affinity membranes and monoliths for efficient removal of albumin and to compare the three different affinity supports: commercial resin, membranes and monoliths. In particular, this work describes the experimental comparison between the performance of three different affinity chromatography media: membranes and monoliths modified with Cibacron Blue F3GA and a commercial column HiTrap™ Blue HP, produced by GE Healthcare.

In Chapter 1 the principles of affinity chromatography are introduced and the various steps of a chromatographic cycle are described. In the last part of the chapter the main advantages and disadvantages of the different chromatographic supports studied are discussed.

In Chapter 2 the materials used during the research project are described in detail. A qualitative description of the chromatographic cycles performed is also presented, along with the explanation of the procedure employed for data

elaboration and the description of the analytical assays performed during the research activity.

In Chapters 3 and 4 the experiments performed with membranes and monoliths are described in detail and results are discussed, while in Chapter 5 the comparison among the affinity supports is described.

In Appendix I is listed the composition of all solutions used, in Appendix II the calibration realized for calculations of the results.

## Affinity Chromatography

### 1.1. Introduction to Chromatography

Chromatography is a separation technique based on differential partitioning between the mobile and stationary phases.

In a chromatographic process a mixture of molecules is carried by a liquid, called mobile phase, through a column containing a porous solid substance, called stationary phase, which remains fixed in the column. The stationary phase acts as a restraint on many of the components in the mixture, which travel at different speeds. The movement of the components is controlled by the significance of their interactions with the mobile and/or stationary phases. Some components will move faster than others according to the differences in solubility in the mobile phase and according to the strength of their affinities with the stationary phase. In this way the separation of the components within the mixture is facilitated.

The chromatographic methods are among the most widely used separation techniques for the purification of proteins, they are classified according to the nature of the interactions that are established between the protein and the stationary phase.

Various types of chromatographic techniques are used for protein separation. These methods are based on different supports such as silica gel, glass plates, paper and liquids.

**Paper chromatography** uses a piece of specialized paper. It is a planar system in which cellulose filter paper represents the stationary phase. The separation of compounds occurs on the stationary phase.

**Gel filtration or Size Exclusion Chromatography (SEC)** separates molecules according to differences in size as they pass through a gel filtration medium packed in a column, using mild conditions.

**Thin layer chromatography (TLC)** is used frequently to visualize components of a mixture. The common TLC plate is a rectangular piece of glass coated with silica powder. The silica is the stationary phase because it remains adhered to the glass plate and it does not move during the chromatographic process.

**Ion Exchange Chromatography (IEC)** separates molecules by reason of differences in their surface charge. Molecules vary significantly in their charge properties and will exhibit different levels of interaction with charged media according to differences in their surface charge distribution, density and overall charge. An IEC medium, stationary phase, consists of a matrix of spherical particles substituted with ionic groups that are negatively or positively charged.

**Hydrophobic Interaction Chromatography (HIC)** separates according to the reversible interaction between the target protein and the hydrophobic ligand bounded to the chromatographic matrix.

**High Performance Liquid Chromatography (HPLC)**, in this technique the mobile phase is pumped through the column, composed by small particles which offer a great surface area for the interaction between the stationary phase and the molecules, under high pressure. An HPLC system consists of a pump, sample injection, detection and data-processing unit.

**Affinity Chromatography (AF)**, this technique exploits the properties of proteins to interact specifically with a ligand. The affinity ligand is immobilized on a solid matrix to create the stationary phase while the target molecules are in the mobile phase. The interactions between ligand and target proteins are typically reversible and so it is possible to recover proteins using a specific eluent.

## **1.2. Affinity chromatography**

Affinity chromatography is one of the most used methods for the protein purification. This technique allows to obtain high purity products at a relatively low cost.

Affinity chromatography is based on the specific interaction between a ligand and a target protein. The high specificity and capacity of affinity chromatography allows the use of high speeds of the mobile phase in small matrix volumes obtaining fast separations [5].

The ligand is immobilized on an inert support, in this way it can interact with the target molecule, called ligate. Ligand and ligate form a complex bonded on the support. Usually, the interactions between protein and ligand are weak chemical bonds as Van der Waals forces, electrostatic forces, hydrogen bonds and hydrophobic interactions. The interactions are reversible and they ensure the link between the two substances, and the subsequently release of the protein varying the conditions. These conditions are varied sufficiently to cause the release of the ligate from the complex, but not to cause significant release of the ligand from the support.

The affinity separation occurs in three steps: adsorption, washing and elution. The simplicity of the chromatographic process is represented in the Figure 1.1.

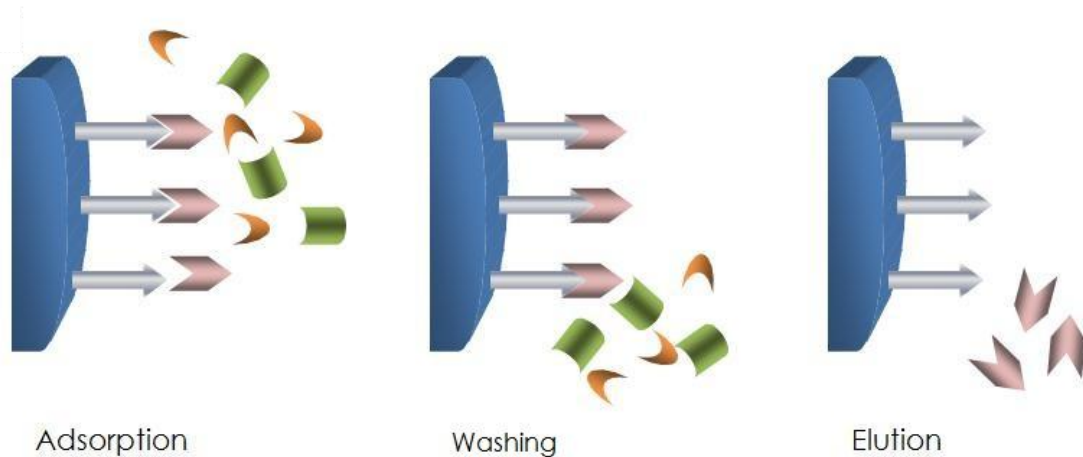


Figure 1.1 – Schematic diagram of affinity chromatography.

In the first step, adsorption, the protein interacts with the ligand immobilized on the support.

Thereafter, in the washing step, the molecules nonspecifically linked to the matrix are removed from the support.

Finally, elution allows the desorption of the target molecule using an appropriate elution buffer. Elution can be performed in a competitive or non-competitive manner. In the competitive elution, the buffer contains a compound that has a great affinity with the target biomolecule and it competes with the ligand for the active sites. The non-competitive elution consists in a change of the operating conditions, which can be achieved by varying the pH, temperature and ionic strength [6].

The fourth step consists in the regeneration and/or sanitization of the solid support with a strong alkali or acid, in order to reuse it for subsequent cycles.

Breakthrough analysis (BTC) is a method used for the evaluation of a chromatographic process. The breakthrough curve (BTC) is defined as the plot of effluent concentration versus time, or versus effluent volume, Figure 1.2.

A solution containing a known concentration of the ligate is applied continuously to an affinity column. As this ligate is bound to the ligand, the ligand becomes saturated and the amount of ligate eluted from the column increases, forming a characteristic breakthrough curve.

An ideal BTC increases instantaneously from zero to the feed concentration when the adsorbent becomes saturated; actual BTCs are broadened by the non-idealities of real flow systems, like dead volume mixing and slow sorption kinetics. A broad BTC means that the system is inefficient, because if the loading step is performed until ligand saturation, protein will be lost in the effluent [7].

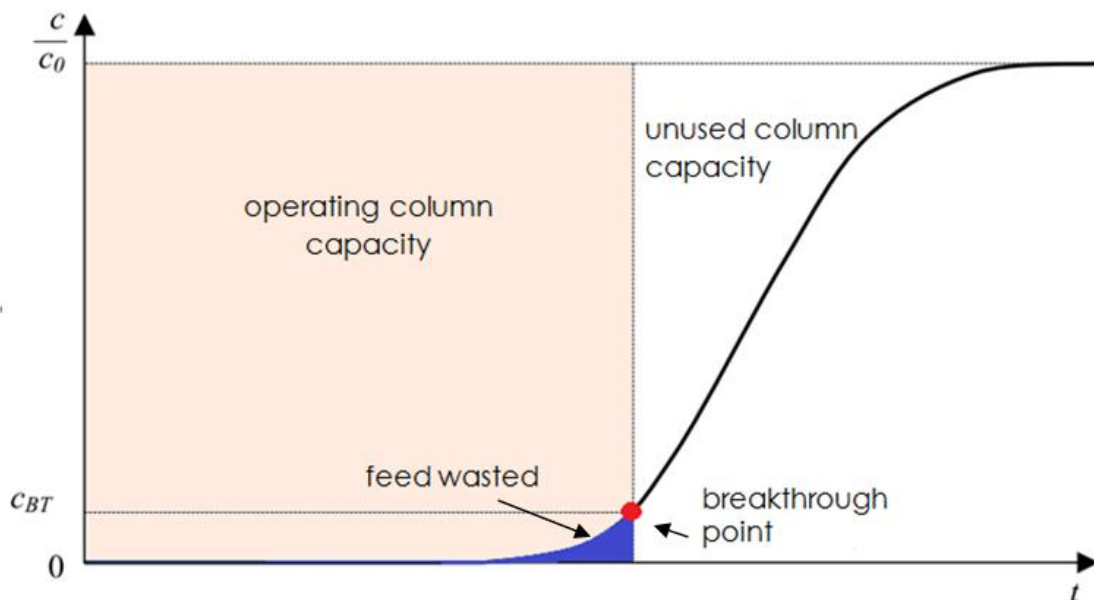


Figure 1.2 – Breakthrough analysis for a typical chromatographic process.

In this figure, the solute in the feed is completely retained by the column at short times. After a while the effluent concentration increases with time, until the column becomes saturated and the effluent concentration becomes equal to

the feed concentration. The maximum capacity of the column for a given feed concentration is equal to the area behind the breakthrough curve, while the amount of solute that exits from the column is the area under this curve [8].

In industrial processes the adsorption step is usually concluded before column saturation, at breakthrough point, when the solute reaches a specified concentration,  $C_{BP}$ , in order to reduce the loss of product. In this case the breakthrough curve can be used to determine how much of the column capacity is exploited, how much solute is lost in the effluent and the processing time [8]. It is desirable to work with systems that have a high binding capacity and in which the breakthrough curve is very steep.

The position of the breakthrough curve on the volume axis depends on the column capacity and on the feed concentration: increasing the capacity at a fixed feed concentration or decreasing the feed concentration at a fixed capacity, the volume of feed that can be processed increases and shifts the breakthrough to the right [8].

Although the performance of a chromatographic process depends strongly on the adsorption step, it is important to consider also washing and elution steps.

### **1.2.1. Chromatographic supports**

The main technologies available for chromatographic separations employ different supports: conventional resins (diffusive), perfusive resins membranes or monoliths.

The solid supports traditionally used in the stationary phase are functionalized resins or polymeric matrices, such as agarose, formed by beads with spherical shape and variable size. This method is based on the use of a column packed with a porous adsorbent in which the ligand is immobilized.



Particles are typically 50 to 100  $\mu\text{m}$  in diameter to minimize pressure drops [9]. These particles exhibit high throughputs, because of the high superficial area, but they have various limitations.

First, pressure drop across a packed bed is high and increases during a process due to the combined effects of bed consolidation and column obstruction caused by the accumulation of colloidal material. Another major limitation is the dependence on intra-particle diffusion for the transport of solute molecules to their binding sites within the pores. This increases the process time since diffusive transport of macromolecules is slow, especially when it is hindered [10]. Consequently, the volume of the elution buffer also increases and biomolecules may be denatured because of a long exposition to aggressive conditions. Smaller particles with a higher superficial area and a lower diffusive distance could be employed to solve this problem, but pressure drop would drastically increase.

Another problem is the possible formation of flow passages due to cracking of the packed bed (channeling). This results in short-circuiting of material flow, leading to poor bed utilization. Furthermore, the complexity of the transport phenomena makes scale-up of packed bed chromatographic process complicated [1].

Perfusion chromatography is based on the use of bidisperse porous particles on which the ligand is immobilized. These particles have a network of large pores, through pores, in which the particles transit, and also a network of smaller interconnecting pores between the through pores. In this media, the intraparticle convective velocity is non-zero; this property helps to overcome the limitations encountered in conventional processes with purely diffusive particles.

An alternative to packed beds is represented by supports with polymeric matrix as membranes and monoliths. These materials provide advantages over the conventional chromatography packed columns, especially in relation to processing time and activity recovery [11].

Membranes act like short and wide chromatographic columns in which the adsorptive packing consists of one or more microporous or macroporous membranes in series, each derivatized with adsorptive portions. They are basically derived from filtration modules and consequently they exist in a similar variety of configurations, as flat or spiral sheets, hollow fibers and cast cylindrical plugs, Figure 1.3.

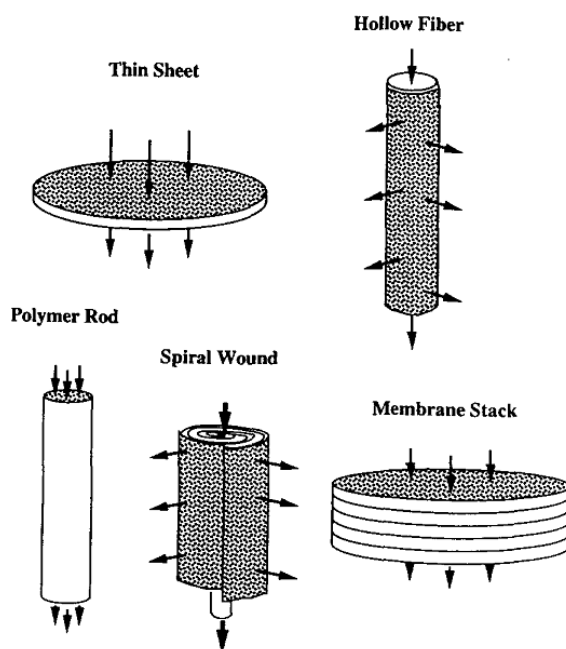


Figure 1.3 - Schematic comparison of the configurations of the membrane adsorbers [12].

Cellulose, regenerated cellulose, nylon, polyethylene, poly(styrene-co-divinylbenzene), poly(HEMA), polyamide, chitin and chitosan are some materials used as substrate in adsorptive membranes [12].

Monolithic supports compete with macroporous membranes since they have similar pore morphology but different manufacturing technology [13,14].

Monolithic supports consist of a single piece of a solid stationary phase cast as a homogeneous column. The use of monolithic supports has been exploited with immobilized low molecular mass ligands, as dyes, inhibitors, chelating species, combinatorial ligands, and high molecular mass ligands, like proteins A and G, antibodies and receptors [15].

Normally, monolithic stationary phases for affinity separations are polymerized using ethylene dimethacrylate (EDMA) or trimethylolpropane trimethacrylate (TRIM) like a cross-linking monomer and glycidyl methacrylate (GMA) as the active monomer for successive immobilization of the ligand [15]. The macroporous poly(glycidylmethacrylate-co-ethylene dimethacrylate) monoliths have been also used for the immobilization of dye in affinity chromatography for protein separations [16].

### **1.2.2. Advantages and limitations of adsorbers**

The main difference between polymeric matrixes, membranes and monoliths, and beads is the mechanisms by which solutes are transported to and from their surfaces, as schematically illustrated in Figure 1.4. Diffusion and convection are the primary types of mass transport. Diffusion is the migration of solutes from the area with high concentration to the area with low concentration through random movement. The mass transport phenomena in beads depend mainly on the diffusion [17]. One important point regarding the diffusion is the process is slow, and it becomes much slower with increasing molecular size. As a result, dynamic binding capacity decreases with increasing of the flow rates [17-20].

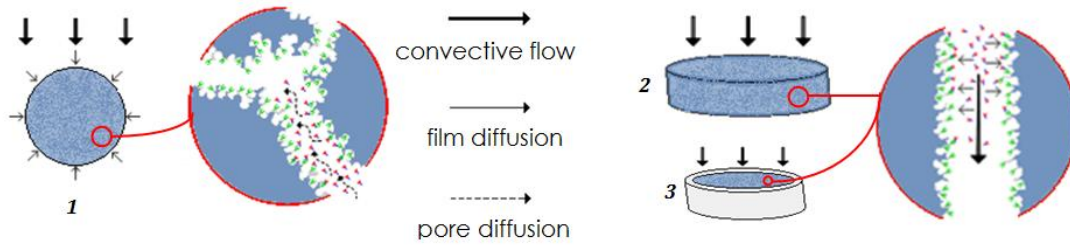


Figure 1.4 – Comparison of mass transport phenomena during adsorption of molecules in generalized structures of membranes stacked, monoliths and beads.

The convective transport of mass is not limited by diffusion or molecular size. The convection is imposed by an external force, in the case of chromatography, the flow of liquid is delivered from the pumps. Instead of beads, membranes and monoliths structures are designed to take advantages of convective mass transport. Capacity and resolution are independent of the flow rate for these supports [21–23, 18, 24, 25]. So, it is possible to work at high flow rates reducing the process time.

Operating pressures in a certain flow rate are lowest on membranes and usually highest on beads. Monoliths create a less back pressure than beads at flow rates lower than one column volume per minute.

Several membrane adsorbers are disposable, that means for a single use application. As a consequence, the costs of the process can be reduced since it is not necessary to realize and validate the steps of cleaning, regeneration and sanitization.

The flow distribution inside the membranes housing is less controlled than monoliths housing or packed columns, resulting in irregularities in the flow and reductions in the binding efficiency [26]. Monoliths are optimized to eliminate areas of uncontrolled dispersion and to provide constant flow distribution in the column.

Furthermore, membranes and monoliths differ from resins by the presence or absence of void volume between the particles. In packed beds, the fluid takes the easiest path which offers lower flow resistance, that is, through the void volume rather than through the particles. The flow through monoliths is laminar that minimizes the shear. This ensures an instantaneous response (to changes) in buffer composition changes, which maximizes elution kinetics and contributes to clear and better resolved elution peaks [25].

### 1.3. Langmuir model

The Langmuir model is most common type of isotherm used to describe the stationary phase adsorption of a biomolecule. Adsorption is a result of the interactions between the biomolecule and the chromatographic support; in general there can be various kinds of interactions, such as electrostatic interactions, hydrophobic interactions, Van der Waals forces.

Langmuir model is based on the hypotheses that the interaction between the biomolecule and the ligand is monovalent, reversible and that the adsorbed molecules do not interact with each other. Another approximation is made by considering the support homogeneous, all the interactions have the same binding energy [27]. Under these hypotheses the interaction can be described with the following reaction:



where  $P$  is the protein,  $L$  is the ligand and  $PL$  represents the protein–ligand complex. The mass balance associated with eq. (1.1) for the adsorbed biomolecule is the sum of two terms, one related to the reaction of formation of

the protein-ligand complex and one related to the reaction of dissociation of this complex.

The formation of the complex depends directly on the interaction between the protein and the support, so it is reasonable to consider a linear dependence of the adsorption rate on the concentration of biomolecule. Moreover, since a protein cannot interact with active sites that are already involved in an interaction with other proteins, the adsorption rate should be proportional to the concentration of free binding sites. The following second order equation results from the combination of these two effects:

$$R_a = k_a c(q_m - c_s) \quad (1.2)$$

where  $R_a$  is the adsorption rate,  $c$  is the local concentration of protein,  $c_s$  is the concentration of protein bound to the stationary phase,  $q_m$  is the maximum binding capacity of the support and  $k_a$  is the kinetic constant of the adsorption reaction.

Similar considerations can be done for the desorption reaction, whose rate is assumed proportional to the concentration of protein adsorbed on the stationary phase. The following first order equation can thus be written:

$$R_d = k_d c_s \quad (1.3)$$

where  $R_d$  is the desorption rate and  $k_d$  is the kinetic constant of the desorption reaction.

The mass balance obtained by coupling eq. 1.2 and 1.3 is

$$\frac{\partial c_s}{\partial t} = k_a c(q_m - c_s) - k_d c_s \quad (1.4)$$

If the system is in equilibrium, the adsorption rate is equal to the desorption rate:

$$k_a c (q_m - c_s) = k_d c_s \quad (1.5)$$

The concentration of adsorbed protein can be easily derived from eq. previous equation:

$$c_s = \frac{q_m c}{K_d + c} \quad (1.6)$$

Equation 1.6 is the Langmuir adsorption isotherm. The parameter  $K_d$  is the Langmuir dissociation constant, equal to the following ratio:

$$K_d = \frac{k_d}{k_a} \quad (1.12)$$

The Langmuir kinetic model contains 3 parameters,  $k_a$ ,  $k_d$  and  $q_m$ , while the Langmuir equilibrium isotherm contains only 2 parameters,  $K_d$  and  $q_m$ , that can be easily calculated from equilibrium data.

## **Materials and methods**

### **2.1. Introduction**

In this chapter materials and experimental methods employed during the work are described. In § 2.2 properties, biological functions and main applications of bovine serum albumin are presented, in order to provide some information about the biomolecule used in the research for the characterization of the chromatographic media examined. In § 2.3 materials used in the experiments are described in detail. In § 2.4 a detailed description of the assays used for protein quantifications. The last paragraph consists in a qualitative description of chromatographic cycles performed is presented, and an explanation of the procedure employed for the elaboration of experimental data.

### **2.2. Protein**

Serum albumin is one of the most widely studied proteins and it is the most abundant protein in the circulatory system. Bovine Serum Albumin, BSA, is often chosen as a model protein for experimental studies due to its low cost and availability, Figure 2.1.

This protein has a capacity of conformational adaptation and so it can bind with high affinity a variety of compounds.



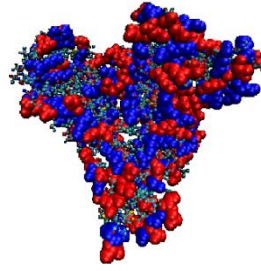


Figure 2.1 – Bovine serum albumin.

BSA is a large globular protein constituted by the twenty essential amino acids in a structure which contains 583 amino acid residues. The molecular weight calculated from different techniques, ranges from 66411 to 66700 Da and the used value for solution is 66500 Da [28]. It has an isoelectric point of 4.7, so it is negatively charged at pH 7 [29].

The structure and properties of BSA in solution can be characterized by a versatile conformation as a function of pH, ionic strength, presence of ions, and others. This protein presents various conformations [30] according to pH of the medium:

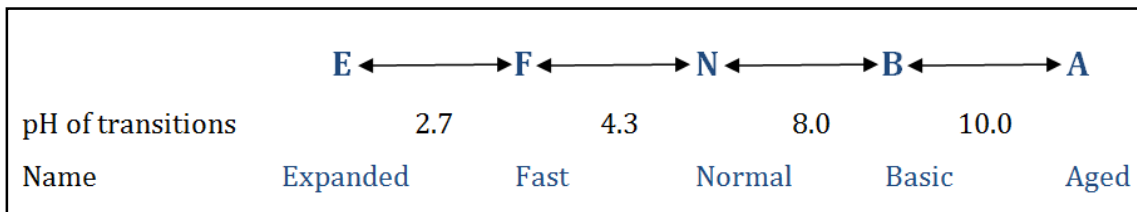


Figure 2.2- Reversible conformational isomerization of serum albumin in function of pH.

BSA conformer N has a globular, compressed structure, that reveals a triangular heart shape [31]. The N to F conformation transition is an abrupt expansion occurring at pH 4.3 [32]. This form is characterized by a an increase of viscosity and a reduction of solubility. Conformer E is found in the pH range of 3.4 - 2.75, so denatures for mutual repulsion of internal amino acid residues

positively charged [33]. At pH 9, albumin changes conformation to B basic form and after three or four days, the protein isomerizes forming the A structure.

The sequence of BSA is 75.8% identical to that of human serum albumin (HSA), the main difference being the presence of a second tryptophan residue in position 131 in the bovine protein [34, 35].

Serum albumin has many physiological functions. It is essential for maintaining the osmotic pressure needed for proper distribution of body fluids between intravascular compartments and body tissues. It is also the principal carrier of fatty acids, steroid, hormones and flavour compounds that are otherwise insoluble in plasma, because of its hydrophobic domains [36].

BSA has numerous applications in biochemistry, including Enzyme-Linked ImmunoSorbent Assay (ELISA) and immunohistochemistry. Moreover, it is also used as nutrient in microbial cultures and it is employed to stabilize some enzymes during digestion of DNA and to prevent adhesion of these enzymes to reaction tubes and other vessels. BSA is also commonly used as standard in protein assays, such as BCA, Bradford and Lowry assays. This protein is widely employed because of its stability, its lack of effect in many biochemical reactions and its low cost since it can be purified in large quantities from bovine blood, a byproduct of the cattle industry.

## **2.2. Ligand**

There are several pigments capable of interacting with proteins, especially enzymes, and, in some cases, in a very specific way. The pigments are classified as affinity ligands, they mimic the structure of coenzymes and enzyme cofactors and interact with the active site of enzymes [37-40].

Dye ligands have been considered as an important alternatives to natural homologues for specific affinity chromatography, in order to overcome many of their disadvantages [37, 43- 45].

The majority of reactive dyes used as affinity ligands consists of a chromophore, such as anthraquinone, attached to a reactive group as a triazine ring. These compounds also have sulfonic acids in their structure in order to increase solubility in aqueous media.

Although dyes are all synthetic in nature, dye ligands are commercially available, economic, and can be easily immobilized, especially on matrices with active hydroxyl groups. So, triazine dyes, such as Cibacron Blue F3GA, are among the promising ligands for large scale purification of bioproducts.

Cibacron Blue F3GA, that will be indicated throughout this work by the abbreviation CB, was used as the ligand for specific binding of bovine serum albumin.

The reactive group of CB contains a chlorine atom replaceable that provides a convenient chemical immobilization on supports containing hydroxyl groups, forming an ether bond between the dye and the matrix [46].

Figure 2.3 shows the chemical structure of this dye. It contains several possible active sites that can react with proteins as  $\text{NH}_2$ ,  $\text{SO}_3\text{Na}$  and  $\text{NH}$ . CB has aromatic rings in the sulphonated anthraquinone portion that tends to bind preferentially to the active sites of several enzymes, since it resembles the structure of coenzymes such as NADH and FAD, for this reason CB is widely used in the purification of kinases and hydrogenases [47-50].

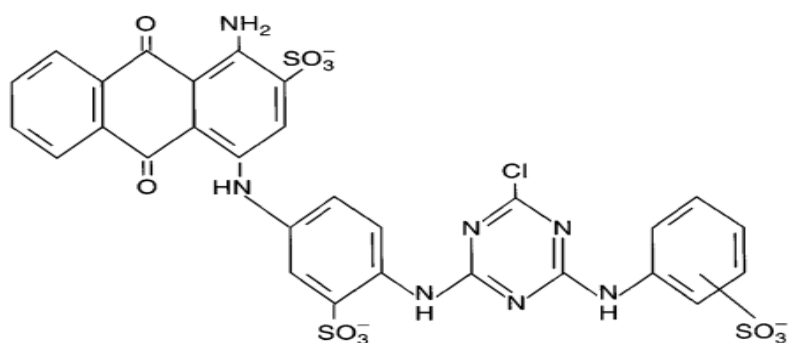


Figure 2.3 - Structure of Cibacron Blue F3GA [51].

The adsorption of albumin, human and bovine, by the CB molecule has been extensively studied using agarose matrices [52], polyamide [53], polystyrene [54], poly (styrene-co-divinylbenzene) [55], and poly (methylmethacrylate) [47].

Although most studies have focused on albumin, other applications for CB were also studied. Doğan *et al.* [56] used a supermacroporous cryogels as a CB affinity adsorbent for interferon purification.

Recently, affinity membranes have become an alternative to chromatographic columns packed with polymeric resin. Nie and Zhu [57] studied CB immobilized on nylon affinity membranes for adsorption of papain.

Hollow-fiber membranes of various polymers containing immobilized CB were tested to purify proteins. Membranes of poly (2-hydroxyethyl) [58], polysulfone and cellulose [59] and polyamide [60] were used to purify albumin, catalase and lysozyme.

Champluvier and Kula [61] studied the commercial Sartobind membranes (Sartorius, Germany) with immobilized CB for the recovery of glucose-6-phosphate dehydrogenase from *Saccharomyces cerevisiae*.

Monoliths are novel alternative supports studied in affinity chromatography. Monoliths composed by poly(EDMA-GMA) [16] and poly(acrylamide-allyl glycidyl ether) [62] with immobilized CB were studied for HSA purification.

## 2.3. Chromatographic supports

### 2.3.1. Resin

Several affinity matrices with immobilized reactive dye are commercially available. Matrices containing Cibacron Blue F3GA are available with varying amounts of dye bound. Some of them are Sepharose CL-6B, Affi-Gel Blue Gel, AcroSep™ and HiTrap™ Blue HP manufactured by Sigma Aldrich, Bio-Rad, Pall Life Sciences and GE Healthcare respectively.

HiTrap™ Blue HP Columns, Figure 2.4, are prepacked columns with Blue Sepharose™ High Performance, that is a specific adsorbent for the purification of albumin, enzymes, coagulation factors, interferons, and related proteins. The carbohydrate nature of the agarose base promotes the coupling due to a hydrophilic and chemically favourable environment. The cross linked structure has a spherical matrix with 34 µm of mean particle size.



Figure 2.4 - HiTrap™ Blue HP Column.

The ligand, CB, is covalently attached to the matrix via the triazine part of the dye molecule.

The columns are made of polypropylene, which is biocompatible and does not interact with biomolecules. The columns used are 1 mL of volume, they can be used either with a syringe, a laboratory pump or a chromatographic system.

The main characteristics of HiTrap™ Blue HP columns are summarized in Table 2.1.

Table 2.1. Characteristics of HiTrap™ Blue HP columns with volume of 1 mL.

|                                |  |
|--------------------------------|--|
| <b>Column dimensions</b>       | 0.7 × 2.5 cm                           |
| <b>Ligand concentration</b>    | 4 mg/mL medium                         |
| <b>Binding capacity</b>        | 20 mg human albumin/mL medium          |
| <b>Mean particle size</b>      | 34 μm                                  |
| <b>Matrix</b>                  | Highly cross-linked, spherical agarose |
| <b>Maximum backpressure</b>    | 3 bar (0.3 MPa)                        |
| <b>Maximum flow rate</b>       | 4 mL/min                               |
| <b>Recommended flow rate</b>   | 1 mL/min                               |
| <b>pH stability</b>            |  |
| <b>Regular use<sup>1</sup></b> | 4–12                                   |
| <b>Cleaning<sup>2</sup></b>    | 3–13                                   |
| <b>Temperature stability</b>   |  |
| <b>Regular use</b>             | 4°C to room temperature                |
| <b>Storage</b>                 | 4°C to 8°C                             |
| <b>Storage buffer</b>          | 20% ethanol                            |

<sup>1</sup> Refers to the pH interval where the medium is stable over a long period of time without adverse effects on its subsequent chromatographic performance.

<sup>2</sup> Refers to the pH interval for regeneration, cleaning-in-place, and sanitization procedures.

### 2.3.2. Membranes

Flat sheet regenerated cellulose membranes were used as solid support for ligand immobilization. Sartobind membranes, kindly provided by Sartorius Stedim Biotech GmbH, Göttingen, Germany, have been used in three different formats: preactivated with epoxy groups, Sartobind® Epoxy; with aldehyde groups, Sartobind® Aldehyde; as well as the unmodified membrane.

These membranes have a base matrix of stabilized and reinforced cellulose: this hydrophilic polysaccharide consists of linear chains of several

hundreds to over ten thousand D-glucose units linked with  $\beta$ 1-4 glycosidic bonds (fig. 2.5). Reticulations between adjacent chains are also possible through  $\beta$ 1-6 glycosidic bonds.

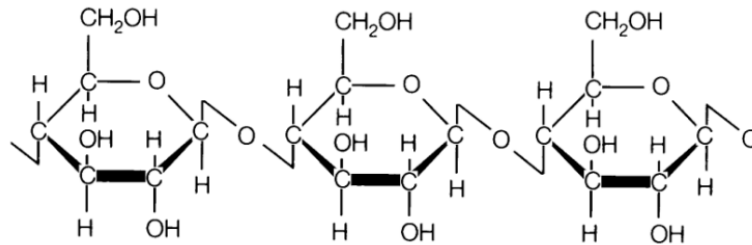


Figure 2.5 – Cellulose structure.

The hydroxyl groups in position 2, 3 and 5 can be activated with functional groups, such as epoxy or aldehydic groups, and then a ligand can be attached to these groups.

### 2.3.2.1. Regenerated cellulose membranes

The unmodified regenerated cellulose membrane is the base matrix of all Sartobind family, figure 2.6. The membranes have an average pore size of 0.45  $\mu\text{m}$  and a thickness in the range of 227 to 252  $\mu\text{m}$ . The thickness of individual sample was measured using Digimatic Disk Micrometer (Mitutoyo Corporation, Japan). These membranes are indicated with RC throughout this work.

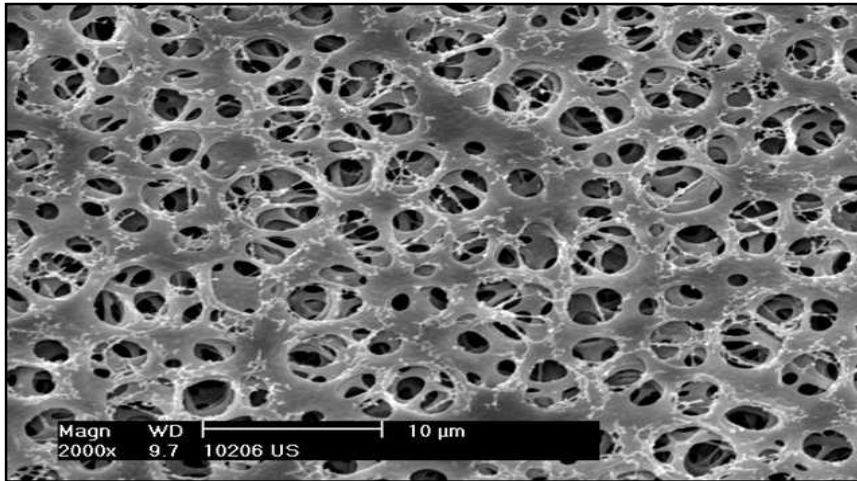


Figure 2.6 - SEM image of matrix in cellulose reinforced and stabilized.

### 2.3.2.2. Membrane Sartobind® Epoxy

The second membrane used for CB coupling was Sartobind® Epoxy, a stabilized reinforced cellulose with active epoxy groups, Figure 2.7.

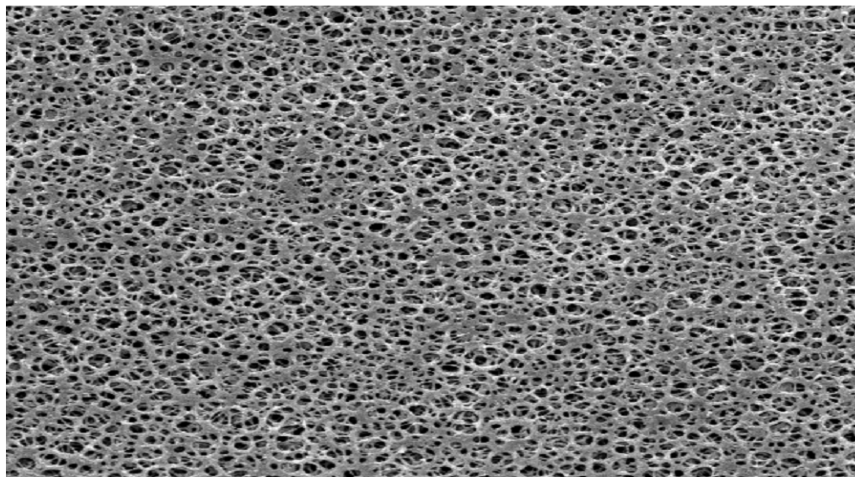


Figure 2.7 - SEM of Sartobind® Epoxy membrane surface view x 1000.

The activation is usually accomplished through grafting technique, using an epoxy monomer. The membrane obtained has a thickness of 275 μm, the average pore size of 0.45 μm and a void fraction of about 64%. The density of the



epoxy monomer on membrane is 1.5  $\mu\text{eq}/\text{cm}^2$ . Membranes characteristics are summarized in table 2.2, in which the information provided in the manufacturer in data sheet is reported. Sartobind<sup>®</sup> Epoxy membranes are indicated with SartoE throughout this work.

Table 2.2 – Main characteristics of SartoE and SartoA membranes.

|   |   |
|---|---|
| <b>Binding capacity of protein</b>            | > 1.1-5.5 mg/mL<br>> 30-150 $\mu\text{g}/\text{cm}^2$ |
| <b>Flow rate at 0.1 MPa (1 bar, 14.5 psi)</b> | > 40 mL/ $\text{cm}^2 \times \text{min}$              |
| <b>Poresize</b>                               | 0.45 $\mu\text{m}$                                    |
| <b>Ligand density</b>                         | 1.5 $\mu\text{eq}/\text{cm}^2$                        |
| <b>1 mL membrane</b>                          | 36.4 $\text{cm}^2$                                    |

### 2.3.2.3. Membrane Sartobind<sup>®</sup> Aldehyde

Membranes in cellulose with aldehyde activation Sartobind<sup>®</sup> Aldehyde membranes, for simplicity indicated with the abbreviation SartoA, are constituted by the same reinforced and stabilized cellulose used for all Sartobind membranes, Figure 2.8.

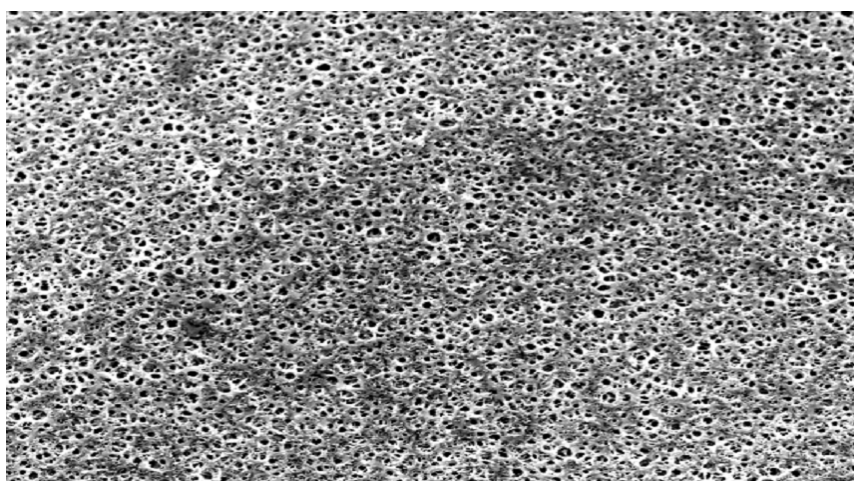


Figure 2.8 - SEM of Sartobind<sup>®</sup> aldehyde surface view x 500.

The activation is achieved through grafting technique, in this case using an aldehyde monomer which is a spacer arm and provides functional groups for subsequent immobilization of the ligand. Thickness, average pore size and porosity are equal to the membranes SartorE as specified in Table 2.2.

### 2.3.3. Monoliths

A monolithic column is constituted of a single piece of separation media which presents high permeability and low resistance to mass transfer. For this reason monolithic material is especially suited for the separation of analytes with low diffusion constants, like proteins, peptides, nucleic acids and synthetic polymers [63].

The monolithic supports used in this work were kindly provided by BIA Separations GesmbH. Monoliths with two different activation chemistry, epoxy and EDA, were used as a chromatographic support for CB immobilization, Figure 2.9.

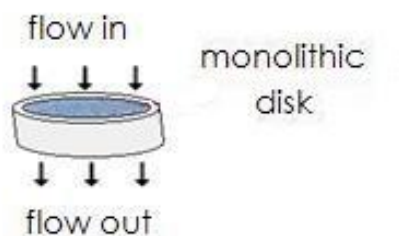


Figure 2.9 - Convective interaction media (CIM) disks.

These monoliths have a diameter of 12 mm and thickness of 3 mm, volume of 0.34 mL, placed in an appropriate housing [64], Figure 2.10, which was connected to a FPLC system.

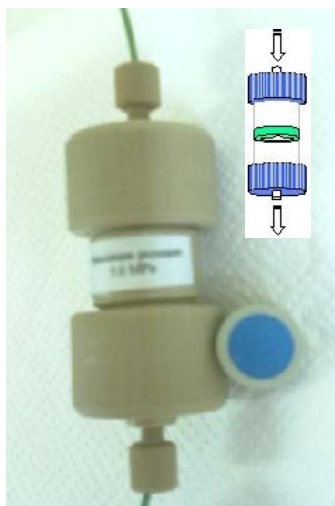


Figure 2.10 –CIM® housing and CB-Epoxy disk.

This monolith contains a homogeneous base matrix of poly(glycidyl methacrylate-co-ethylene dimethacrylate), Figure 2.11, and a non-porous, self-sealing fitting ring that ensures only axial flow through the disk and prevents any sample and mobile phase leakage or bypass.

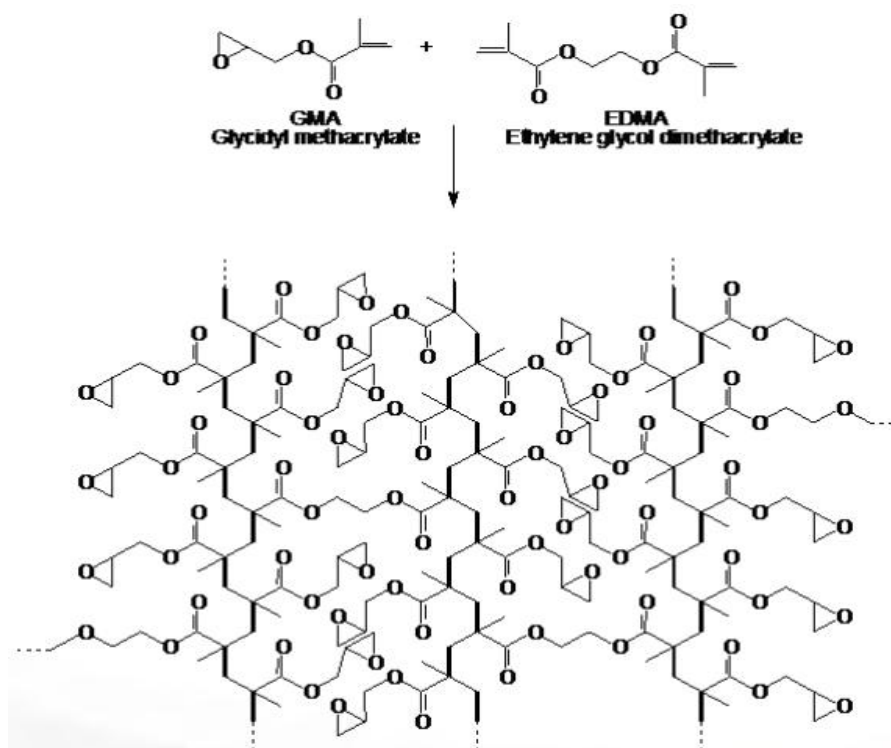


Figure 2.11 – Monolith chemical structure.

The main characteristics of CIM disks are summarized in Table 2.4.

Table 2.4. Comparison of the characteristics of CIM Epoxy and EDA disks.

| <b>Disk chemistry</b>          | Epoxy  | EDA  |
|--------------------------------|--|------|
| <b>Channel size</b>            | Average pore radius: 600 – 750 nm                      |      |
| <b>Matrix</b>                  | poly(glycidyl methacrylate-co-ethylene dimethacrylate) |      |
| <b>Working system pressure</b> | Up to 50 bar (5 MPa)                                   |      |
| <b>pH Working range</b>        | 1-14   | 2-13 |
| <b>Storage buffer</b>          | 20% ethanol  |      |

## 2.4. Analytical methods

### 2.4.1. Protein concentration determination methods

Accurate protein quantification is essential to all experiments related to proteins in many research projects.

During the last century several methods have been developed to quantify proteins either to determine the total protein content and also as a specific assay to quantify a single protein.

Total protein quantification methods include traditional methods such as the UV adsorption at 280 nm ( $A_{280}$ ), bicinchoninic acid (BCA) and Bradford assays, as well as alternative methods like Lowry or novel assays developed by commercial suppliers.

#### 2.4.1.1. UV adsorption

UV adsorption is one of the simplest and effective methods for the measurement of the concentration of pure protein solutions. When an electromagnetic radiation hits a substance, this substance absorbs a portion of the incident radiation. If  $I_0$  indicates the incident radiation intensity and  $I$  indicates the intensity of the radiation that has passed through the sample, the transmittance  $T$  is defined by the following relationship:

$$T = \frac{I}{I_0} \quad (2.1)$$

while the absorbance  $A$ , for liquid solutions, is defined by the following relationship:

$$A = \log_{10} \left( \frac{I_0}{I} \right) = -\log_{10}(T) \quad (2.2)$$

Proteins absorb at 280 nm mainly for the presence of tyrosine and tryptophan residues and cysteine, disulfide bonded cysteine residues.  $A_{280}$  method is based on the protein capacity to absorb the radiation in the near ultraviolet (UV). Usually the wavelengths used are 215 and 280 nm according to the absorbance peaks of proteins.

Some conditions that alter the protein tertiary structure as buffer type, pH and reducing agents, can affect its absorbance. Nevertheless, measuring the absorbance at 280 nm is often used because few other chemicals also absorb at this wavelength.

In the range of 20 to 3000  $\mu\text{g/mL}$ , the relationship between absorbance and concentration of an absorbing species is linear and can be described by the Lambert Beer law. The general Lambert Beer law is usually written as:

$$A = \varepsilon \cdot b \cdot c \quad (2.3)$$

where  $A$  is the measured absorbance,  $\varepsilon$  is the molar absorptivity coefficient dependent to wavelength having units of  $\text{M}^{-1} \text{cm}^{-1}$ ,  $b$  is the path length and  $c$  is the analyte concentration [65].

The absorbance measurements were performed with a spectrophotometer UV1601 (Shimadzu) and with the UV detector module of the FPLC System ÄKTA Purifier 100 (GE Healthcare), that will be described in Section 2.6.1.3.

Due to the use of two UV cells with different path length it was necessary to determine a conversion factor between the two instruments. This coefficient is 209.7.

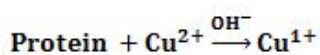
#### 2.4.1.2. BCA assay

Another method used to determine the total amount of protein is the bicinchoninic acid assay, BCA. The BCA Protein Assay Reagent Kit (Pierce Biotechnology, Inc.) was used as indicated in the manufacturer instructions specified for the standard protocol, as experimental conditions: 37 °C for 30 minutes in a working range of 20 - 2,000  $\mu\text{g}/\text{mL}$ .

The principle of the bicinchoninic acid (BCA) assay is based on the formation of a  $\text{Cu}^{+2}$  protein complex under alkaline conditions, followed by reduction of the  $\text{Cu}^{+2}$  to  $\text{Cu}^{+}$  (Biuret reaction). The amount of reduction is proportional to the protein present. It has been shown that cysteine, tryptophan, tyrosine and the peptide bond are able to reduce  $\text{Cu}^{+2}$  to  $\text{Cu}^{+1}$ [66]. The reaction result in an intense purple colour with an absorbance maximum at 562 nm. The

coloured reaction product of this assay is formed by the chelation of two molecules of BCA with one cuprous ion, Figure 2.12.

**STEP 1**



**STEP 2**

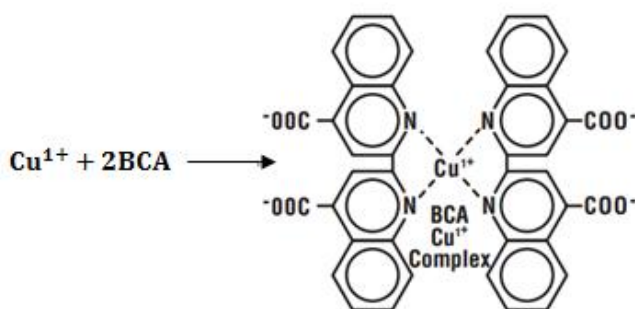


Figure 2. 12 – Reaction representation of the BCA assay. In step 1 the chelation of copper with protein is shown and in step 2 the chelation of two BCA molecules with one cuprous ion.

Since the production of  $\text{Cu}^+$  in this assay is a function of protein concentration and incubation time, the protein content of unknown samples may be determined spectrophotometrically by comparison with known protein standards.

The BCA protein assay was performed using a ShimadzuUV-1601 spectrophotometer (Kyoto, Japan). The samples and their corresponding blanks were assayed in triplicate by the BCA method, using BSA as the standard, for these data see Appendix II.

### 2.4.1.3. Electrophoresis

Proteins have a net average charge in solution at any pH other than their isoelectric point, allowing to analyze heterogeneous protein samples. The proteins migrate by action of an electric field due to their charges. This migration is different for each protein and it depends on its charge density, that is, a ratio charge/mass. As a result, proteins have characteristic migration rates that can be exploited for the purpose of separation as in electrophoresis.

The force acting on a protein is equal to  $Ez$ , being  $E$  the electric field applied and  $z$  the net charge on the protein. This force is opposed by viscous forces in the moving medium proportional to the viscosity  $\eta$ , the particle radius  $r$  (Stokes radius) and the velocity  $v$ .

In a steady state

$$Ez = 6\pi\eta rv \quad (2.4)$$

The specific mobility, defined as velocity per unit of electric field  $\frac{v}{E}$  is therefore

$$u = \frac{z}{6\pi\eta r} \quad (2.5)$$

From this relation, it is evident that the final mobility of a charged protein is a function of both net charge and size.

The support frequently used to carry out an electrophoresis separation is a polymeric gel. The electrophoresis gel is a three dimensional network of filaments forming pores of various sizes, acting as a screening towards proteins of different dimensions. As a consequence, the effective viscosity of the gel  $\eta$



varies as a function of protein size, causing mobility, Eq. 2.5, to be a more complex function.

Lastly, gel electrophoresis separates according to both net charges and molecular size.

The different electrophoresis procedures using polyacrylamide gels as a medium are Native electrophoresis, Urea gel, Sodium dodecyl sulphate gel electrophoresis (SDS-PAGE) and Gradient gels.

SDS-PAGE is adopted to determine the molecule weight and purity of a protein sample. It provides a platform to analyze multiple samples simultaneously and multiple components in a single sample.

This method involves denaturing the protein with sodium dodecyl sulphate (SDS). SDS binds noncovalently to protein in a manner that confers an overall negative charge on the proteins, the same charge/mass ratio for all proteins and a long rod-like shape on the proteins instead of the tertiary conformation. As a result, the separation occurs only due to the screening effect through the pores of the gel.

The separation of molecules of the same size is not realizable, despite of the best resolution achieved with this method.

It is possible to compare unknown samples in the gel using standard polypeptides of known molecular weight in terms of mobility against size.

Electrophoresis technique can be used during purification process to identify whether the desired product is pure or contains impurities. When the product is completely isolated only a band is expected.

#### 2.4.1.3.1. *Experimental procedure*

The apparatus available in our laboratory requires the use of precast gel, Figure 2.13. The precast gel used is Tris-HCl Criterion™ Gel 4-20% Linear Gradient (Bio-Rad) 13.3 cm of width, 8.7 cm of length and thickness of 0.1 cm.



Figure 2.13 – Electrophoresis apparatus.

The procedure adopted is as follow:

- ❑ Mix in Eppendorf tubes 80  $\mu\text{L}$  of protein samples with 20  $\mu\text{L}$  of CPB (classic protein buffer) solution. At the same time, mix 80  $\mu\text{L}$  of protein markers with 20  $\mu\text{L}$  of CPB. For the composition of these solution see Appendix I.
- ❑ Heat the sample at 90-95°C for 10 min.
- ❑ Prepare the running buffer solution, Appendix I.
- ❑ Remove the gel from the package. Remove the comb and rinse the wells with deionized water. Thereafter, remove the tape from the bottom of the cassette into one of the slots in the cell tank.
- ❑ Fill the cell tank with running buffer until the mark Fill.
- ❑ After having inserted the precast gel to the cell tank, load 25  $\mu\text{L}$  of markers in the terminal wells and 25  $\mu\text{L}$  of protein samples in the wells available.

- ❑ Set the power supplier working at 140 V and 40 mA and connect the power supply to the cell tank and run the gel for about one hour and thirty minutes.
- ❑ After electrophoresis is complete, turn off the power supply and disconnect the electrical leads. Remove the cover from the tank and remove the gel from the cell. Remove the gel from the cassette carefully.
- ❑ Soak the gel in staining solution, Comassie Brilliant Blue (Bio-Safe Comassie, Bio-Rad) for about one hour.
- ❑ Destain overnight in water for few hours.

#### 2.4.1.4. HPLC

Classic liquid chromatography has severe limitations as a separation method. When the solvent is driven by gravity, the separation is very slow, and if the solvent is driven by vacuum, in a standard packed column, the plate height increases and the effect of the vacuum is negated.

The limiting factor in liquid chromatography was originally the size of the column packing, once columns could be packed with particles as small as 3  $\mu\text{m}$ , faster separations could be performed in smaller and narrower columns. High pressure was required to force the mobile phase and sample through the column.

The use of high pressures in a narrow column allowed for a effective separation to be achieved in much less time than was required for others forms of liquid chromatography.

General instrumentation, for this technique called High Performance Liquid Chromatography (HPLC), has following components:

- ❑ **degasser**, the solvent is passed through a very narrow bore column and any contaminant could at worst plug the column, or at the very least add

variability to the retention times during repeated different trials. Therefore HPLC solvent must be kept free of dissolved gases, which could come out of solution mid-separation, and particulates.

- ❑ **pump**, to deliver the mobile phase with varying range of pressure up to several hundred atmospheres to achieve reasonable flow rates.
- ❑ **injector**, the chromatographic process begins by injecting the solute into the injector connected to the top of the column.
- ❑ **guard column** to prevent contamination of the main column.
- ❑ **column**, the most important part of the system is the column where the separation occurs. Separation column contains packing to accomplish desired separation.
- ❑ **detector**, capable enough of measuring the solute concentration. The method used for detection is dependent upon the detector used.
- ❑ The response of the detector, a chromatogram, is displayed on a chart recorder or computer screen. To collect, store and analyze the chromatogram, integrators and other data-processing equipment are frequently used.

The concentrations of BSA eluted and the other components of the mixture were determined by the use of HPLC Watters Alliance 2695, Figure 2.14.

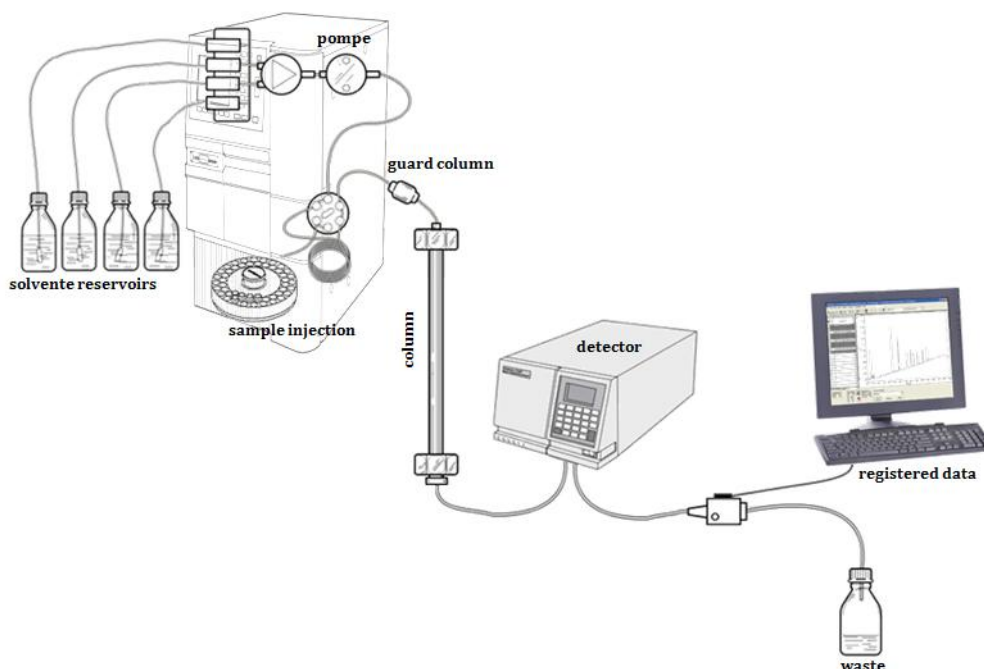


Figure 2.14 – Schematic diagram of High Performance Liquid Chromatography.

The chromatographic method applied to our separation is based on differences in size or shape, that is Size Exclusion Chromatography (SEC). In this case the separation is due to a specific distribution of the solutes between the mobile phase and the stationary phase. The characteristic of SEC is its gentle non-adsorptive interaction with the sample, enabling high retention of biomolecular activity.

On analytical scale, columns with small size beads are preferred since the resolution is more an issue than flow rate.

The column used for this procedure was BioSuite™ 250 4  $\mu\text{m}$  UHR SEC Columns Waters, with internal diameter 4.6 mm and length 300 mm.

The method used is isocratic with SEC Buffer, for the composition of this solution see Appendix I. The flow rate used is constant and equal to 0.35 mL/min.

The samples, before injection, are filtered in filters 0.22  $\mu\text{m}$ . The injection volume used is 10  $\mu\text{L}$ .

## 2.4.2. Chromatographic apparatus

The characterization of the chromatographic devices tested was done with a Fast Protein Liquid Chromatography (FPLC) system. The commercial name of the FPLC employed during the research project is Äkta Purifier 100, produced by GE Healthcare Life Sciences. Äkta Purifier 100 is a chromatographic system designed for development and optimization of biomolecular purifications at lab scale. An Äkta Purifier 100 is shown in fig. 2.15.

FPLC ÄKTA Purifier 100 is a system for protein separation and purification. This equipment is used for protein separation by different chromatographic techniques such as affinity, ion exchange, gel filtration, hydrophobic interaction and reversed phase chromatography.

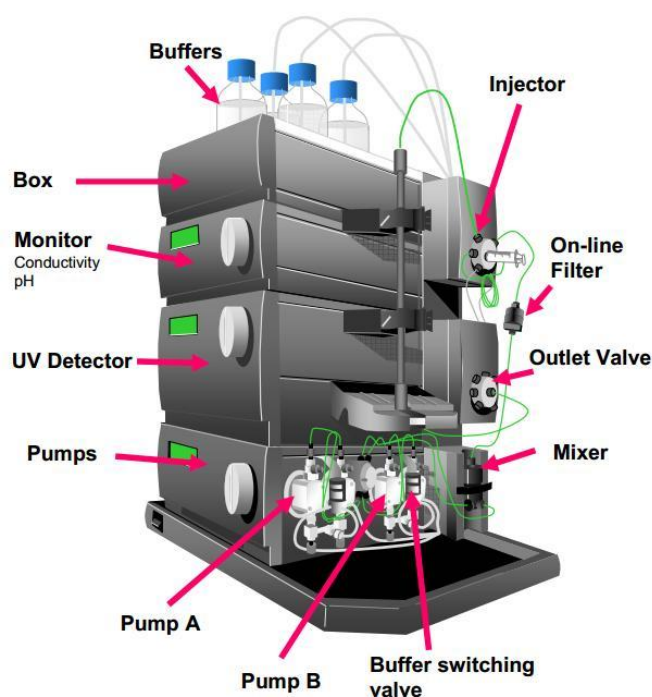


Figure 2.15 –FPLC ÄKTA Purifier 100.

The system includes a **pump** P-901 capable of providing flows from 0.01 to 100 mL/min until a maximum pressure of 10 MPa (100 bar). It also includes a **gradient mixer** M-925 with a 2mL chamber capable of using two pads simultaneously to flow 30 mL/min. The **sample injection** is made by INV-907 module that allows to use loops of different volumes or use a pump P-960 for loading large volumes of sample flows can reach up to 50 mL/min pressures up to 2 MPa (20 bar).

For the chromatographic separation control system includes a **detection module** Monitor UV-900 absorbance can monitor up to three wavelengths simultaneously in the range 190-700 nm, with a module that includes pH/C-900, **detector conductivity and pH** probe that control the gradients of solvents used. Following **separation valve** PV-908 allows the separation of waste products or the collection of fractions using a fraction collector Frac-920. A representative flow diagram for a Äkta Purifier 100 is shown in fig. 2.16.

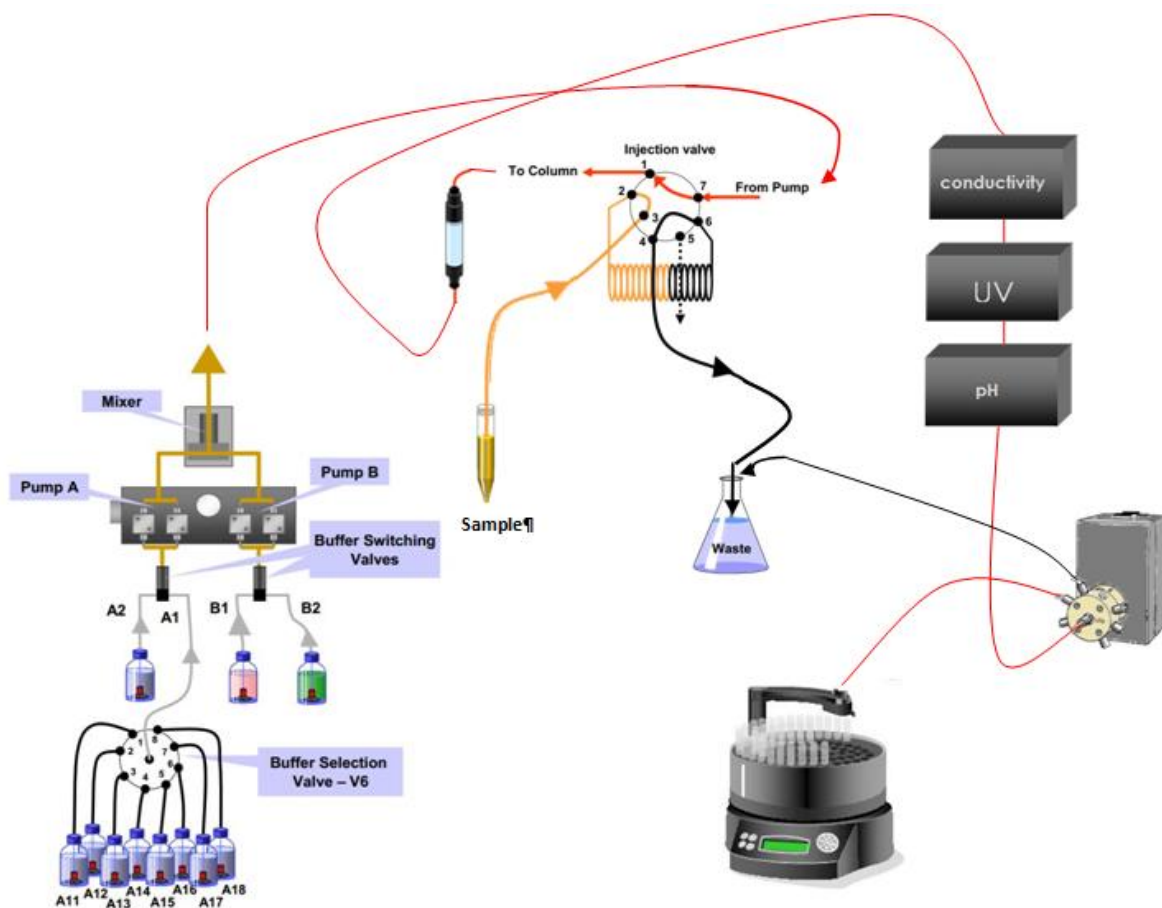


Figure 2.16 – Flow diagram for a FPLC Äkta Purifier 100.

In addition to the components described above, there are some accessory items, such as valves, a fraction collector, and others. Eleven different buffer lines can be used to load buffers into the system: 8 of them (from A11 to A18) belong to the group of lines A1, the other are the lines A2, B1 and B2. An 8 -port fractionation valve is used for the choice of the line of the group A1.

The system of pumps is constituted of 4 heads, two of them belonging to the couple of pumps A and the other two belonging to the couple of pumps B. The two pumps of a certain couple run in parallel, in order to provide a constant flow rate. The couple of pumps A can process either one of the lines of the group A1 or the line A2, while the system B can process either the line B1 or the line B2. The choice between the lines 1 and 2 is determined by the position of a switch valve; thus, the chromatographic system can process simultaneously



two different buffers, one from a line A and the other one from a line B. The lubrication of pumps is performed with a proper system, in which a fluid flows in a closed circuit with a velocity proportional to that of the pumps. The lubricant is a 20% (v/v) of ethanol aqueous solution.

After the pumps, a magnetic, single chamber mixer homogenizes the solutions that come from different lines. Then, these solutions are filtered with a polypropylene filter with 2  $\mu\text{m}$  pores and reach a 7-port injection valve. This valve can assume three different positions: Load, Inject and Waste. These positions are shown in fig. 2.17.

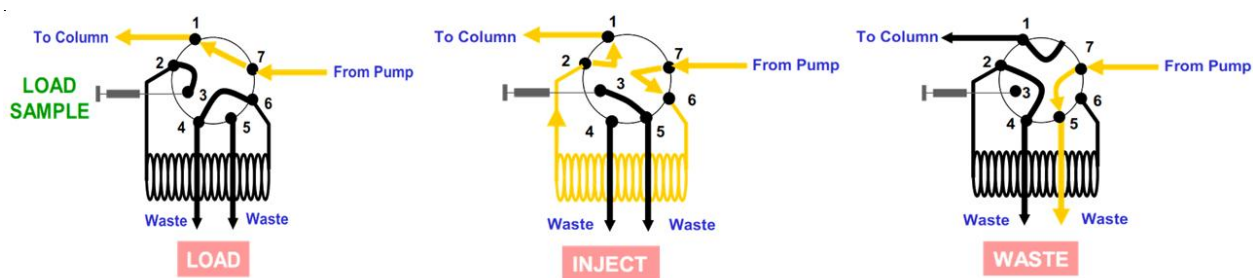


Figure 2.17 – Positions that can be assumed by the injection valve.

When the valve is in the Load position, the buffer is directly sent to the flow direction valve placed immediately after the injection valve. In this position, it is possible to load a sample from the port 3 while the chromatographic column is equilibrated. A loop, a simple tube of known volume that contains the sample, is connected to the ports 2 and 6. When the valve moves to the Inject position, the sample is pushed to the flow direction valve by the buffer; when the valve assumes the Waste position the column is disconnected from the circuit and the buffer pumped is discharged into the waste. This position is useful when it is necessary to change buffer, since it allows washing the volumes before the column.

The flow direction valve is a 7-port valve that, basing on the position assumed, directs the flow either downward or upward through the column.

After this valve there is a column valve. 8 chromatographic devices can be simultaneously connected to the Äkta system; the column valve directs the flow to the desired column. After the column there are the UV monitor and the pH/conductivity monitor. Before the outlet valve there is a flow restrictor, a device that generates a pressure drop. Because of the presence of this flow restrictor, the pressure in the UV and pH monitors is sufficiently high to avoid the formation of air bubbles that could lead to inaccurate measurements.

After this device there is another 8-port valve, the outlet valve. It can direct the buffer stream either to the waste or to another system, such as a fraction collector. A fraction collector FRAC-902 was connected to the Äkta Purifier 100.

Unicorn™ 5.0 is the software employed for the control of the chromatographic unit and for data elaboration. It has a 4 windows structure; the sections of the program are:

- ❑ Manager: this window is used to organize data, such as result files and user set up. It is divided into two columns: in the left one the working methods are displayed, in the right one the experimental results are saved.
- ❑ Method editor: in this window it is possible to create, modify and save working methods.
- ❑ System control: this is the most important window, since it allows to view run data in real time and to control the instrument manually with immediate effect on the process;
- ❑ Evaluation: this window is used to elaborate experimental data. A lot of different operations can be performed, such as peak integration, curve normalization, curve smoothing and curve differentiation. Results can be exported into other programs, like Excel worksheets, for further elaboration.

### 2.4.2.1. Qualitative description of chromatographic cycles

All protein solutions employed during chromatographic experiments were filtered with 0.45  $\mu\text{m}$  Sartorius filters made of cellulose nitrate. The filter material was hydrophilic, so, non-specific adsorption of BSA was minimized.

The experiments were performed as chromatographic cycles in bind and elute mode. This kind of chromatographic process is usually constituted of the following steps:

- Equilibration: a buffer with pH and ionic strength similar to those of the sample under examination is flushed into the column, in order to obtain uniform working conditions along the chromatographic media. The duration of this step depends on the column volume.
- Loading: in this step the sample is fed to the column. Its duration depends on the purpose of the chromatographic process: in industrial operations, the step is interrupted when the outlet concentration reaches a certain value, called Breakthrough concentration. In lab scale experiments, the adsorption step can be prolonged until the column is completely saturated; thus the maximum binding capacity of the column can be measured. In the cycles done during this study both these working modes were employed, see Chapters 4 and 5.
- Washing: in this step the solute molecules present in the dead volumes and those not specifically bound to the stationary phase are removed from the system. The buffer used is usually identical to that employed during the equilibration step. The wash ceases when the absorbance signal is close to zero, thus its duration depends on the column volume.
- Elution: the buffer flushed during this step breaks the bonds between the target biomolecule and the ligand and allows the recovery of the protein.

The duration is dependent on both the column volume and the desorption kinetic.

- Regeneration: the purpose of this step is to restore the primitive conditions of the column. Regeneration buffers usually have a pH acid or basic, in order to promote the denaturation of adsorbed proteins and their detachment. In some applications regeneration is performed after each cycle, in other cases it is sufficient to regenerate after a certain number of cycles.
- Riequilibration: the equilibration buffer is loaded again to the column.

In the experiments carried out during the work, for resin 0.1 M Tris-HCl pH 8, membranes 0.05 M Tris-HCl containing 0.05 M NaCl pH 8 and monoliths 25mM phosphate buffer containing 0.1 M NaCl pH 7.4 were employed for the equilibration, washing and riequilibration steps. The duration of the various steps varied from one cycle to another: the experimental protocols will be reported in detail in chapters 4 and 5. All buffers were loaded with buffer lines of the group A1. For elution the same buffer solution was used for all supports, 0.05M Tris-HCl containing 0.05 M NaCl and 0.5 M NASCN pH 8.0. Fractions were collected during the elution steps of each experiment and their concentration was measured with UV absorbance readings at 280 nm, since pure protein solutions were loaded during the runs.

### **2.4.3. Elaboration of experimental data**

The purpose of the chromatographic cycles performed was the determination of the binding capacity at saturation,  $DBC_{100\%}$ , and of the dynamic binding capacity at 10% of the maximum breakthrough height,

$DBC_{10\%}$ , at different flow rates of the affinity membranes and monolith selected for comparison with the resin. These parameters are defined in the following way:

$$DBC_{100\%} = \frac{m_{ads,100\%}}{V} \quad (2.6)$$

$$DBC_{10\%} = \frac{m_{ads,10\%}}{V} \quad (2.7)$$

where  $m_{ads,100\%}$  is the mass of adsorbed proteins on the stationary phase when the mobile phase and the adsorbent are in equilibrium,  $m_{ads,10\%}$  is the mass of protein adsorbed when the height of the breakthrough curve is equal to the 10% of the saturation BTC height and  $V$  is the volume of the adsorbent, total volume of the membranes, monolith or resin bed.

$DBC_{10\%}$  is an extremely important indicator of column performance and the knowledge of its dependence on the superficial velocity is fundamental for industrial applications, since at industrial scale the adsorption step is usually interrupted when the BTC height reaches a certain fraction of the height at saturation, otherwise too much protein would be lost.

The  $DBC_{10\%}$  usually decreases when the superficial velocity increases, because of mass transfer and kinetic limitations. These phenomena are particularly important when the stationary phase is a resin bed.

The binding capacities can also be referred to the adsorbent surface area  $A$ :

$$DBC_{100\%} = \frac{m_{ads,100\%}}{A} \quad (2.8)$$

$$DBC_{10\%} = \frac{m_{ads,10\%}}{A} \quad (2.9)$$

After the washing step, a fraction of the mass of protein loaded to the system is bound to the adsorbent and the other fraction has been lost; no protein is present in the system dead volumes. Thus, the mass of protein adsorbed can be easily calculated with the following equation:

$$m_{ads} = c_0 V_{loaded} - m_{lost} \quad (2.10)$$

where  $c_0$  is the concentration of the feed,  $V_{loaded}$  is the volume of protein solution loaded to the system and  $m_{lost}$  is the mass of protein lost. This last term can be calculated by integrating the area under the breakthrough curve during the loading and the washing steps, this operation can be easily performed with Unicorn™.  $m_{ads}$  can be either the mass of protein adsorbed at saturation or the mass of protein adsorbed at 10% of the maximum BTC height, depending on whether the load step is interrupted at 10% of the BTC height at saturation or it is prolonged until saturation.

The  $DBC_{10\%}$  can also be calculated from a breakthrough prolonged until saturation; in this case the previous equation must be corrected in order to keep in consideration the amount of protein that is present in the system dead volume at 10% of the maximum BTC height. Indeed, the washing step is not performed immediately after the BTC reaches the 10% of its maximum height, so at that point some protein occupies the system dead volumes.

The quantity of protein not specifically bounded to the stationary phase can be estimated by multiplying the feed concentration times the system dead volume.

This calculation introduces an approximation, since the concentration of the protein is considered uniform over the entire system and equal to the feed concentration, while, especially in the dead volume of the adsorbent media, it is lower.

$$m_{ads,10\%} = c_0 V_{loaded,10\%} - m_{lost,10\%} - c_0 V_{sys} \quad (2.11)$$

where  $V_{loaded,10\%}$  is the volume of protein solution loaded at 10% of the maximum BTC height,  $m_{lost,10\%}$  represents the mass of protein lost at 10% of the BTC height at saturation, calculated by integration of the area under the curve until the 10% of the maximum BTC height, and  $V_{sys}$  is the total system dead volume.  $V_{sys}$  can be calculated by loading a solute that is not adsorbed on the stationary phase from one of the buffer lines.

Other important parameters of a chromatographic process are the recovery and the yield:

$$recovery = \frac{m_{elu}}{m_{ads}} \quad (2.12)$$

$$yield = \frac{m_{elu}}{m_{loaded}} \quad (2.13)$$

where  $m_{elu}$  is the mass of protein eluted,  $m_{loaded}$  is the mass of protein fed to the system and the other terms have the meanings previously specified. In the experiments performed, the mass of protein eluted was calculated by integration of the area under the elution peaks.

## 2.5. Buffers and protein

BSA used in the experiments was purchased from Sigma-Aldrich and had a purity  $\geq 96\%$ . All buffers employed were prepared in our labs; the preparation methods of all solutions employed are described in Appendix I.

## *Affinity Membranes*

### **Experimental procedures and results**

#### **3.1. Ligand immobilization**

Cellulose membranes were cut into circular pieces of 26 mm of diameter and were equilibrated overnight in phosphate buffered saline (PBS) solution at pH 7.0.

Following this step, the membranes underwent specific treatments depending on the activation of the matrix. The protocols are described in details in the following paragraphs.

##### **3.1.1. SartoE membranes**

Two different procedures of immobilization were tested on these membranes: the first one involves the direct opening of the epoxy ring, the second one considers the addition of a spacer arm. The reaction schemes of the two protocols are reported in the Fig. 3.1.



*Protocol 1:*

The first step, the epoxy ring opening, was made by soaking the membranes in a 0.3 M NaOH aqueous solution, with 10 mg/mL of dissolved CB ligand and 1 mg/mL sodium borohydride ( $\text{NaBH}_4$ ). This reaction was carried out with gentle agitation at 37 °C for about 20 h [6]. Sometimes it was necessary to intervene with a glass rod to detach the membranes that adhered to the container walls. The epoxy ring opening is performed by reaction with a strong nucleophile or with an acid, in this case, it was the presence of  $\text{NaBH}_4$ .

In order to stimulate the reaction between the hydroxyl groups produced on the membranes and the ligand a solution of 20 %(w/v) NaCl at 60 °C was added. After 30 minutes, this reaction was catalyzed with 25 %(w/v)  $\text{Na}_2\text{CO}_3$  at 80 °C for 4h [57, 60, 67]. After ligand immobilization, the impurities were removed by an extensive cleaning procedure. The affinity membranes obtained with this protocol will be indicated as CB-SartoE1.

*Protocol 2:*

The immobilization of CB by addition of a spacer arm, was performed by a chemical conversion of the epoxy groups present on the membranes in amino groups with incubation with ethylenediamine (EDA) and then coupled with the ligand.

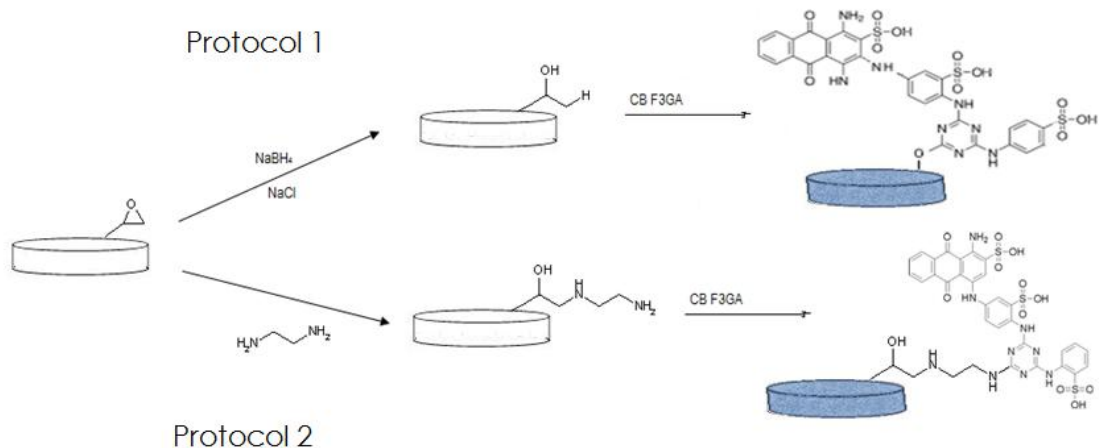


Figure 3.1- Immobilization reaction for Sartoe membranes with Cibacron Blue F3GA.

The membranes were incubated in EDA for 4h at 60 °C, followed by hydrolysis of the remaining epoxy groups into diol groups by treatment with an aqueous solution of 0.5 M sulphuric acid at 80 °C for 2h.

Ligand immobilization on membranes was performed by incubation in 10 mg/mL CB at 60 °C for 1 h, during this phase the membranes were continuously stirred. This reaction was followed by addition of 20 % (w/v) NaCl aqueous solution. After 1 h, an aqueous solution of 25% (w/v) Na<sub>2</sub>CO<sub>3</sub> aqueous solution was added to accelerate the reaction between dye and membrane which took place for 4 h at 80 °C [57, 60, 67]. The affinity membranes obtained by this procedure will be indicated throughout this work as CB-Sartoe2.

Finally, the affinity membranes were washed with hot water, 20% (v/v) methanol, 2 M NaCl aqueous solution, adsorption and elution buffers, and sequentially, water, 20% (v/v) methanol and 2 M NaCl several times until all the unbound dye was removed.

The membranes were stored at 4 °C in 0.05 M phosphate aqueous solution pH 7.0 containing 0.02 %wt. sodium azide to prevent microbial contamination [68].

### 3.1.1. *SartoA* membranes

With *SartoA* membranes two different procedures of immobilization were performed. One protocol considers the reduction of aldehyde groups with sodium borohydride and the second considers a direct immobilization of CB. The two reaction schemes are shown in Fig 3.2.

#### *Protocol 3:*

In order to obtain the reduction of aldehyde groups, the membranes were treated with sodium borohydride with a final concentration of 1 mg/mL and a concentration of CB ligand of 5 mg/mL. This reaction was carried out with gentle agitation at 37 °C for different time length. Sometimes it was necessary the intervention with glass rod to detach the membranes that remained adherent to the container walls.

The reaction between the hydroxyl groups produced on membranes and the ligand was stimulated adding 20 %(w/v) NaCl in an aqueous solution at 60°C. After 30 minutes, this reaction was catalyzed with 25 %(w/v) Na<sub>2</sub>CO<sub>3</sub> at 80°C for 4h [57, 60, 67]. After the dye-attachment phase, the impurities were removed by an extensively cleaning procedure. The affinity membranes obtained with this procedure will be indicated throughout this work as CB-*SartoA*3.

#### *Protocol 4:*

To perform the direct immobilization of CB, the ligand solution was left in contact with the aldehyde groups of the membrane.

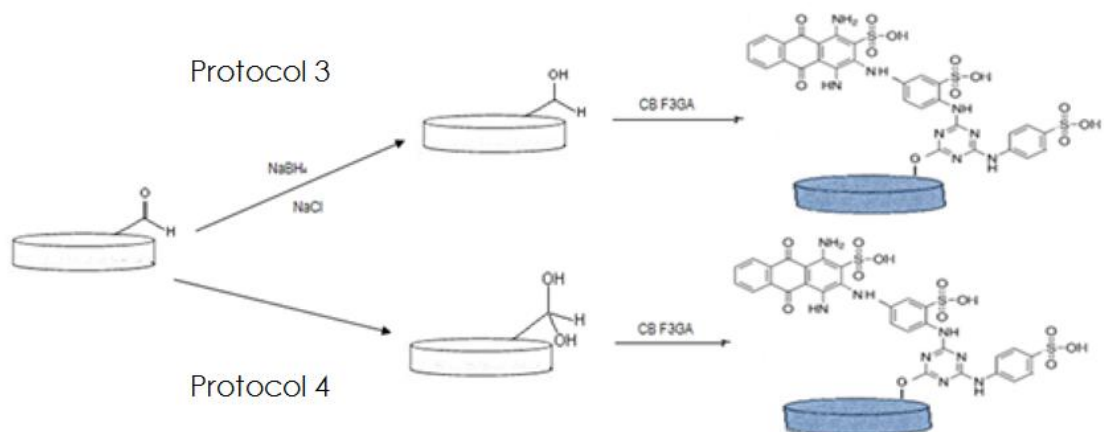


Figure 3.2 - Immobilization reaction for SartoA membranes with Cibacron Blue F3GA.

This immobilization was performed by incubation of membranes in 10 mg/mL CB at 60 °C for 1 h, during this phase membranes were continuously stirred. The reaction was followed by addition of an aqueous solution of 20 % (w/v) NaCl. After 1 h, an aqueous solution of 25% (w/v) Na<sub>2</sub>CO<sub>3</sub> was added to accelerate the reaction between dye and membranes which took place for 4 - 6 h at 80 °C [57, 60, 67]. The affinity membranes obtained with this procedure will be indicated throughout this work as CB-SartoA4.

After these steps the affinity membranes were washed with hot water, 20% (v/v) methanol, 2 M NaCl, adsorption and elution buffers, and sequentially, water, 20% (v/v) methanol and 2 M NaCl several times until all the unbound dye was removed.

The membranes were stored at 4 °C in 0.05 M phosphate buffer pH 7.0 containing 0.02 % wt. sodium azide to prevent microbial contamination [57].

### 3.1.2. RC membranes

Since the regenerated cellulose has free hydroxyl groups available, a protocol for direct immobilization of the ligand was developed as follows.

#### *Protocol 5:*

Membranes were soaked in a beaker containing aqueous solution of 10 mg/mL CB, stirred at 60°C in a water bath for 1h. The reaction was followed by addition of 20 %(w/v) NaCl to the solution. After 1h, 25 %(w/v) Na<sub>2</sub>CO<sub>3</sub> was added to accelerate the reaction between the replaceable chloride of the triazine ring and the membranes, this phase took place for 4h at 80°C.

At the end, the membranes were washed quickly with hot water to stop the reaction. Then, additional washing with methanol, 2 M NaCl, adsorption and elution buffers, and sequentially, water, methanol and 2 M NaCl aqueous solution was performed several times until all the unbound dye was removed. The membranes were stored at 4 °C in 0.05 M phosphate buffer pH 7.0 containing 0.02 %wt. sodium azide to prevent microbial contamination [68].

### 3.2. Ligand density

The membrane ligand density was determined spectrophotometrically following the protocol developed by Ruckenstein and Zeng [69]. Unmodified and CB-membranes were hydrolyzed with 2 mL of 12 N hydrochloric acid for 30 min at 80°C. This solution was diluted to 6 N with distilled water and then neutralized with 4 mL of 6 N sodium hydroxide aqueous solution [45].

The dye concentration in solution was measured by absorbance readings at a wavelength of 610 nm, using the appropriate extinction coefficient for the dye  $\epsilon = 13.6 \text{ mM}^{-1} \text{ cm}^{-1}$  [70, 62, 71].

### ***3.3. Ligand leakage***

Dye leakage was evaluated in three different solutions at room temperature to estimate the amount of molecules of CB that were released. The dye concentration in the medium was measured with UV readings at wavelength of 610 nm.

The solutions were chosen in different range of pH values: acid, neutral and basic to simulate the pH conditions of the buffers used in the purification process.

In particular, the membranes were soaked in 0.05 M sodium acetate solution pH 3.0, 0.05 M potassium phosphate solution pH 7.0 and 0.05 M sodium carbonate solution pH 11 for 2 months [57, 72].

## **3.4. Results and discussion**

### **3.4.1. Efficiency evaluation of the membrane modification procedure**

In order to evaluate the efficiency of the modification reaction some parameters were studied. These parameters are the temperature and the ligand concentration in the immobilization solution.

The first parameter investigated is the temperature of the reaction as reported in fig. 3.3. From the data reported in the figure it can be observed that ligand density increases with the reaction temperature. In table 3.1 are reported

the results of experiments performed with SartoE membranes to obtain the optimum reaction temperature. The temperature was changed over a range from 40 °C to 90°C according to the literature [73-77].

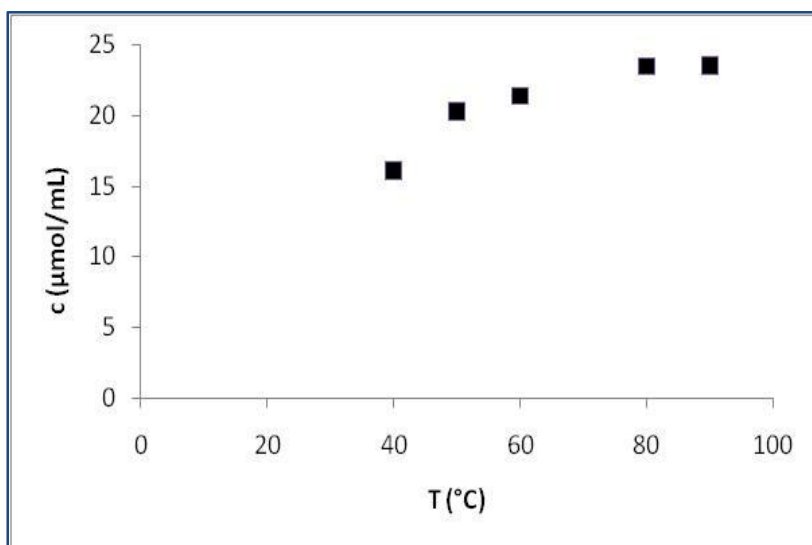


Figure 3.3 – Concentration of CB immobilized onto the membranes CB-SartoE1 as a function of temperature of reaction.

According to the experimental results, ligand immobilization was realized at 60°C and 80°C. The experimental data obtained at these temperatures are summarized in table 3.1.

Table 3.1 – Ligand density at two different immobilization temperatures for SartoE1 membranes.

| c <sub>CB</sub><br>(mg/mL) | CB density<br>(μmol/mL) |       |
|----------------------------|-------------------------|-------|
|                            | 60 °C                   | 80 °C |
| 0.6                        | 1.26                    | 3.27  |
| 1.5                        | 14.6                    | 22.4  |
| 3.0                        | 29.4                    | 33.5  |

The second parameter investigated is the ligand concentration in the coupling reaction as it is shown in Figure 3.4, where the ligand density is reported as a function of the concentration of CB in the immobilization solution.

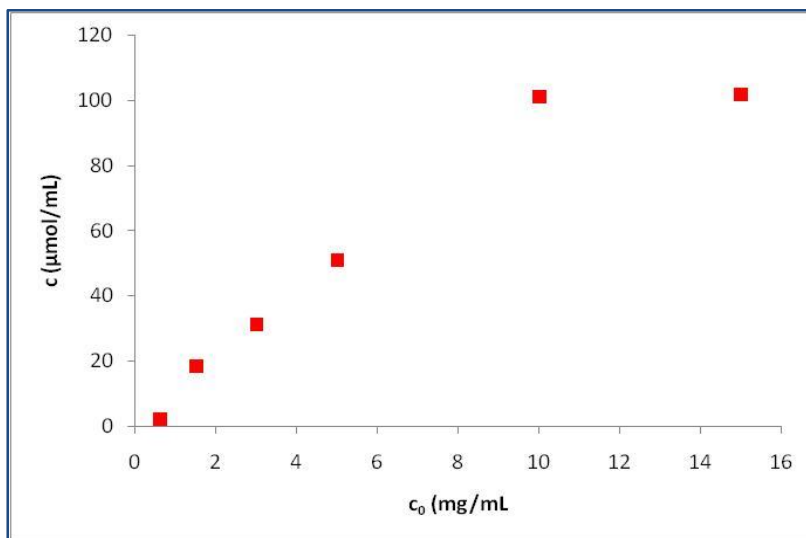


Figure 3.4 - Concentration of CB immobilized onto the membranes CB-SartoE1 as a function of initial solution of ligand at 80°C.

As it can be observed in the figure, that reports experimental data for the immobilization of CB on SartoE1 membranes at 80°C, the ligand density increases as the ligand concentration in the immobilization solution increases.

The amount of immobilized ligand on membranes was determined with the method described in § 3.2. Values of ligand density in all the membranes studied, CB-SartoE, CB-SartoA and CB-RC, are reported in Table 3.2.



Table 3.2 – Ligand density in the membranes CB-SartoE, CB-SartoA and CB-RC.

| Membrane   | $c_{CB}^1$ (mg/mL) | CB density ( $\mu\text{mol/mL}$ ) |
|------------|--------------------|-----------------------------------|
| CB-SartoE1 | 0.6                | 2.27                              |
|            | 1.5                | 18.5                              |
|            | 3.0                | 31.45                             |
|            | 5                  | 51.2                              |
|            | 10                 | 101.2                             |
| CB-SartoE2 | 10                 | 83.1                              |
| CB-SartoA3 | 5.0                | 46.3                              |
| CB-SartoA4 | 3.0                | 78                                |
|            | 5.0                | 96.5                              |
| CB-RC      | 5                  | 63.4                              |
|            | 10                 | 151.8                             |

<sup>1</sup>Initial concentration of the ligand in the immobilization solution.

A comparison of ligand density on the different membranes studied at the optimal immobilization conditions, temperature and ligand concentration, is reported in Figure 3.5, the experimental data were analysed according to the method explained in § 3.3.

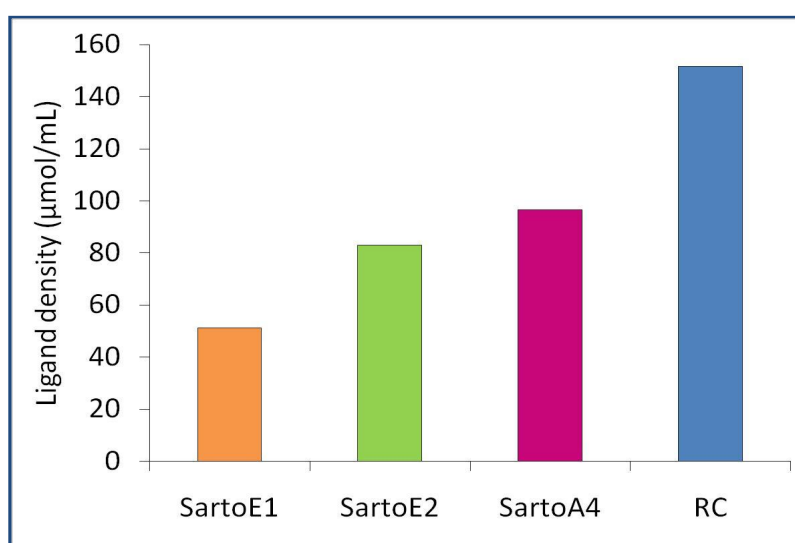


Figure 3.5 – Ligand density of Cibacron Blue F3GA on membranes.

The amount of CB immobilized on membranes varies between 51 to 152  $\mu\text{mol/mL}$  with CB initial concentration of 10 mg/mL, according to the immobilization protocol used.

Results of ligand leakage experiments are shown in Figures 3.6 and 3.7, where the amount of Cibacron Blue F3GA released from membranes is plotted as a function of solution pH.

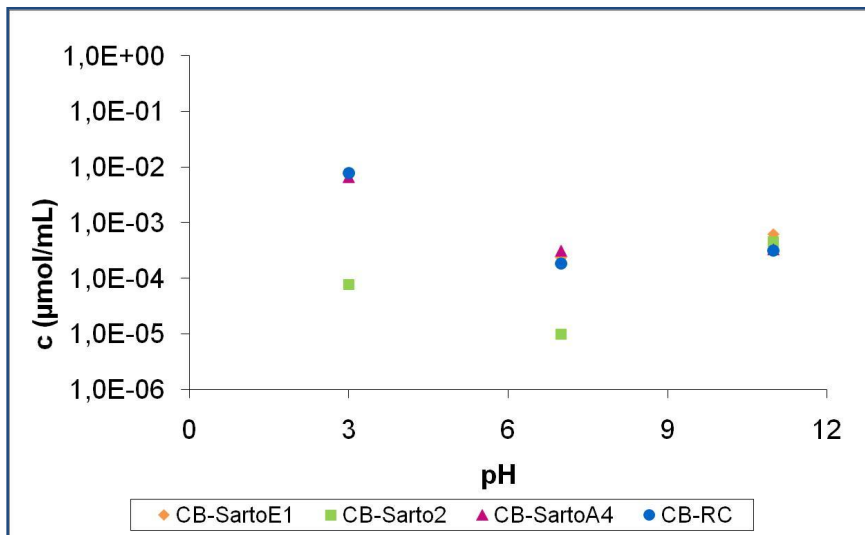


Figure 3.6 – Dye released from membranes at different values of pH.

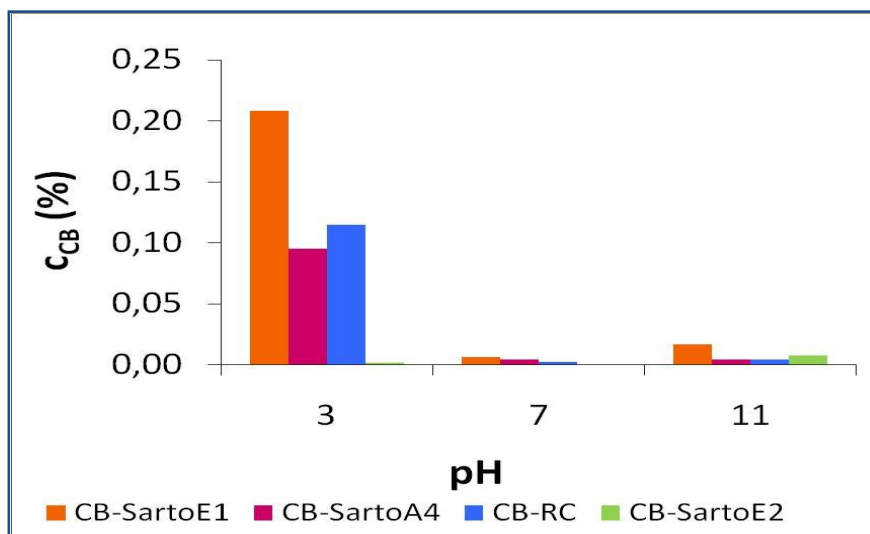


Figure 3.7 – Percent values of Cibacron Blue F3GA released in three different solutions from CB-membranes as function of pH.

Ligand leakage experiments indicated that there is nearly no release of dye molecules in the neutral (pH 7.0) and alkaline (pH 11.0) media, while in the acidic (pH 3.0) medium the dye leakage was less than one percent for all membranes. These tests showed that there was no significant ligand leakage from pH 7.0 – 11.0 during adsorption studies, or even for a long period of storage time, more than 2 months.

### **3.5. Characterization of the modified membranes with batch tests**

Separation of BSA from aqueous buffered solution of pure protein was studied in batch experiments in order to determine the static binding capacity of the CB-affinity membranes.

An affinity purification process is generally performed as a sequence of steps: adsorption → washing → elution.

In the adsorption step, 2 mL of protein solution, BSA in 0.05 M Tris-HCl containing 0.05 M NaCl pH 8.0, was loaded in a beaker containing four new CB-affinity membranes. The step ends up when an equilibrium condition between the protein in solution and the protein onto the membranes is reached. After several experiments it was observed that generally three hours were sufficient to reach equilibrium conditions.

At the end of the adsorption stage, the CB-membranes were immediately extracted from the protein solution and were washed in a beaker, with 2 mL of equilibration buffer. The washing step allows to remove the fraction of not specifically adsorbed protein. At the end of this step, only the protein immobilized remains on the support.

In the elution step the immobilized protein was recovered and brought in solution. During this step, the membranes were kept for 2 h 30 min in a beaker containing 2 mL of elution buffer at room temperature.

All the steps were conducted keeping the beaker at a room temperature and under continuous agitation on shaking platform. In all steps samples of liquid phase were analyzed via UV adsorption ( $A_{280}$ ) at regular intervals, to monitoring the protein concentration in solution. Experiments were performed at two different concentration of BSA in the adsorption solution, namely 0.5 and 1 mg/mL.

### **3.5.1. Experimental results**

At the beginning kinetic experiments to determine the time necessary to reach equilibrium were performed for both adsorption and elution stages. The typical trend of concentration in solution observed during these steps is presented in Figure 3.8.

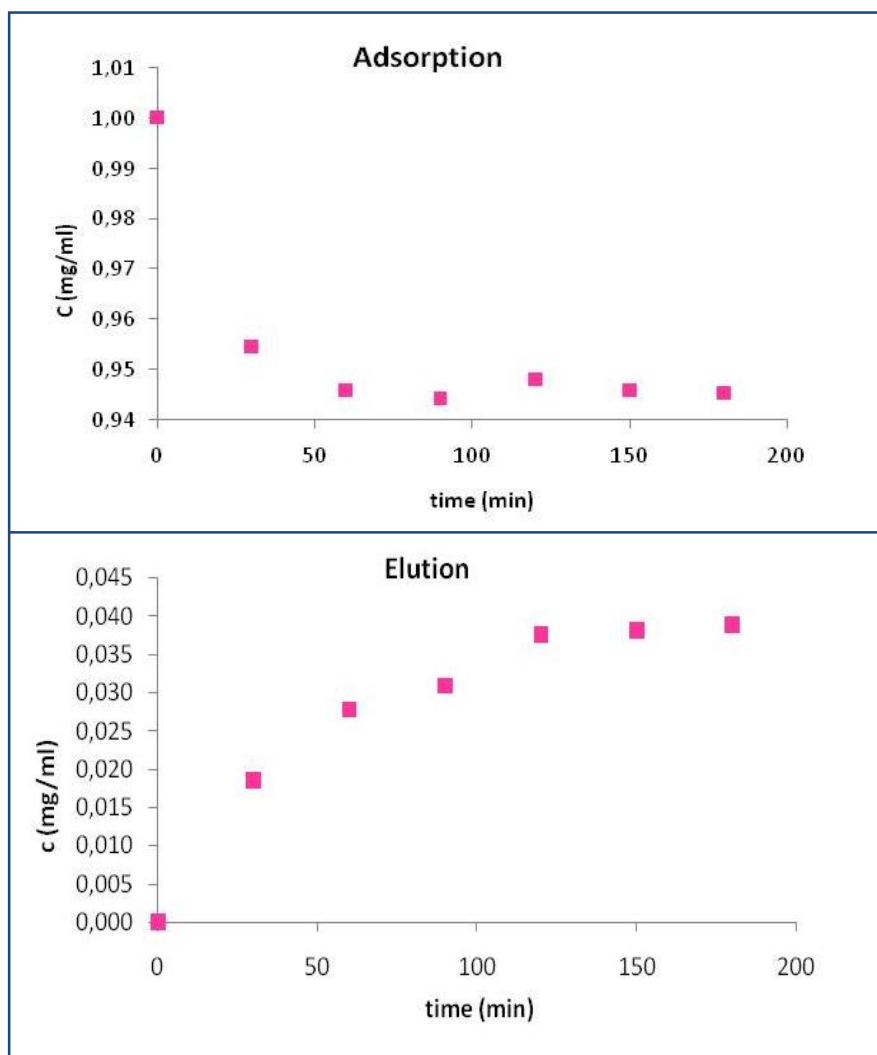


Figure 3.8 – BSA concentration as a function of time in adsorption and elution steps of experiments performed with CB-SartoE1.

Each experiment provides information in terms of kinetics and equilibrium conditions. From the mass balance on the adsorption step, the amount of protein immobilized onto the membranes can be calculated, thus the concentration of protein, in mass per unit of surface area or volume, in equilibrium with the concentration left in solution. In an analogous way one can proceed for the elution step.

A comparison of the adsorption kinetic on CB-SartoE1, CB-SartoA4 and CB-RC membranes is reported in Figure. 3.9; the tests were conducted at the

same operating conditions: membrane area of 7.07 cm<sup>2</sup>, initial concentration of BSA 1 mg/mL, duration of the adsorption step of 2 hours.

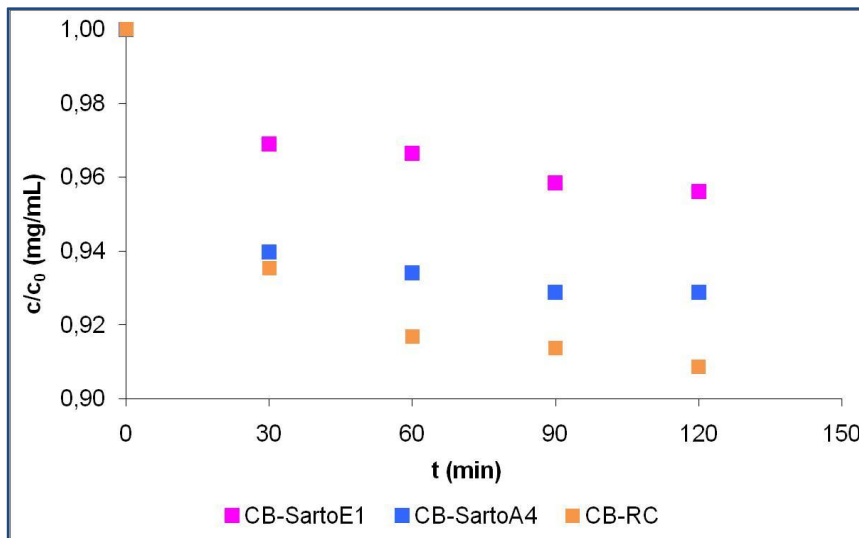


Figure 3.9 – Comparison of experimental data obtained from adsorption kinetic experiment with CB-SartoE1, CB-SartoA4 and CB-RC membranes.

From the experimental data it appears that CB-RC membranes have a faster kinetic than CB-SartoE1 and CB-SartoA4 membranes. However, the difference among the curves is minimal and can be consider comparable.

Equilibrium experiments were performed with BSA solutions of different concentration to determine the static binding capacity of the affinity membrane. In Figure 3.10, the capacity of CB-SartoE1 membranes is reported together with the equilibrium isotherm calculated with the Langmuir model as described in § 1.3.1. The terms  $c_{eq}$  and  $q_{eq}$  represent respectively the concentration value of protein in solution and the concentration value of protein adsorbed onto the membranes at equilibrium.

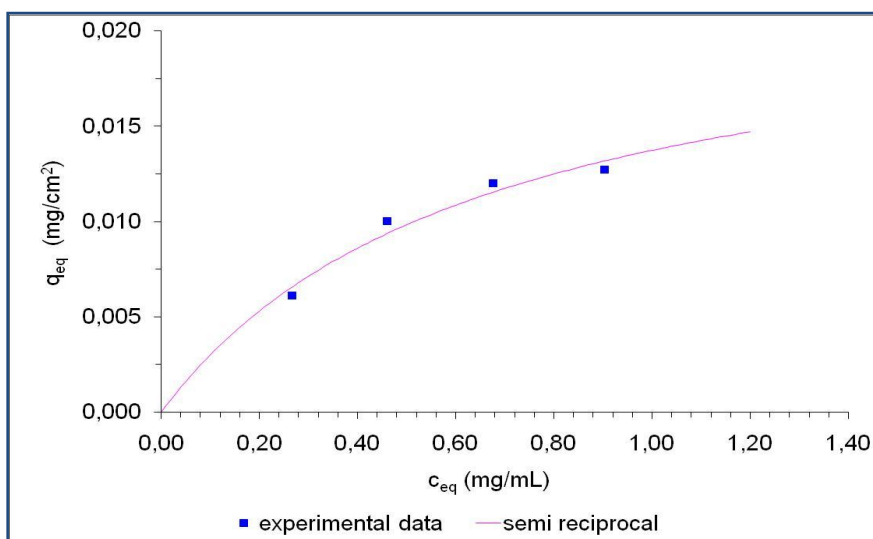


Figure 3.10 – Experimental data and adsorption isotherm of BSA on CB-SartoE1 affinity membranes.

The values of the Langmuir parameters  $K_d$ , the dissociation constant, and  $q_m$ , the maximum binding capacity, for CB-SartoE1 membranes are summarized in Table 3.3.

Table 3.3 - Langmuir parameters determined by the semi reciprocal method.

| <b>SartoE1-CB</b>           |        |
|-----------------------------|--------|
| $q_m$ (mg/cm <sup>2</sup> ) | 0.0128 |
| $K_d$ (mg/mL)               | 0.187  |

### 3.5.1.1. Elution step

The elution step consists in the cleavage of the bond between ligand and protein created during the adsorption in order to recover the protein. During elution the biomolecule of interest is recovered by changing the mobile phase composition.

There are different elution techniques, in this way the elution can be performed in a selective or non-selective way.

In the competitive elution, selective elution buffer contains a compound that competes either for binding to the target protein or for binding to the ligand.

The non-competitive elution consists in a change of the operating conditions, which can be achieved by varying the pH, high concentration of chaotropic agents and ionic strength. A change in pH alters the ionization of charged groups on the ligand or the bound protein. This fact may affect the binding sites reducing their affinity or cause alterations in the conformation. The mechanism for elution through the changes in ionic strength will depend upon the specific interaction between the ligand and target protein. This method consists in a mild elution using a buffer with increased ionic strength, in our case we used NaCl and KCl. The use of chaotropic agents in elution buffers causes alterations in the protein structure. Chaotropic agents tend to denature the eluted protein.

The elution tests was carried out using buffers at room temperature. The BSA adsorbed supports were placed in the elution medium and stirred for 2 h 30 min at a stirring rate of 100 rpm. The final BSA concentration within the elution medium was determined by using  $A_{280}$  and BCA assay. The elution ratio was calculated from the amount of BSA adsorbed on the supports and the amount of BSA eluted into the medium.

Different eluents were tested in order to evaluate which would provide better performance. In sequence the different elution solutions tested are listed:

- 0.05M  $\text{KH}_2\text{PO}_4$  + 1.5M KCl pH 7
- 0.05M  $\text{KH}_2\text{PO}_4$  + 1.5M KCl pH 9
- 0.05M Tris-HCl + 0.5M NaCl pH 8
- 0.05M Tris-HCl + 1 M NaCl pH 8
- 0.02M  $\text{Na}_2\text{HPO}_4/\text{NaH}_2\text{PO}_4$  + 2M NaCl pH 9



- ❑ 0.05M Tris-HCl + 0.5M NaSCN pH 8
- ❑ 0.05M Tris-HCl + 0.5M NaCl + 0.5M NaSCN pH 8

The elution carried out with saline solution of 0.05M  $\text{KH}_2\text{PO}_4$  containing 0.5 M KCl by absorbance readings at 280 nm has not detected the presence of protein even after an elution time of 4 hours.

The elution experiments performed using 0.02M  $\text{Na}_2\text{HPO}_4/\text{NaH}_2\text{PO}_4$  containing 2 M NaCl at pH 9.0, 0.05 M Tris-HCl buffer at pH 8.0 containing 0.5 M and 1 M NaCl had initially brought to encouraging results, showing increasing values of absorbance at 280 nm with increase the time. However, during support regeneration with a NaOH solution it was detected the presence of protein thus indicating that the elution was not complete.

The elution methods with addition of a competitor, 0.5 M NaSCN, showed better results. The strongest elution may be attributed to the disorganization of the structure of water by NaSCN [77].

In Figure 3.11 is reported the comparison of elution tests with the same membranes previously studied, CB-SartoE1, CB-SartoA4 and CB-RC.

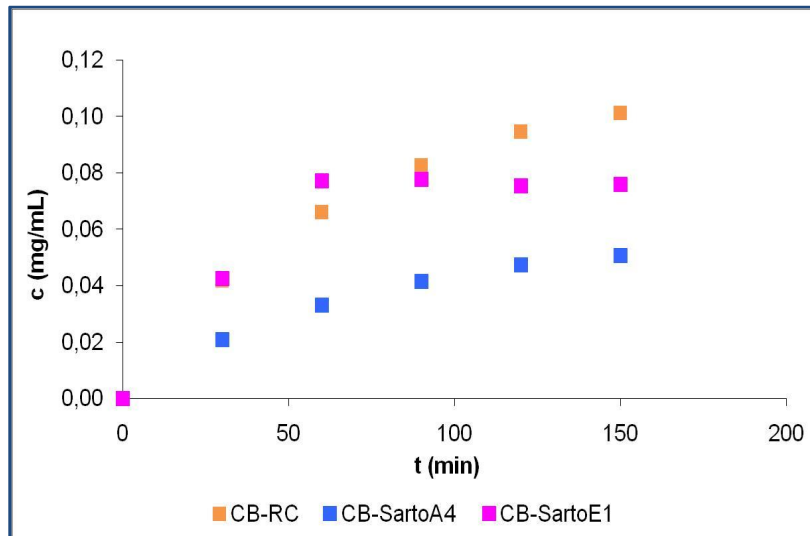


Figure 3.11 – Comparison of experimental data obtained from elution kinetic experiment with CB-SartoE1, CB-SartoA4 and CB-RC membranes.

In the elution stage the CB-SartoE1 and CB-SartoA4 membranes show the same behaviour, that is, about two hours to achieve steady state. The CB-RC membranes need more time than others to achieve the steady state. In addition, during elution step CB-SartoA4 membranes did not present the same performance of the CB-SartoE1 and CB-RC membranes. CB-RC and CB-SartoE1 membranes adsorbed more protein in specific manner than CB-SartoA4 membranes, although the analysis conditions and procedure were the same.

### 3.5.2. Dynamic experiments

After batch tests, the membranes were characterized in dynamic experiments using an ÄKTA Purifier 100 system, described in Section 2.4.2. At the beginning the affinity membranes, CB-SartoE1, CB-SartoE2, CB-SartoA4 and CB-RC were tested with pure BSA solutions to obtain breakthrough and elution profiles at different flow rates and concentration of BSA in the feed.

We modified the FPLC methods applied to columns with chromatographic resins for BSA purification. The developed methods resulted from the improvement of these procedures together a basic knowledge of membranes preparation and chemical reactions.

Dynamic tests were performed through the method created specifically for these membranes in Unicorn™ Software. The tests were conducted in a column with a membrane bed volume of 0.53 mL. BSA concentration in the feed solution ranged from 0.25 to 1.5 mg/mL. The flow rate in all process steps varied from 0.5 to 10 mL/min. Ten membranes with circular form and 2.6 cm of diameter were inserted into the cell, fig.3.12.



Figure 3.12 -Membrane module used in flow tests.

The dynamic experiments with the membranes were performed according to the procedure described in § 2.4.2.

The CB membranes were subjected to several cycles of experiments with the aim to determine their dynamic binding capacity as shown in Figure 3.13 where the comparison of the binding capacity of the membranes studied is reported.

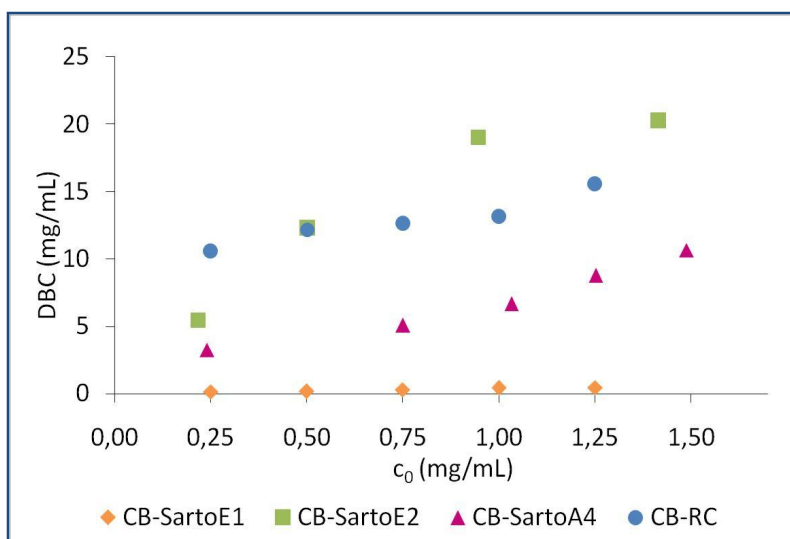


Figure 3.13- Dynamic binding capacity as function of protein feed concentration.

SartoE membranes with spacer arm, in this case ethylenediamine attached to the supports after rupture of the epoxy ring, named CB-SartoE2, showed a dynamic binding capacity of about 20 times higher than CB-SartoE1 membranes which showed nearly non adsorption of BSA. CB-SartoA4 membranes showed maximum value of dynamic capacity of approximately 11 mg/mL and CB-RC membranes presented values of binding capacity from 11 to 16 mg/mL.

The capacity values obtained with all membranes can be compared with the experimental data of the, membranes produced by Zeng and Ruckenstein, they used poly(ethersulfone) chitosan with adsorption capacity of 10.2 mg/mL [45].

The percentage of BSA eluted from the membranes is reported in Figure 3.14.

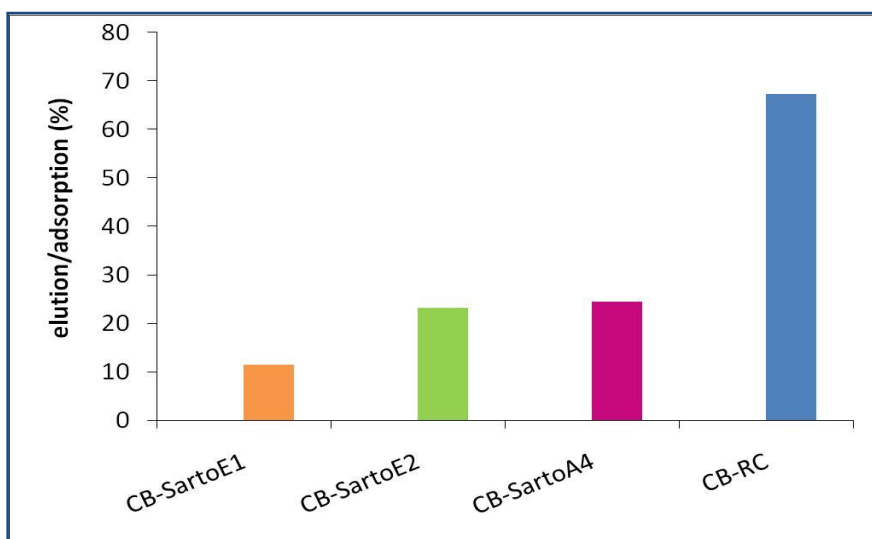


Figure 3.14 – BSA percentage eluted from different affinity membranes.

CB-SartoE2 membranes presented better results than CB-SartoE1, this fact ensures the efficiency of the space arm attachment. CB-SartoE1 membranes showed percent concentrations lower than 15%. In contrast with CB-SartoE2 membrane shaving values close to 25% and CB-SartoA4 membranes presented percentages of elution under 30%. CB-RC membranes are the membranes which higher BSA recovery, with values around 70% that can be compared with data from Wolman obtained CB poly(ethylene) hollow fibers membranes 50-77% [78].

An attempt to increase the ligand density of CB-RC membranes was performed by repeating the immobilization procedure. In this way, the process of CB immobilization was performed two times in sequence. The membranes with double immobilization were compared with the CB-RC affinity membranes. A comparison of the effect of double immobilization is shown in Figure 3.15 were two complete chromatographic cycles with pure BSA are reported.

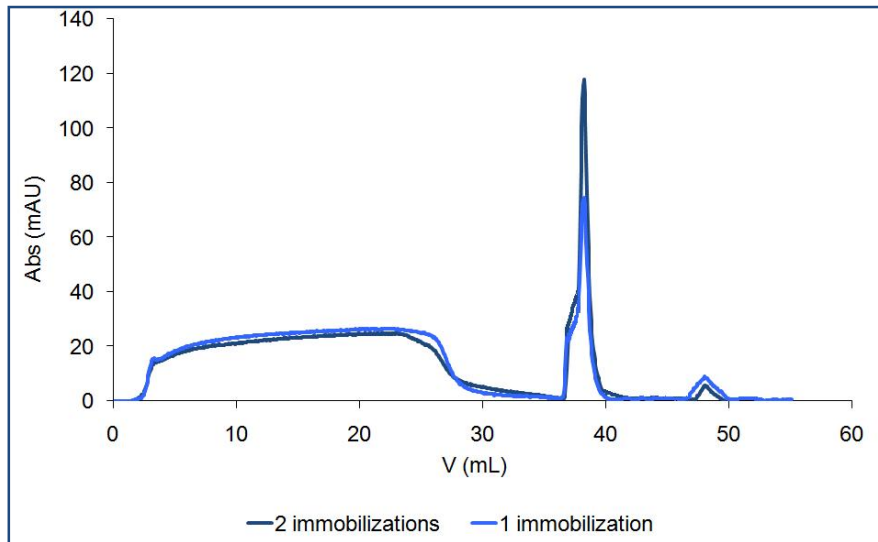


Figure 3.15- Comparison between CB-RC affinity membranes with 1 e 2 CB immobilizations. Operating conditions: flow rate of 1 mL/min and BSA feed concentration of 0.25 mg/mL.

The curves of the complete chromatographic cycle for these experiments present the same profile with similar adsorption values, while the elution peak is higher for the membranes with double immobilization.

The membranes were tested at different values of BSA concentration in the feed and the results in terms of dynamic binding capacity are shown in Figure 3.16.

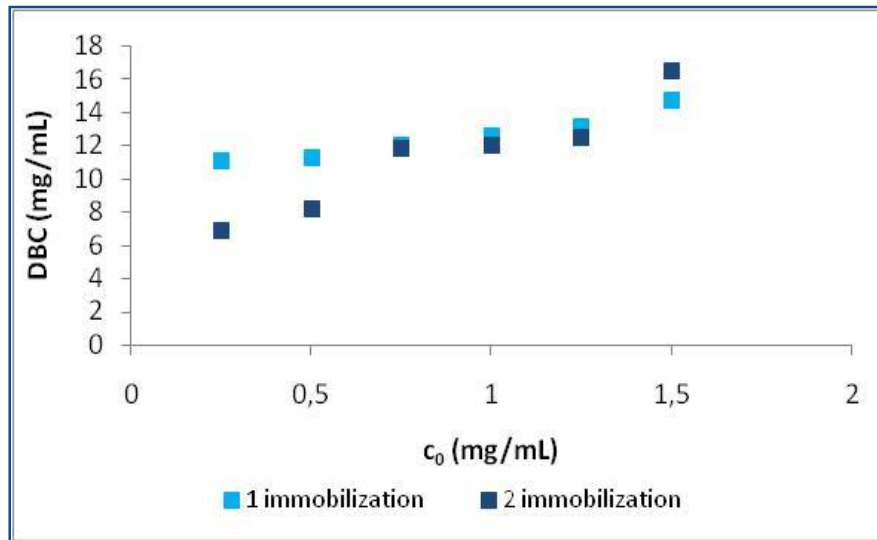


Figure 3.16–Comparison of DBC on membranes with one and two ligand immobilizations at flow rate of 0.5 mL/min.

The effect of flow rate on double immobilization is reported in Figure 3.17 in which dynamic binding capacity measured at a constant of concentration of BSA in the feed are reported.

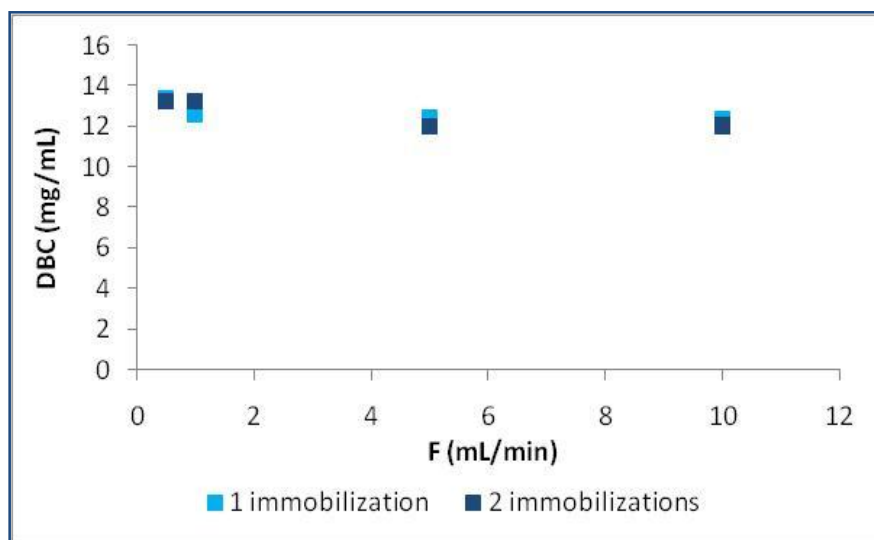


Figure 3.17 – The influence of the flow rate on binding capacity for membranes with one and two CB immobilizations with BSA feed concentration of 1 mg/mL.

It is evident that the dynamic binding capacities are comparable and the inclusion of this new step in the protocol it is not beneficial since it does not increase the BSA membrane capacity.

According to the results obtained so far, CB-RC affinity membranes with a single CB immobilization are the membrane that give better performances. For this reason they were chosen for the comparison with the different chromatographic supports, resin and monoliths, and they performance have been investigated in detail in the following.

Complete chromatographic cycles were performed at different flow rates, namely 0.5, 1, 5 and 10 mL/min, and at different values of BSA concentration in the feed, namely 0.25, 0.5, 1.0 and 1.5 mg/mL. The adsorption isotherms for CB-RC membranes are presented in Figure 3.18.

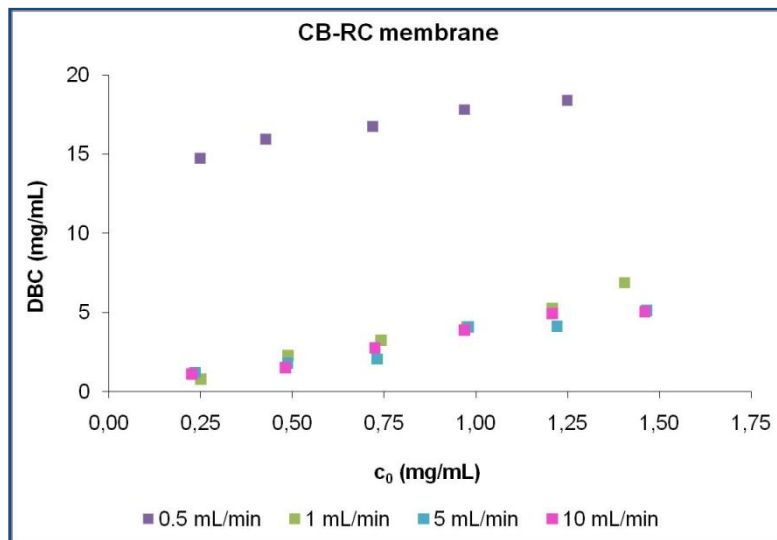


Figure 3.18 – Dynamic binding capacity at 100% breakthrough as function of feed protein concentration at flow rate of 0.5 to 10.0 mL/min.

The results obtained at 0.5 mL/min show values of dynamic binding capacity higher than the ones obtained at higher flow rates. It is possible to explain the differences in the values of binding capacity for CB-RC membranes



at flow rates less than 1 mL/min with a possible change in the structure of the membranes, which might be caused by the process of ligand immobilization. To verify this hypothesis the permeability of binding buffer through unmodified and modified, CB-RC, membranes were performed and the results are reported in Figure 3.19.

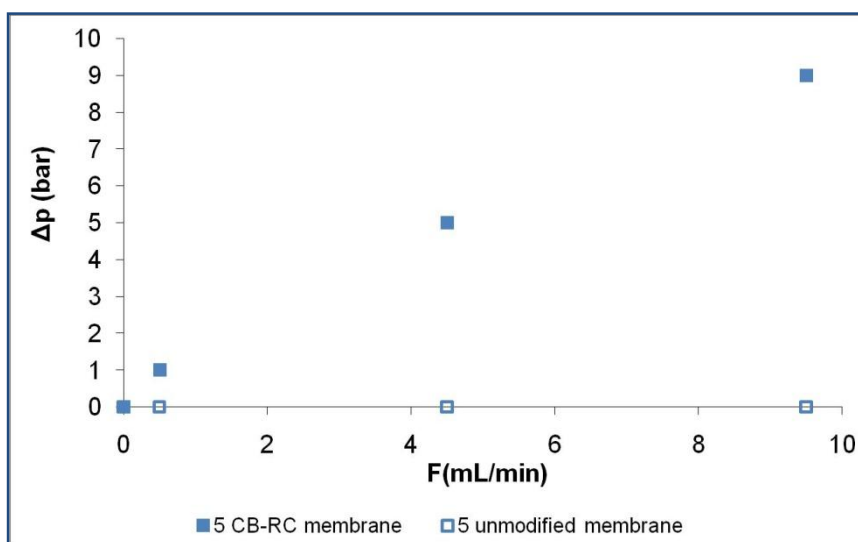


Figure 3.19–Pressure drop vs flow rate for experiment with 0.05M Tris-HCl + 0.05M NaCl, pH 8 through a stack of 5 unmodified and CB-RC membranes.

The unmodified membranes show no significant variations, resulting in values close to zero, while the modified membranes present an increase of pressure drop with the flow rate. Ruckenstein and Zeng [69] investigated the permeability of the binding buffer through ten macroporous Cibacron Blue F3GA – chitosan membranes under different pressure drops. According to these workers, the swelling of the membranes is diminished and its compressibility decrease because the dye is immobilized. By these conditions, the relationship between flow rate and pressure drop is linear at low pressure studied.

The influence of flow rate on the binding capacity was studied by increasing the flow from 1 to 10 mL/min as reported in Figure 3.20.

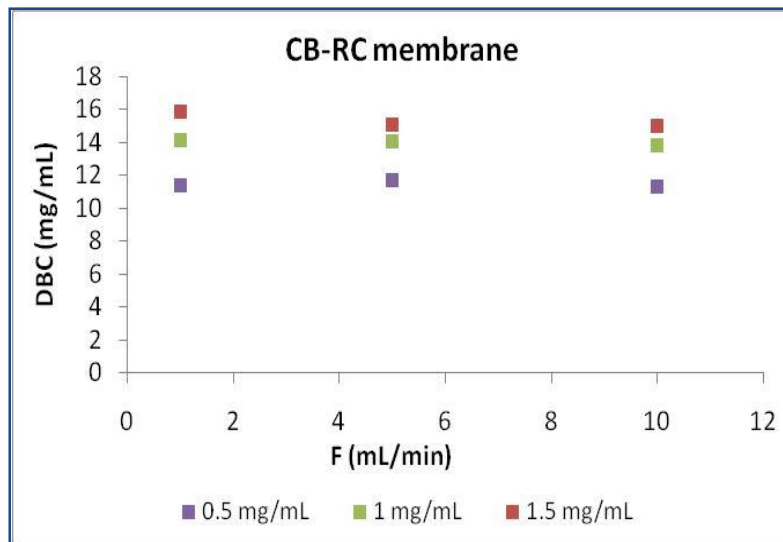


Figure 3.20 – Dynamic binding capacity at 100% breakthrough as function of flow rate at feed protein concentrations of 0.25 to 1.5 mg/mL for CB-RC membranes.

The affinity CB-membranes used in the tests show values of adsorption capacity are independent from the flow in the range of flow rate and concentration investigated.

Since bioproducts have generally a high added value, the purification process is stopped in the early stages of breakthrough in order not to lose valuable product. This point, called the point of breakthrough, BTP, is the point in which the concentration in outlet of the column correspond to a fraction, usually 10%, of the feed concentration.

In this thesis experiments were carried out at 10% breakthrough: pure BSA solutions were loaded until the maximum breakthrough curve, BTC, height was 10% of the saturation height. All other experimental conditions and methods were the same used for experiments at saturation.

The results of the experiments realized at  $DBC_{10\%}$  as a function of initial feed protein solution are presented in fig.3.21.

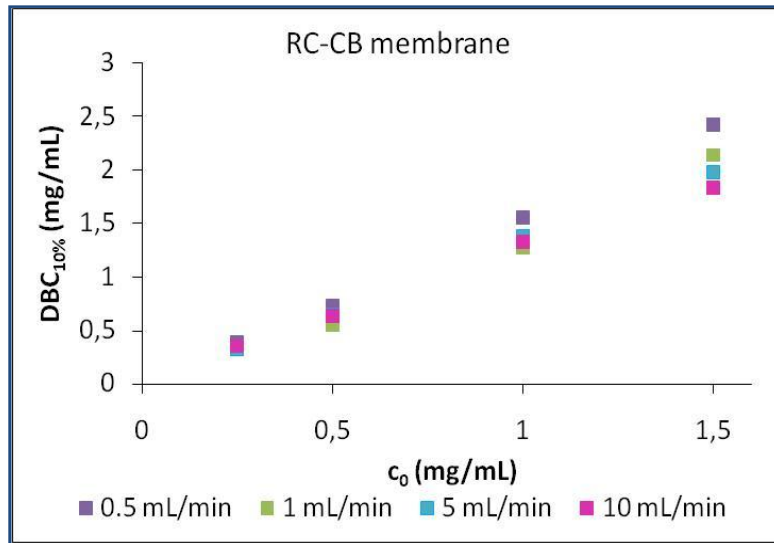


Figure 3.21 - Dynamic binding capacity at 10% breakthrough as a function of initial feed protein solution.

The results show the influence of the flow rate on dynamic binding capacity, in particular, the dynamic binding capacity at 10% BT increases with the protein concentration in the feed.

The effects of flow rate on dynamic binding capacity are presented in Figure 3.22, as it can be observed the  $DBC_{10\%}$  values are independent from the flow rate in the range of flow rates and concentration studied.

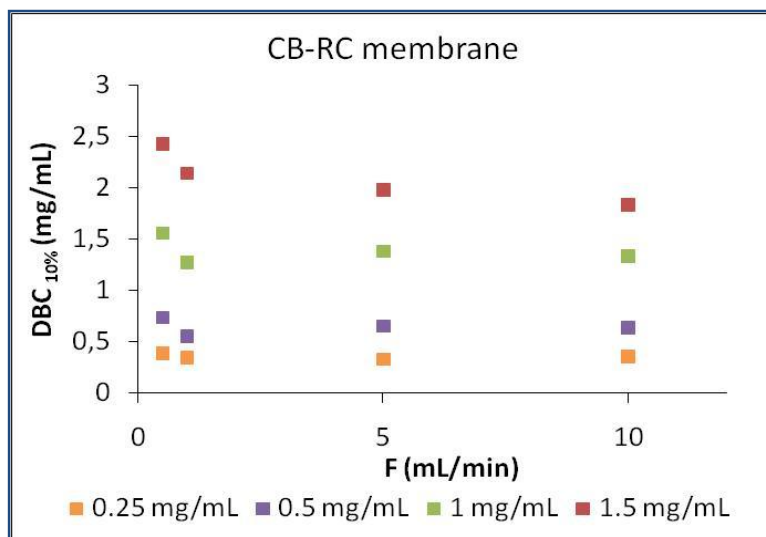


Figure 3.22 - Dynamic binding capacity at 10% breakthrough as a function of flow rate.

## *Affinity Monoliths*

### **Experimental procedures and results**

#### **4.1. CB immobilization on CIM disks**

The immobilization of CB on monoliths was performed in a flow system especially constructed for this process illustrated in Figure 4.1.



Figure 4.1 – Plexiglas module for CB immobilization in a single disk monolith.

The module is made of a synthetic polymer of methyl methacrylate, called poly(methyl methacrylate). It has been sold under a variety of trade names, including Plexiglas. Plexiglas is a lightweight material having, high

impact resistance, good chemical resistance and excellent thermoformability. This material is a compatible and non-interactive with the reagents used.

Inside the module there are plastic grids at the top and bottom of the reserved space for the monolithic disk, which are composed by polyethylene, Figure 4.2.

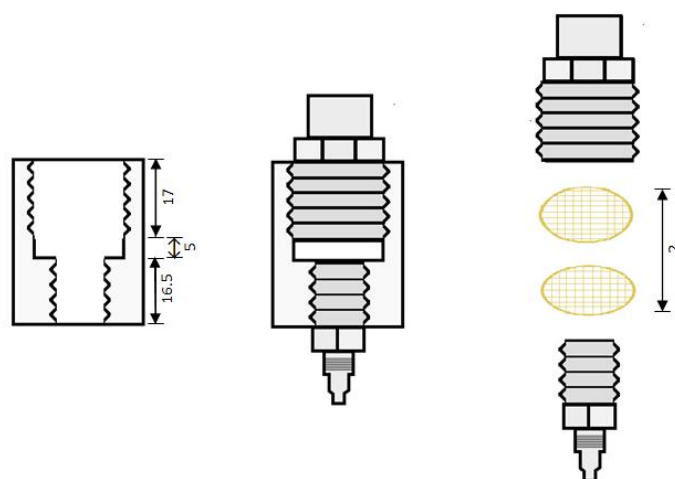


Figure 4.2 –Scheme of the module for immobilization on monoliths.

The module was connected to a peristaltic pump (Minipuls 3/Gilson), and the immobilization on the monolithic bed was performed by recirculation. This module was fixed on a thermostatic water bath (GTR 2000 LLX/ISCO) with temperature control, the process scheme is illustrated in Figure 4.3.

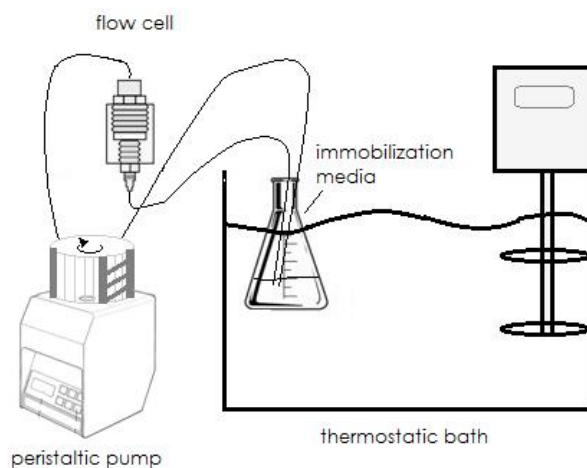


Figure 4.3 – Experimental set-up used for CB immobilizations on monoliths.

Before ligand immobilization the monolith was thoroughly washed with 50 mL of water.

### Protocol 1

With CIM EDA disks, the chemical modification of the copolymer GMA-EDMA, matrix of the monoliths, was carried out using the reaction of ethylenediamine with the epoxide groups of the copolymer. For this reason, the reactive amino groups are available for the covalent immobilization of CB, as shown in the reaction scheme of Figure 4.4.

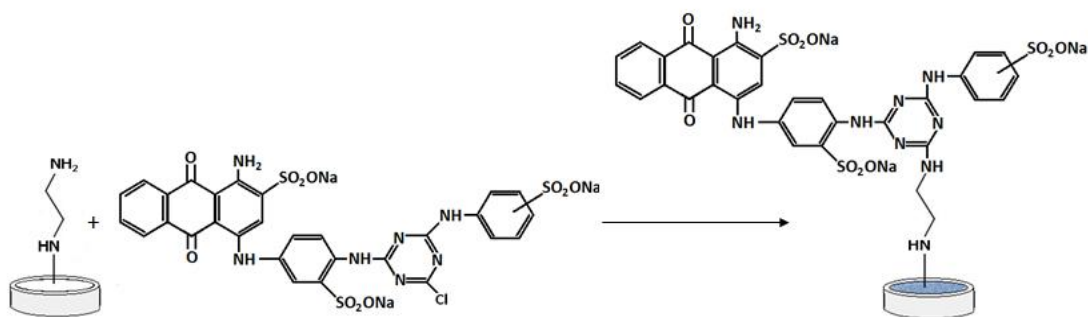


Figure 4.4 – Immobilization reaction of Cibacron Blue F3GA on EDA monoliths.

0.25 g of Cibacron Blue F3GA were dissolved in a solution of 37.5 mL deionized water and 12.5 mL methanol followed by the addition of 10 mL of 20 % (w/v) NaCl. The solution was pumped into the channel at a flow rate of 0.5 mL/min at 60 °C. After one hour, 6 mL of 25% (w/v) Na<sub>2</sub>CO<sub>3</sub> were added to the solution and temperature increased to 80 °C. The reaction was carried out for 3h. The modified monolith was finally washed with water.

## Protocol 2

CB immobilization on CIM Epoxy Disks, called Epoxy, was carried out in the same recirculation system described previously.

50 mL of 5 mg/mL Cibacron Blue F3GA solution containing 1 M NaOH was pumped through the column under recirculation at 80 °C for 3h.

Under these experimental conditions, a chemical reaction took place between the group of the CB containing chloride and the epoxide group of the monolith, as shown in Figure 4.5. The adsorption was followed by monitoring the decrease in UV absorbance at 280 nm.

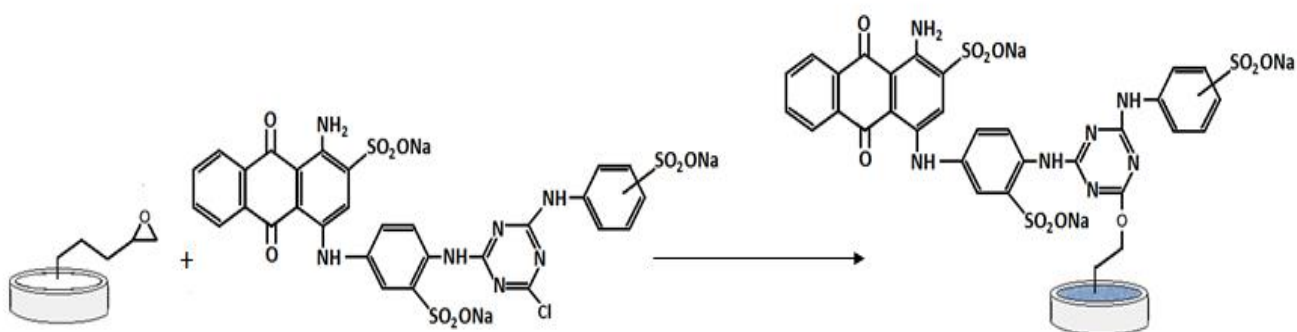


Figure 4.5 - Immobilization reaction of Cibacron Blue F3GA on Epoxy monoliths.

After incubation, the CB-Epoxy monolith was washed with distilled water and 20% methanol aqueous solution until all the physically adsorbed CB was removed.

The modified monoliths, both monolith CB-EDA and CB-Epoxy, were then stored at 4 °C with 0.02% sodium azide to prevent microbial contamination.

Figure 4.6 shows a summary of the process applied to immobilization of the ligand on monoliths with two types of activation.



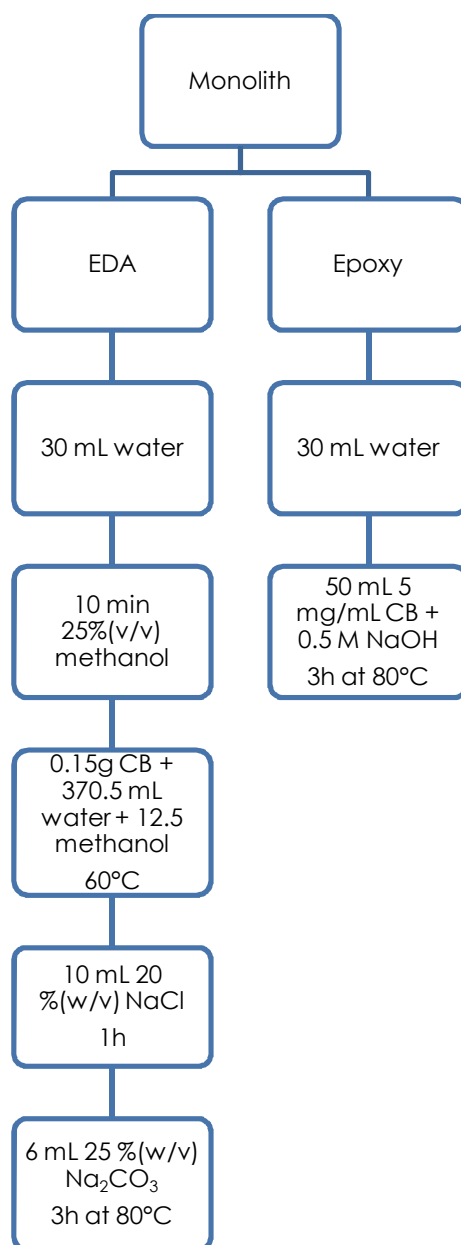


Figure 4.6–Scheme of ligand immobilization on monoliths.

#### **4.2. CB-monoliths characterization through the separation of pure BSA solution in batch system**

The CB monoliths were initially characterized in batch with pure protein solutions at different concentrations, from 0.25 to 1.5 mg/mL. In each test a single monolith was used and the process was realized at room temperature. The experimental procedure for the separation was conducted according to the following subsequent steps.

4 mL of pure BSA solution in 0.05 M phosphate buffer pH 7.4 containing 0.1 M NaCl was loaded in a beaker with one CB monolith. Samples of the liquid phase were analysed via UV adsorption at 280 nm, at regular intervals, to monitor the protein concentration with time. When the steady state was finally achieved the adsorption step was considered concluded.

At the end of the adsorption stage, the monoliths were extracted from the protein solution and washed with 0.05 M phosphate buffer pH 7.4 containing 0.1 M NaCl for one hour to remove the protein not specifically bound to the active sites.

The last step is the elution of the adsorbed protein from the support. During this stage, the monolith was kept for about 2 hours in a beaker containing the elution buffer, 0.05 M tris-HCl buffer solution pH 8 containing 50 mM NaCl and 0.5 M NaSCN. Also in this step the protein in solution was measured via A<sub>280</sub>.

All steps were conducted keeping the beaker in gentle agitation in shaker platform at room temperature.

### 4.3. Dynamic experiments

The aim of batch experiments was to select the monolith which obtained better performance, but these tests showed no significant differences between the two CB affinity monoliths. Flow tests were conducted in order to select the monolith that provide the best characteristics.

Dynamic binding experiments were performed using an Äkta Purifier 100 system (GE Amersham Pharmacia Biotech) as already described for membranes and described in section 2.4.2.. All buffers were pre-filtered through a 0.45  $\mu\text{m}$  cellulose membrane (Sartorius Stedim Biotech) using a vacuum system. The monoliths were tested using a commercial CIM<sup>®</sup> module, shown in Figure 4.7.

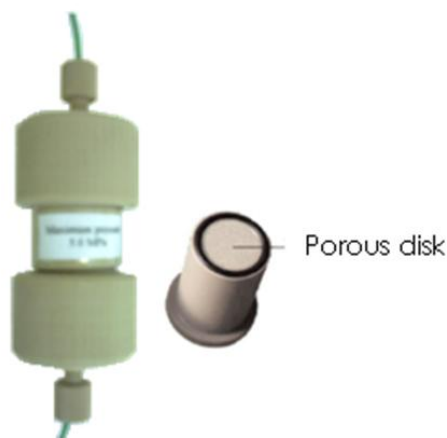


Figure 4.7 –CIM disk holder.

After equilibration with 25 mM phosphate buffer containing 100 mM NaCl pH 7.4, 10 mL of BSA in equilibration buffer, with concentration from 0.25 to 1.5 mg/mL, were loaded at a flow rates from 1 to 5 mL/min. The monolith was washed with 5 mL of 0.05 M phosphate buffer pH 7.4 containing 100 mM NaCl. Elution was performed with 5 mL of 0.05 M tris-HCl buffer solution pH 8 containing 0.05 M NaCl and 0.5 M NaSCN for 3 h.

The dynamic binding capacity at saturation, DBC, and the dynamic binding capacity at ten per cent breakthrough,  $DBC_{10\%}$ , were calculated from there levant breakthrough curves.

Complete chromatographic cycles of pure BSA solutions at different concentrations at a flow rate of 1 mL/min for CB-Epoxy monoliths are reported in Figure 4.8.

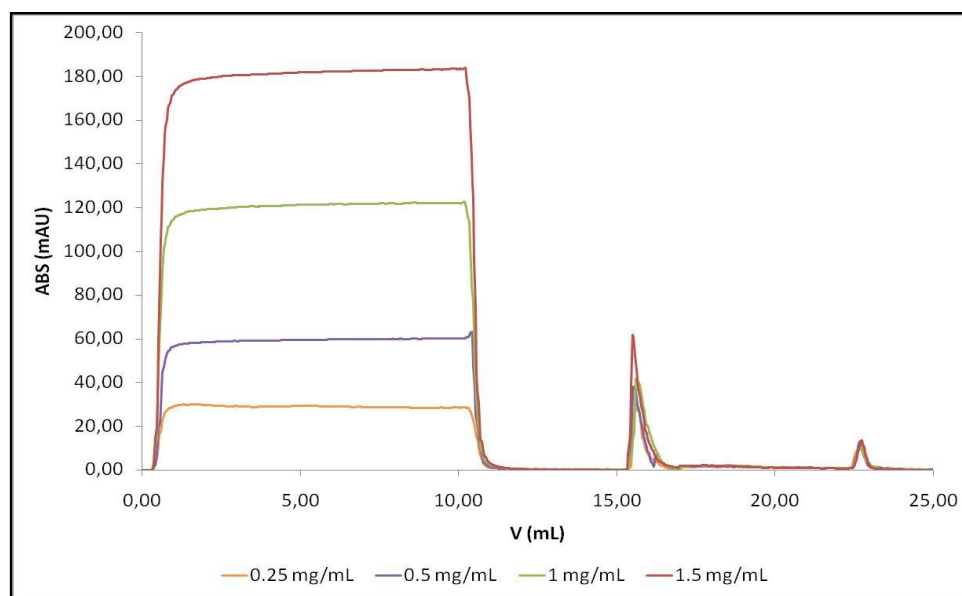


Figure 4.8 – Effect of BSA feed concentration on chromatographic cycles through a CB-Epoxy monoliths at constant flow rate of 1mL/min.

## 4.4. Results and Discussion

### 4.4.1. Ligand immobilization

To verify the ligand immobilization on monoliths, a visual inspection, that is, the color of the affinity monolith, and absorbance measurement at 610 nm were utilized.

### 4.4.2. Batch tests

Kinetic experiments with pure BSA solutions were performed in batch for an initial characterization of the affinity monoliths.

The behaviour of solution concentration observed during the adsorption and elution steps is presented in Figure 4.9.

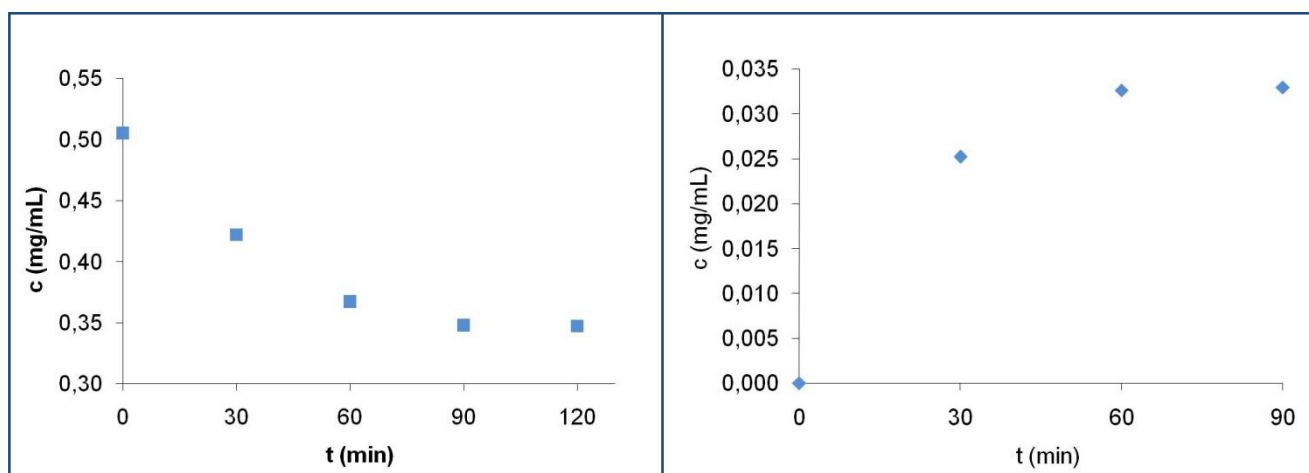


Figure 4.9 – BSA concentration with time in adsorption and elution tests with CB-EDA monoliths.

These experiments provide information about the quantity of protein adsorbed on the support and the amount of protein recovered that can be easily calculated from the mass balance.

A comparison of adsorption kinetic experiments between CB- EDA and CB-Epoxy affinity monoliths is reported in Figure 4.10 while in Figure 4.11 is shown the comparison of the kinetic experiment of elution. In particular, the tests were conducted at the same operating conditions, area of monoliths of 1.13 cm<sup>2</sup>, initial BSA concentration of 1 mg/mL, duration of the adsorption step of 2 hours.

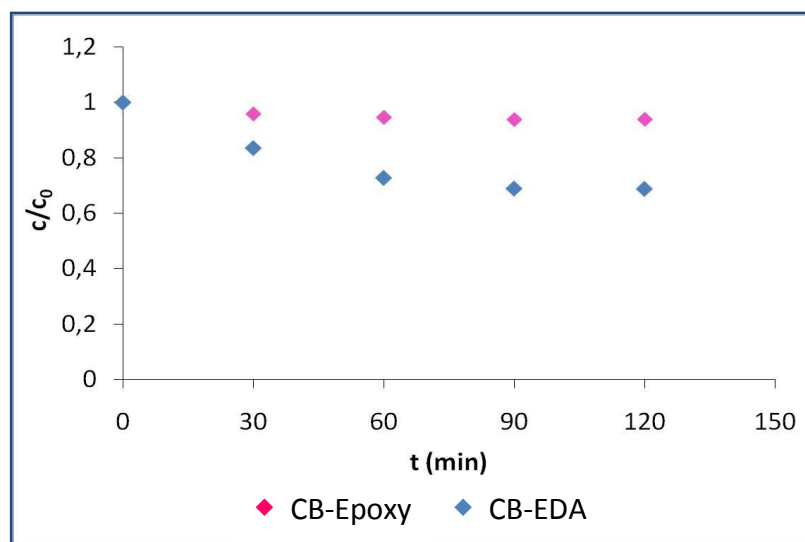


Figure 4.10 - Experimental data obtained of adsorption steps with CB-EDA and CB-Epoxy monolithic disks.

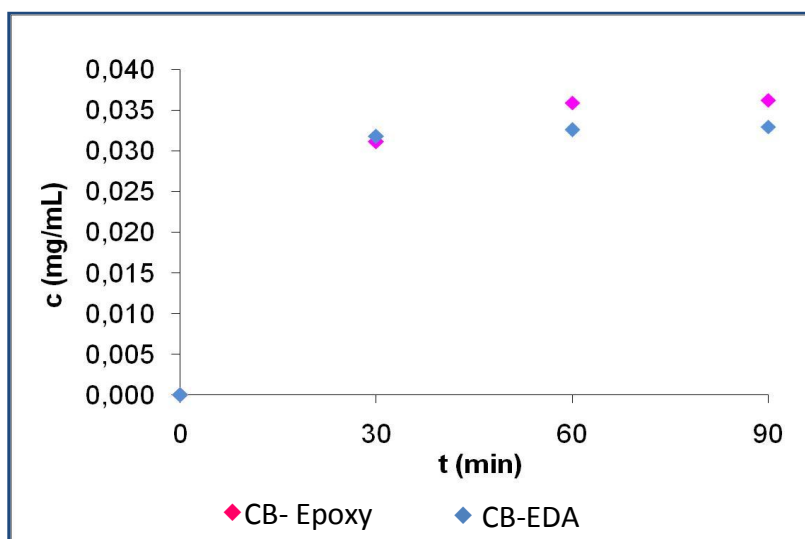


Figure 4.11 - Experimental data obtained of elution with monoliths CB-EDA and CB-Epoxy.

From the analysis of experimental data, obtained through the adsorption kinetics tests performed, we highlight different behaviors of the types of monoliths tested. In particular, CB-Epoxy monolith reaches the condition of steady state in about 30 min while the CB-EDA monolith instead, reaches equilibrium after 90 min of adsorption. That is, the monolith Epoxy is saturated faster than EDA monolith.

The elution curves show similar results and it can be observed that, in both cases, elution reaches the steady state in a time of about 1 hour. The difference in the adsorption curves indicate that the CB-EDA monolith adsorbs more protein than the CB-Epoxy monolith, but the two monoliths have a similar elution behavior. A possible reason could be the difference in the amount of protein adsorbed in a non-specific way as it is confirmed by the amount of protein removed in the washing step, as confirmed by the values reported in Table 4.2.

Table 4.2 – Mass balance of the batch tests with monoliths.

| Monolith | $m_0$ (mg) | $M_{ads}(mg)$ | $M_{wash}(mg)$ | $M_{elu}(mg)$ |
|----------|------------|---------------|----------------|---------------|
| EDA      | 2.5264     | 0.7897        | 0.6223         | 0.1649        |
| Epoxy    | 2.0318     | 0.1278        | 0.0029         | 0.1227        |

#### 4.4.3. Dynamic experiments

The CB affinity monoliths were characterized in terms of dynamic binding capacity at saturation and dynamic binding capacity at 10% breakthrough ( $DBC_{10\%}$ ) using solution of pure protein.

The experimental values of dynamic binding capacity at saturation are reported in Figure 4.12 and the ratio of BSA recovered with elution tests are reported in Figure 4.13.

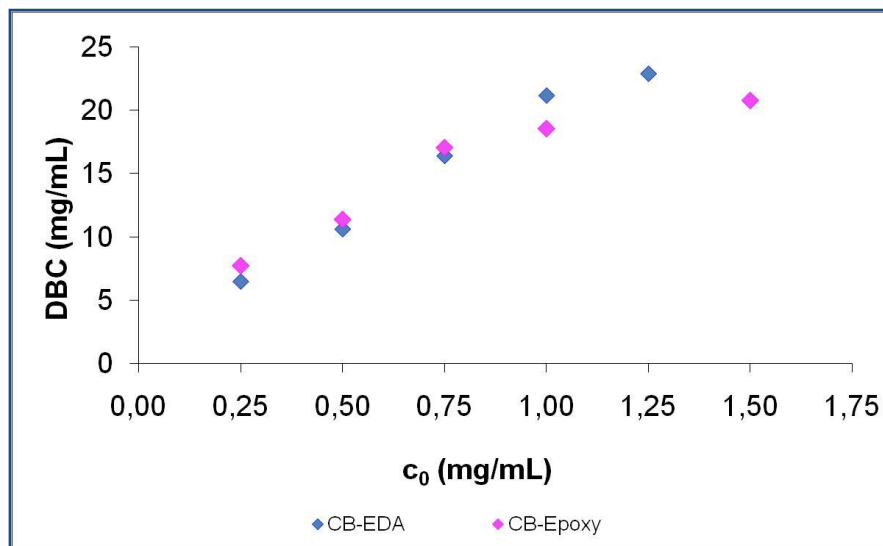


Figure 4.12–Dynamic binding capacity of CB-EDA and CB-Epoxy monoliths in experiments performed at a constant flow rate of 1mL/min.



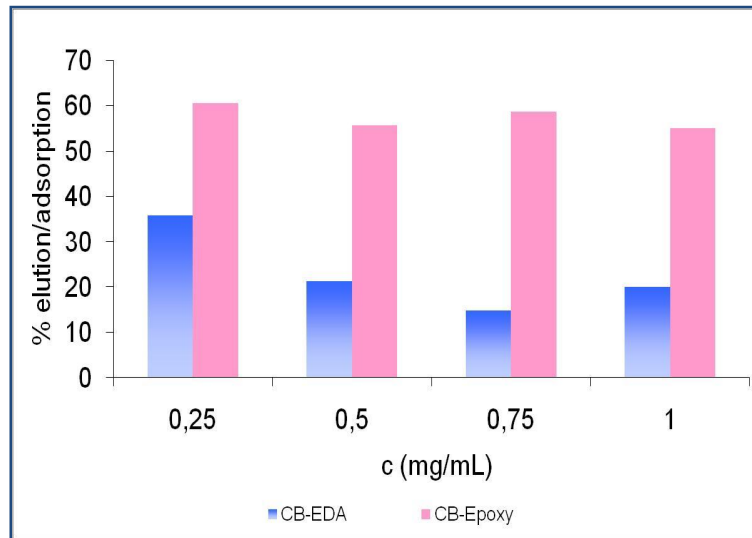


Figure 4.13–Recovery of BSA from CB-EDA and CB-Epoxy monoliths.

The first graph shows the adsorption isotherms as a function of protein feed concentration. Monoliths show a similar behavior, that is, similar dynamic binding capacity (DBC) values. However, the percentage of protein eluted for the CB-Epoxy monolith is higher than the values obtained with CB-EDA monolith as it can be observed from the data reported in Figure 4.13.

Therefore, the CB-Epoxy affinity monoliths are the ones that offer better performances and will be characterized in more detail in order to be compared with the other chromatographic supports, membranes and resin.

Tests with the CB-Epoxy monoliths were performed at flow rates of 1, 2.5, 4 and 5 mL/min and at feed protein concentration of 0.25, 0.5, 1.0 and 1.5 mg/mL. The dynamic binding capacity of the CB-Epoxy monolith as a function of BSA feed concentration are presented in Figure 4.14.

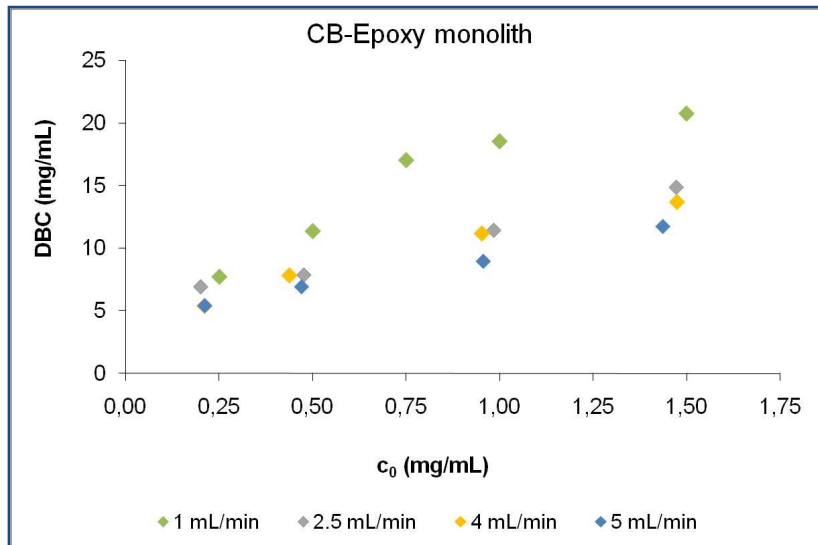


Figure 4.14 – Dynamic binding capacity of BSA at different flow rates.

The dynamic binding capacity of CB-Epoxy monoliths as function of flow rate are showed in the figure 4.15.

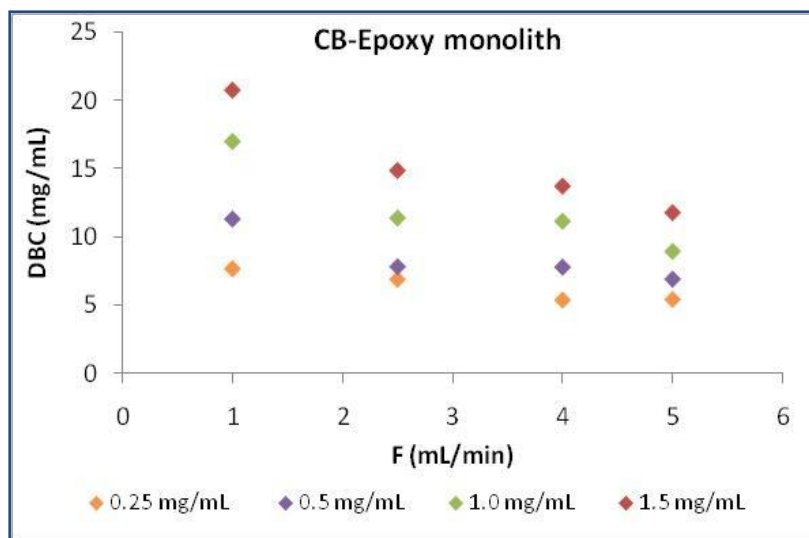


Figure 4.15–Effect of flow rate on dynamic binding capacity of BSA at different flow rates.

From the data it can be observed that the dynamic binding capacity is reduced with the increase of the flow rate, indicating a dependence of the binding capacity with respect to flow rate for the monoliths studied.

As for membranes, experiments were performed at 10% breakthrough, results of these experiments are shown in Figure 4.16 where  $DBC_{10\%}$  as a function of initial feed protein solution are reported.

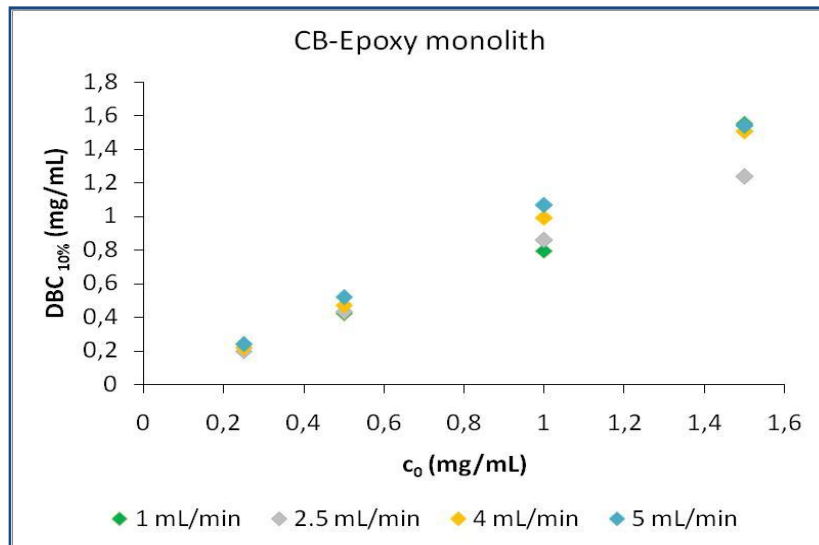


Figure 4.16 - Dynamic binding capacity at 10% breakthrough as a function of initial feed protein solution.

It is quite evident the strong influence of concentration on the dynamic binding capacity at 10% BTC.

In addition, it was studied the influence of the flow rate on  $DBC_{10\%}$ . The results are presented in Figure 4.17.

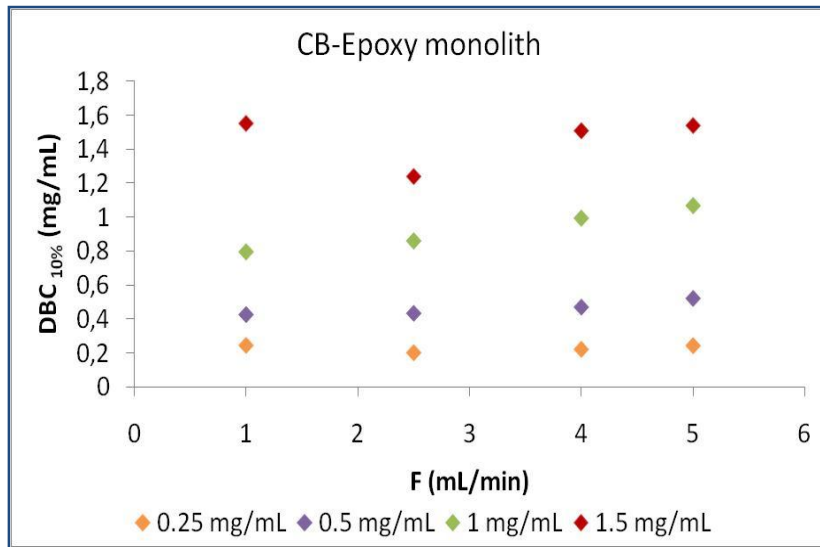


Figure 4.17- The influence of flow rate on dynamic binding capacity at 10% breakthrough.

Experimental values of dynamic binding capacity at 10% BTC as a function of the flow rate are plotted in Figure 4.17. These results reveal that the variation of flow rate shows little impact on dynamic binding capacity indicating that the convection is the dominant transport phenomena.

## Comparison of the affinity supports

### 5.1. Introduction

The purpose of this work is to compare side by side the performance of affinity membranes and monoliths with a packed column in terms of binding capacity at saturation, dynamic binding capacity at 10% breakthrough and productivity using BSA as a target protein.

### 5.2. Dynamic binding capacity

The experiments with CB-RC membranes module were performed at 0.5, 1.0, 5.0 and 10.0 mL/min. The maximum flow rate used was 10 mL/min due the weak resistance of the membranes to higher flows. The same kind of experiments realized with CB-Epoxy monoliths were performed at flow rates of 1.0, 2.5, 4.0 and 5.0 mL/min, according to the indications of manufacturer, in fact the working flow rate indicated is 2 – 4 mL/min. While, the experiments realized with resin, previously characterized [79], were performed at 1.28, 1.92, 2.57 and 3.21 mL/min.

Due to the different formats of the supports the appropriate parameter to consider for a proper comparison is the superficial velocity defined as:

$$u = \frac{F}{\pi r^2} \quad (5.1)$$

where  $F$  indicates the volumetric flow rate and  $r$  the radius of the chromatographic column. The superficial velocities corresponding to the flow rates at which the supports were tested and calculated with eq. 5.1 are shown in Table 5.1.

Table 5.1 – Flow rates and corresponding superficial velocities for the studied supports.

| Resin         |               | Membranes     |               | Monolith      |               |
|---------------|---------------|---------------|---------------|---------------|---------------|
| F<br>(mL/min) | $u$<br>(cm/h) | F<br>(mL/min) | $u$<br>(cm/h) | F<br>(mL/min) | $u$<br>(cm/h) |
| 1.28          | 200           | 0.50          | 7.89          | 1.00          | 53.06         |
| 1.92          | 300           | 1.00          | 15.78         | 2.50          | 132.63        |
| 2.57          | 400           | 5.00          | 78.92         | 4.00          | 212.21        |
| 3.21          | 500           | 10.00         | 157.84        | 5.00          | 265.26        |

### 5.2.1. Dynamic experiments with pure BSA solutions loaded until saturation

CB-RC membranes and CB-Epoxy monoliths were characterized in terms of binding capacity at saturation (DBC) and dynamic binding capacity at 10% breakthrough (DBC<sub>10%</sub>) using solutions of pure BSA in the equilibration buffer. In this work, the binding capacity at saturation is indicated as dynamic binding capacity at 100% breakthrough (DBC<sub>100%</sub>) for the sake of consistency with the

symbol used for indicating the dynamic binding capacity at 10% breakthrough, even if it is not technically a dynamic binding capacity, since it is not influenced by the flow rate.

Experiments were performed at different flow rates in order to study the influence of flow rate on the dynamic binding capacity.

The protocol, reported in table 5.2, was the same for all the flow rates inspected.

Table 5.2 - Experimental protocol of the chromatographic runs with BSA solutions loaded up to complete saturation of the supports.

| <b>Chromatographic step</b> | <b>Buffer</b>                                      | <b>V (mL)</b> |
|-----------------------------|--|---------------|
| <i>Resin</i>                |  |               |
| Equilibration               | 0.1 M Tris-HCl pH8                                 | 10            |
| Loading                     | BSA solution                                       | Varies        |
| Washing                     | 0.1 M Tris-HCl pH8                                 | 25            |
| Elution                     | 0.05 M KH <sub>2</sub> PO <sub>4</sub> + 1.5 M KCl | 10            |
| Regeneration                | -  | -             |
| <i>Membranes</i>            |  |               |
| Equilibration               | 0.05 M Tris-HCl + 0.05 M NaCl pH 8                 | 10            |
| Loading                     | BSA solution                                       | 10            |
| Washing                     | 0.05 M Tris-HCl + 0.05 M NaCl pH 8                 | 10            |
| Elution                     | 0.05 M Tris-HCl + 0.05 M NaCl + 0.5 M NaSCN pH 8   | 10            |
| Regeneration                | 70 % ethanol                                       | 10            |
| <i>Monolith</i>             |  |               |
| Equilibration               | 0.05 M Tris-HCl + 0.05 M NaCl pH 8                 | 10            |
| Loading                     | BSA solution                                       | 10            |
| Washing                     | 0.05 M Tris-HCl + 0.05 M NaCl pH 8                 | 5             |
| Elution                     | 0.05 M Tris-HCl + 0.05 M NaCl + 0.5 M NaSCN pH 8   | 5             |
| Regeneration                | 70 % ethanol                                       | 10            |

Experimental data were elaborated with the procedure described in section 2.4.2.2.

The  $DBC_{100\%}$  as a function of the concentration of feed protein solution is reported in figures 5.1, 5.2 and 5.3 for resin, membranes and monolith.

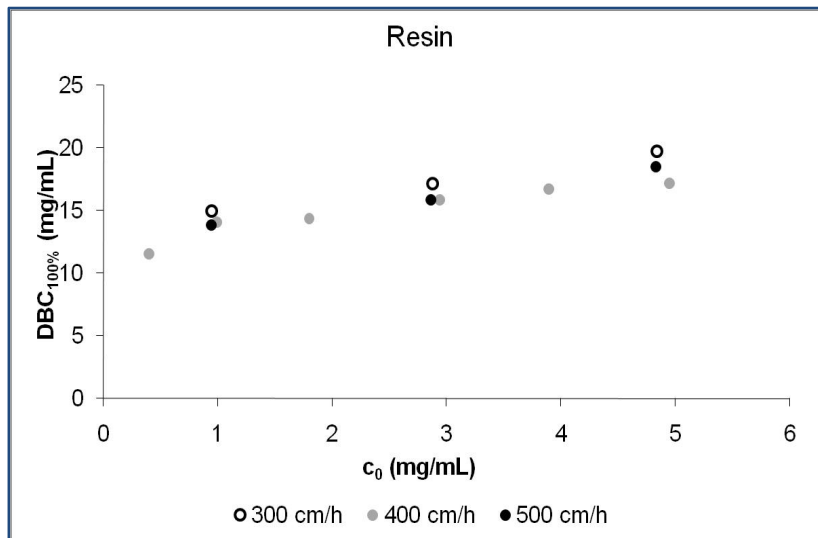


Figure 5.1 -  $DBC_{100\%}$  as function of feed protein concentration at superficial velocity of 300 to 500 cm/h for resin.

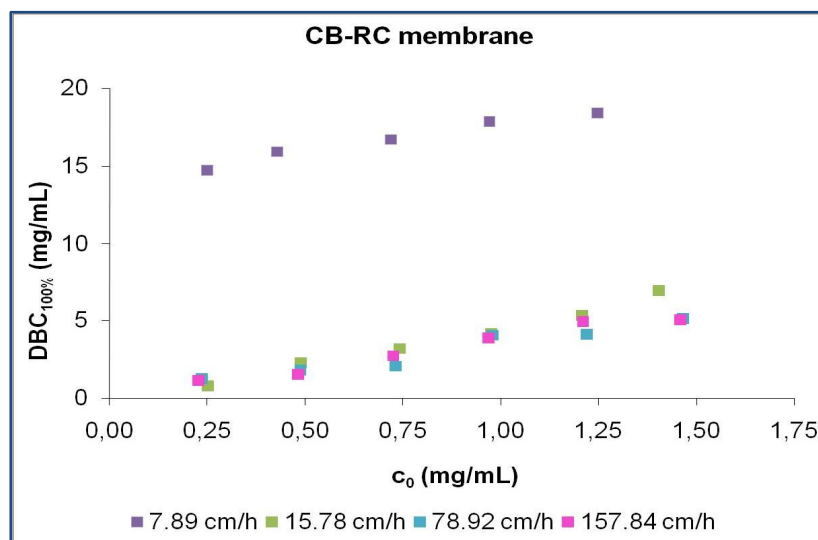


Figure 5.2 -  $DBC_{100\%}$  as function of feed protein concentration at superficial velocity of 7.89 to 157.84 cm/h for membrane.



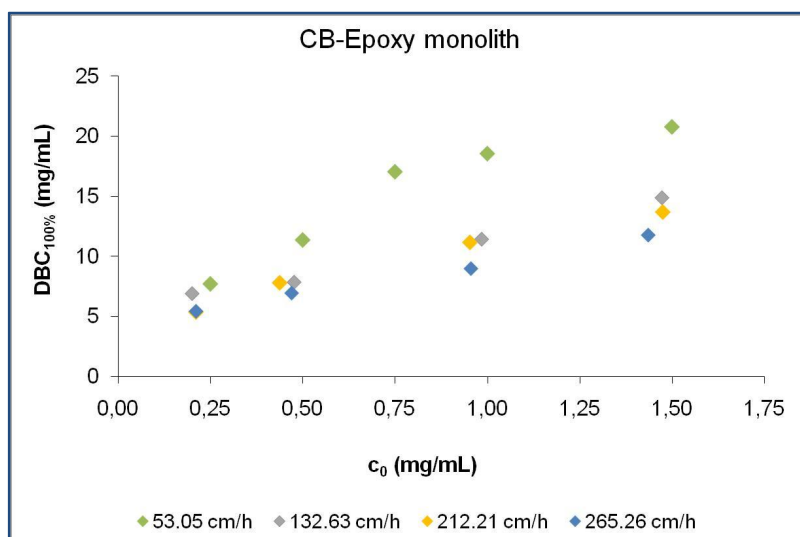


Figure 5.3 -  $DBC_{100\%}$  as function of feed protein concentration at superficial velocity of 53.05 to 265.26 cm/h for monoliths.

The results of the tests with the column and membranes, apart from the experiments at 15.78 cm/h, showed no influence of flow rate in isotherm construction. The discrepancy on membrane behavior at 15.78 cm/h has been already described in §3.5.2 and the behavior of monoliths can be also explained with a possible change in the pore structure, which might be caused by the process of immobilization of the ligand.

The influence of flow on dynamic binding capacity was examined by increasing the superficial velocity from 200 to 500 cm/h for resin, from 15.78 to 157.84 cm/h for membranes and from 53.05 to 265.26 cm/h for monoliths. The results of these experiments at different values of BSA in the feed are shown in Figures 5.4, 5.5 and 5.6 for resin, membranes and monoliths respectively.

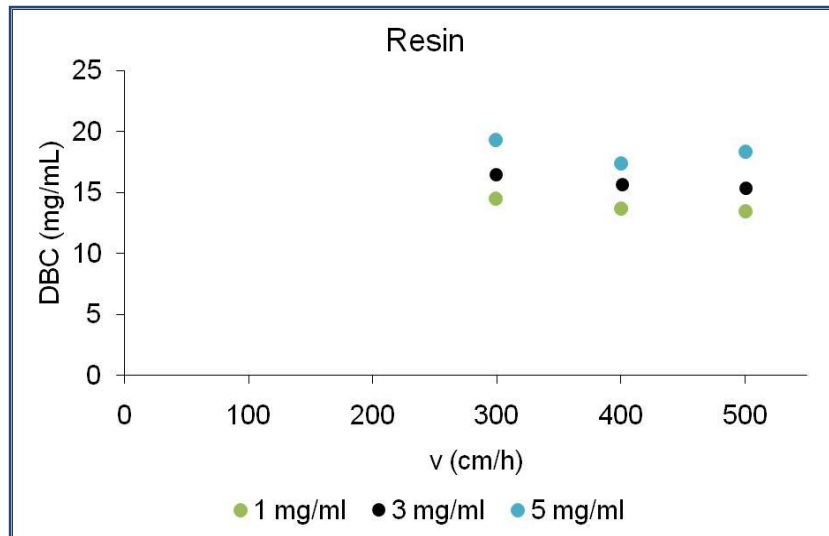


Figure 5.4 -  $DBC_{100\%}$  as function of superficial velocity at feed protein concentrations of 1 to 5 mg/mL for resin.

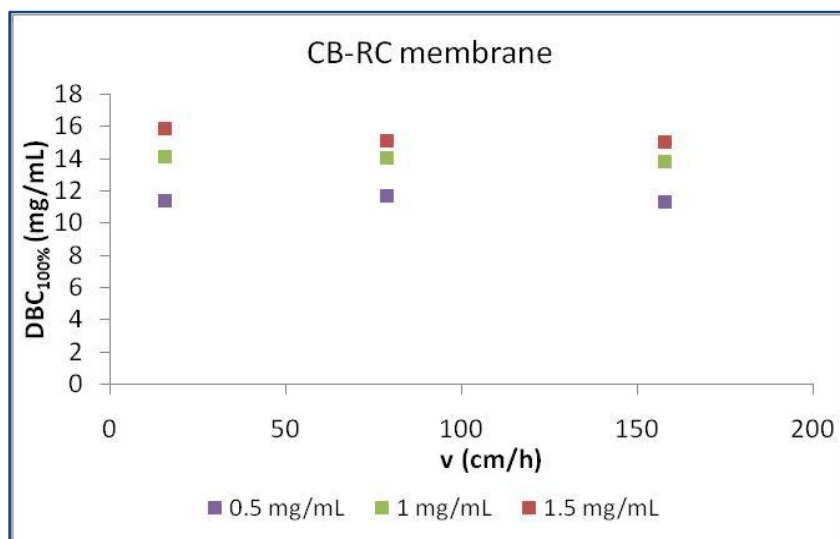


Figure 5.5 -  $DBC_{100\%}$  as function of superficial velocity at feed protein concentrations of 0.25 to 1.5 mg/mL for membranes.

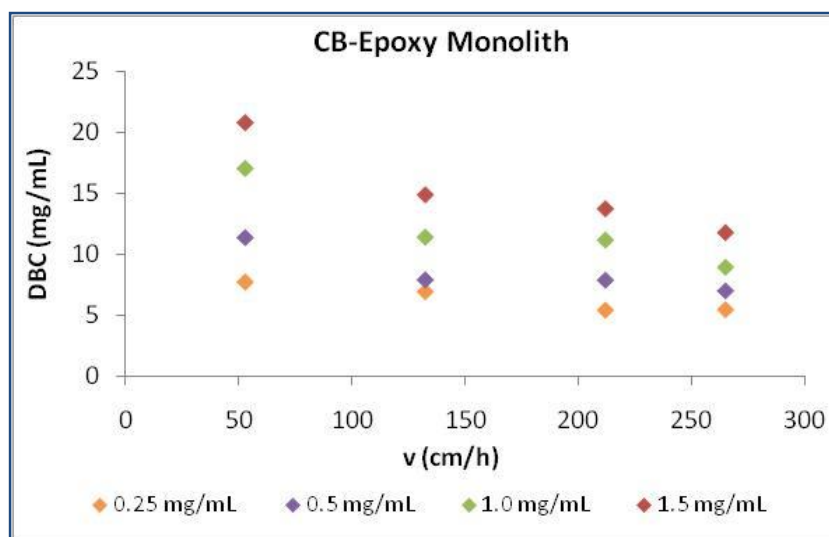
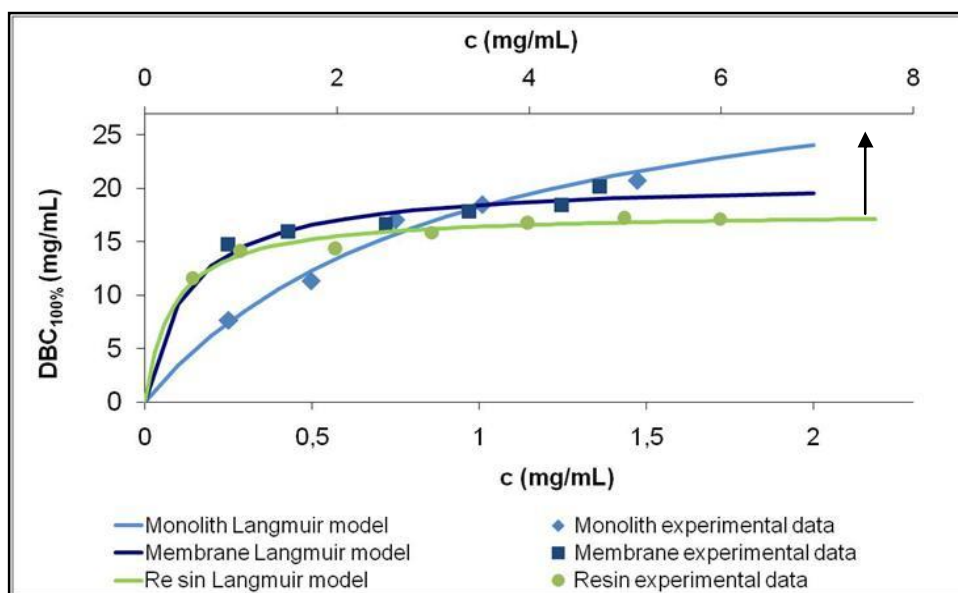


Figure 5.6 –  $DBC_{100\%}$  as function of superficial velocity at feed protein concentrations of 0.25 to 1.5 mg/mL for monolith.

The  $DBC_{100\%}$  of the packed column and of the membranes does not vary with flow rate whereas for monoliths the  $DBC_{100\%}$  decreases with the increase of flow rate.

The adsorption isotherms can be well interpolated with the Langmuir model. The obtained adsorption isotherms are presented in Figure 5.7. The solid line in the figure is the model, Langmuir isotherm, that best fit the experimental data and the Langmuir parameters, the maximum binding capacity,  $DBC_{max}$ , and the dissociation constant,  $K_d$  are reported in Table 5.3.



5.7 - Langmuir isotherm model for CB-RC affinity membranes, CB-Epoxy affinity monolith and HiTrap™ Blue HP column.

Table 5.3 -Langmuir parameters for the affinity supports studied.

| Supporto        | $DBC_{max}$<br>(mg/mL) | $K_d$<br>(mg/mL) |
|-----------------|------------------------|------------------|
| <b>Resin</b>    | 17.54                  | 0.268            |
| <b>Membrane</b> | 16                     | 0.107            |
| <b>Monolith</b> | 17.93                  | 0.523            |

The maximum binding capacity show slight differences, and it is possible to conclude that this parameter is comparable for the three supports used in this work.

### 5.2.2. Dynamic experiments with pure BSA solutions loaded until 10% breakthrough

In this set of experiments, pure BSA solutions were loaded to the module and loading was stopped before the BTC plateau was reached, so that the maximum BTC height reached during these runs was 10%.

It is possible to observe the influence of the protein concentration in the feed on dynamic binding capacity as shown in Figures 5.8, 5.9 and 5.10 respectively for resin, membranes and monoliths.

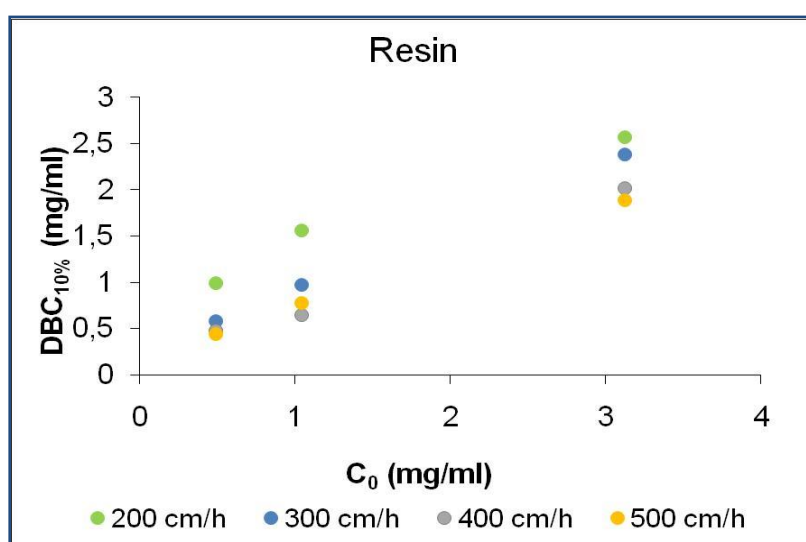


Figure 5.8 – Dynamic binding capacity at 10% breakthrough as a function of initial feed protein solution of HiTrap™ Blue HP.

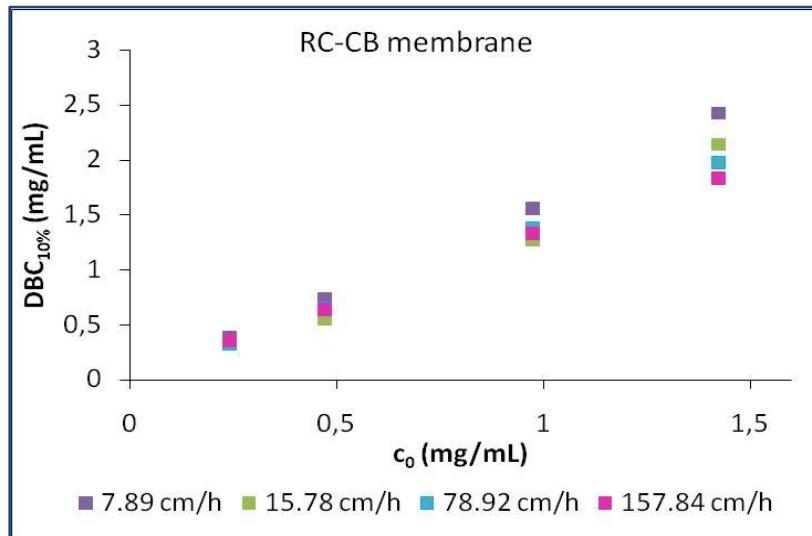


Figure 5.9 -  $DBC_{10\%}$  as a function of initial feed protein solution of modified CB-RC membranes.

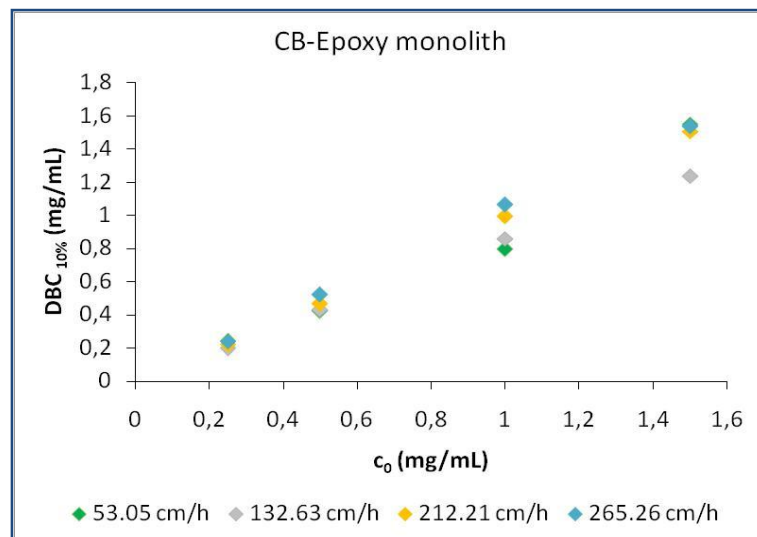


Figure 5.10 -  $DBC_{10\%}$  as a function of initial feed protein solution of CB-Epoxy monoliths.

It was found that the dynamic binding capacity at 10% breakthrough of all supports studied increases with increase feed protein concentration.

The influence of flow rate on the dynamic binding capacity was examined by increasing the superficial velocity from 200 to 500cm/h for resin

(Figure 5.11), 7.89 to 157.84 cm/h for membranes (Figure 5.12) and 53.05 to 265.26 cm/h to monolith (Figure 5.13).

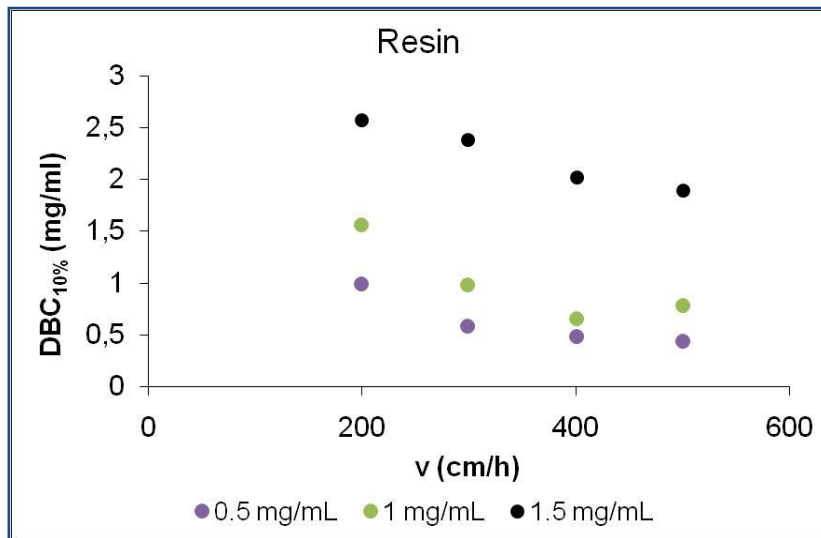


Figure 5.11 - The influence of superficial velocity on the dynamic binding capacity for resins.

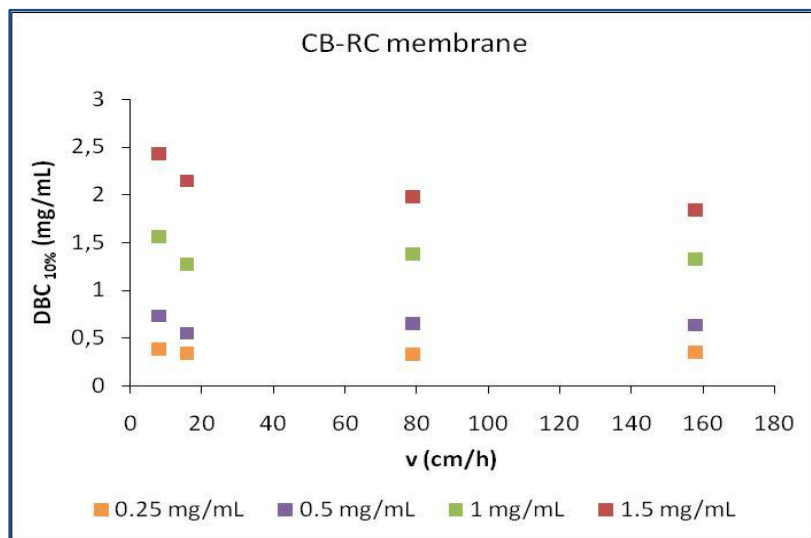


Figure 5.12 - The influence of superficial velocity on the dynamic binding capacity for membranes.

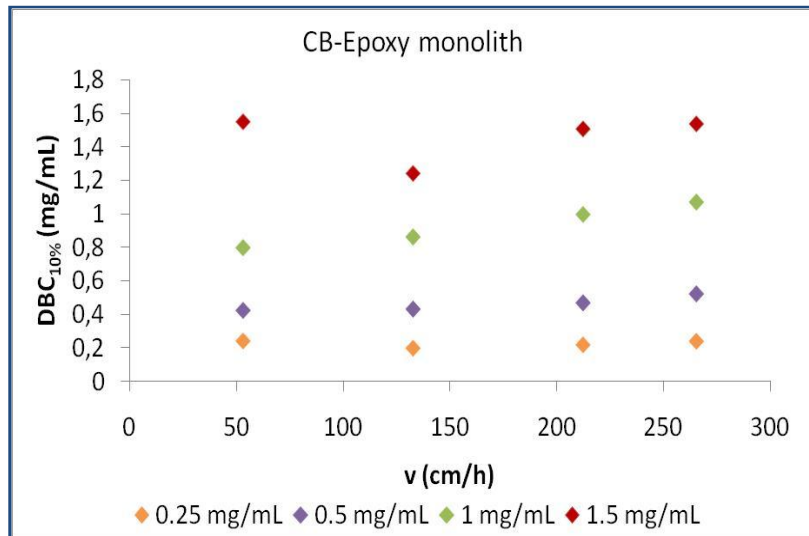


Figure 5.13 - The influence of velocity on the dynamic binding capacity for monoliths.

The DBC<sub>10%</sub> of resin decreases with increase the flow rate. These values of dynamic capacity are comparable with those calculated with an analysis of complete breakthrough curves (§ 5.2.1) and confirm that the system performance is dependent of flow rate. In bead-based packed columns the adsorption process is controlled by diffusion, which means flow rate dependent.

The set of experiments realized with CB-RC affinity membranes confirm that the DBC<sub>10%</sub> is independent of the superficial velocity. The results show a particular behavior of dynamic capacity when the flow rate is increased from 7.89 to 15.78 cm/h, DBC<sub>10%</sub> slight decreases. This behavior can be explained with the fact that, the adsorption is controlled by convection and at low flow rate exists an additional adsorption controlled by diffusion, that is, diffusion of BSA to the active sites in the pores.

For the monoliths, the results of DBC<sub>10%</sub> can be considered independent of the superficial velocity.



### 5.3.Productivity

Biopharmaceuticals production is an expensive process for the industry, where the main cost is due to separation in downstream processing. As mentioned firstly, § 1.1, in industrial processes the adsorption step is usually concluded before column saturation, when the solute reaches a specified concentration  $C_{BT}$ , in order to reduce the loss of product, usually expensive, even with an incomplete exploitation of the column.

The need to optimize chromatography is driven by a continuous demand to minimize production costs and/or to make the process more competitive. The typical parameter optimized in the chromatographic process is the productivity.

Productivity is another way to evaluate the separation performance. In this way, productivity can be defined by the equation 5.1

$$P = \frac{m_{elued}}{t_{cycle}} \quad (5.1)$$

So, productivity is the amount of eluted protein divided by the duration of complete chromatographic cycle. The productivity was investigated for each support as a function of superficial velocity at different values of the feed protein concentrations and the results were reported in Figures 5.14, 5.15 and 5.16.

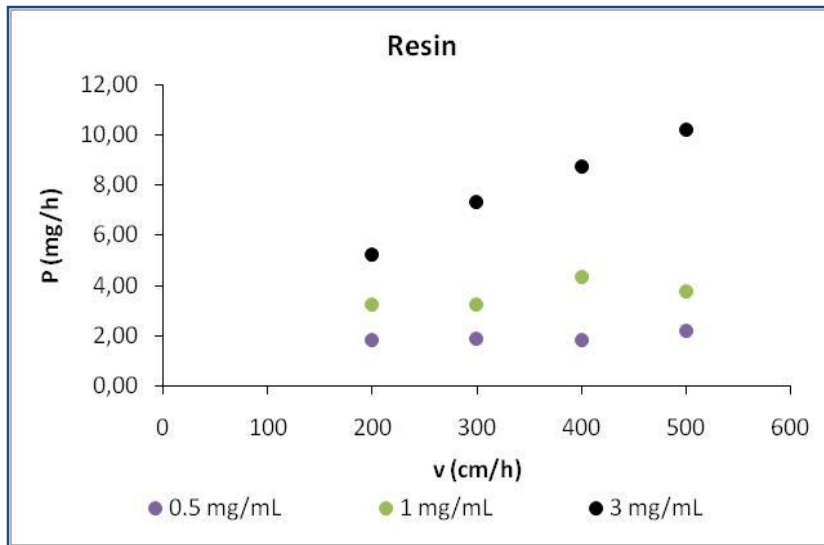


Figure 5.14–Productivity as a function of superficial velocity at different feed concentration for resin.

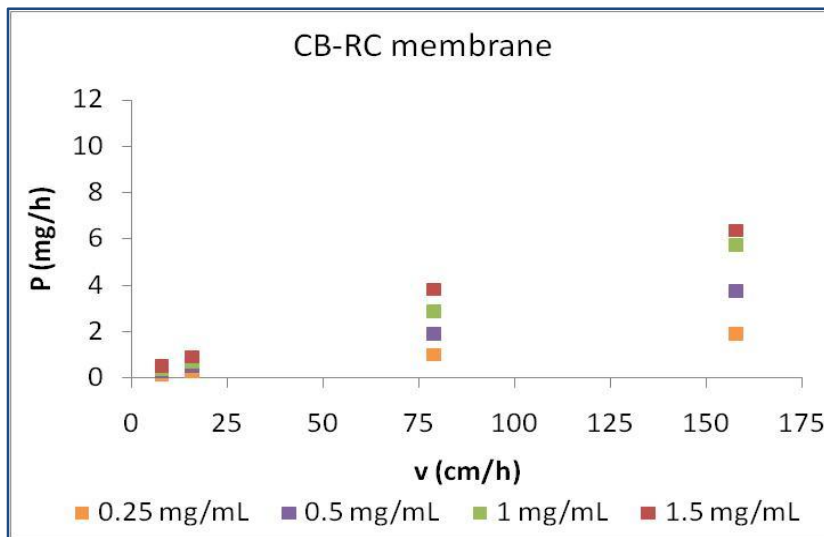


Figure 5.15 - Productivity as a function of superficial velocity at different feed concentration for CB-RC membranes.

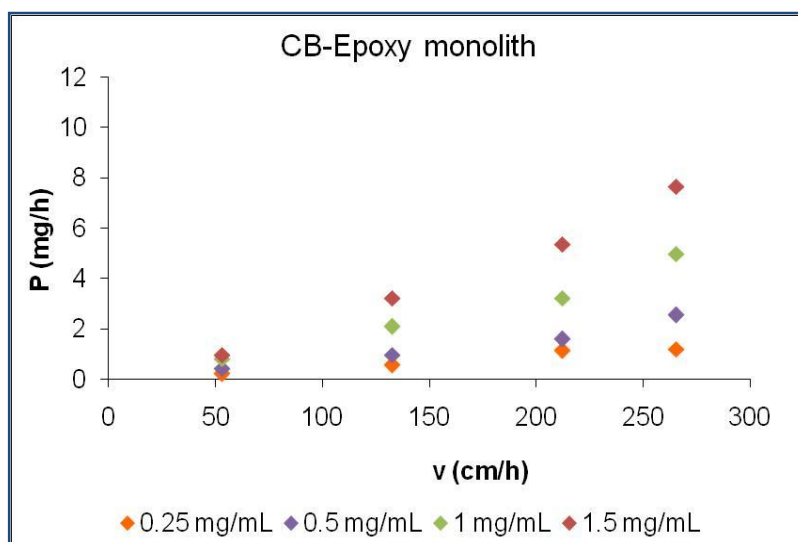


Figure 5.16 -Productivity as a function of superficial velocity at different feed concentration for CB-Epoxy monoliths.

For the resin at low feed concentration the productivity is not affected by flow velocity. However, for concentrations higher than 3 mg/mL is observed that the productivity increases with the superficial velocity in the range studied.

Whereas, for RC-membrane and CB-Epoxy monoliths it can be observed that the productivity increases linearly with superficial velocity, in the range from 7.89 to 157.84 cm/h and 53.05 to 265.26 cm/h respectively, even at lower concentrations, 0.25-1.5 mg/mL.

The graph in Figure 5.17 reports the influence of flow rate on productivity for all affinity supports studied at the same value of BSA concentration in the feed of 1 mg/mL.

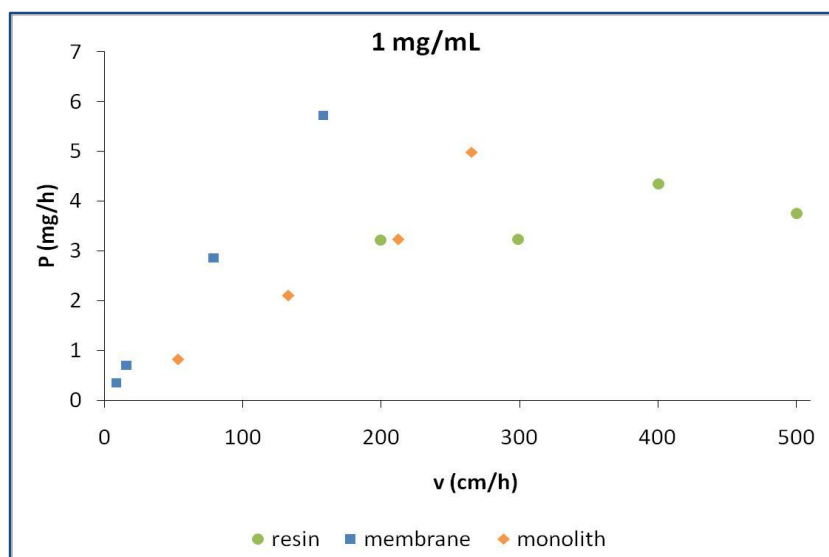


Figure 5.17–Productivity as a function of superficial velocity.

It is quite evident that membranes present a higher productivity than the other supports studied in the range of superficial velocity investigated.

#### 5.4. Tests with bovine serum

Besides the tests with pure BSA solution, which were necessary for the characterization of the supports; tests with bovine serum were carried out, in order to verify the capacity of the supports to separate BSA in the presence of other proteins, that is in complex solution with different proteins and other contaminants.

In these tests bovine serum was diluted fifty times to be used as a feed for the chromatographic process. The method of the chromatographic cycle is identical to the method used in the tests for DBC<sub>100%</sub> with pure BSA.

During the test, the eluate was fractionated in 1 mL sample. These samples were analyzed by SDS-PAGE electrophoresis.

The SDS-PAGE was performed in order to analyze the purity of the fractions eluted from chromatographic tests with the Criterion electrophoresis system from Bio-Rad Laboratories using precast gels.

Each sample was diluted 1:1 with loading buffer, comprising of SDS, glycerol,  $\beta$ -mercaptoethanol, and bromophenol blue in Tris-HCl (pH 6.8) solution. The mixture was then incubated at 95°C for 10 min. The final samples were loaded and run at a current of 140V and 40 mA.

The results of the affinity purification process with affinity supports are reported in a SDS electrophoresis gel. Electrophoresis represents the qualitative confirmation that the separation works, figure 5.18.



Figure 5.18– SDS PAGE of tests with bovine serum with the three affinity supports studied on Tris-HCl Criterion Gel 4-20%. Lines 1 and 18 represents the standards, line 3 the sample of serum, lines 5 and 6 the eluted sample of the test with resin, lines 8 and 9 the eluted sample of the test with monoliths, lines 11 to 16 the eluted sample of the test with membranes and line 17 sample of pure BSA.

It is quite evident the presence of bands of BSA, about 66 kDa, in all the fractions eluted.

The fractions of eluted samples were analyzed also with SEC column (BioSuite Size Exclusion (SEC) 250, 4 $\mu$ m UHR Waters) connected to HPLC (Waters Alliance 2695). From tests carried out with pure BSA it was possible to determine the retention time of the protein, figure 5.19.

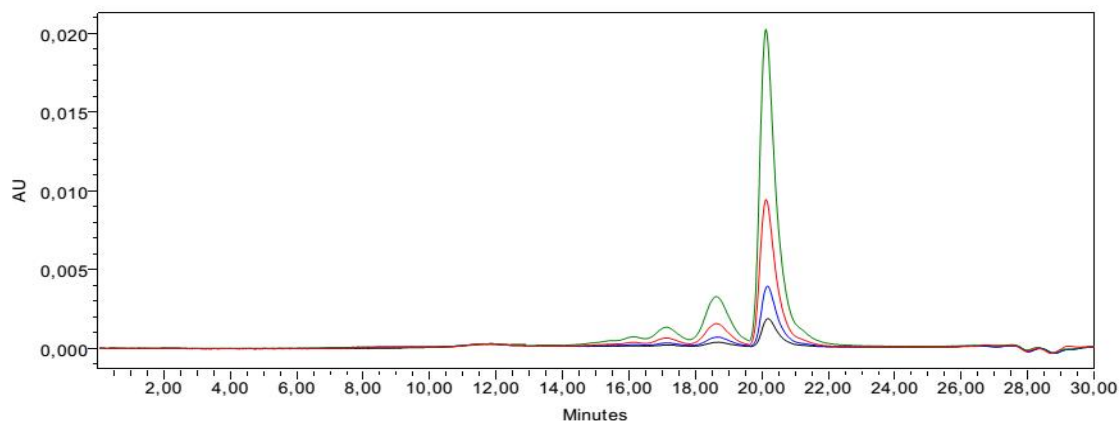


Figure 5.19—Chromatograms, at 280 nm, of standard protein at different concentrations, pure BSA in 0.1 M phosphate buffer, 0.05% M sodimazide, pH 6.7. (—) 0.05 mg/mL, (—) 0.1 mg/mL (—) 0.25 mg/mL and (—) 0.5 mg/mL.

The chromatograms of the samples of the eluted fraction, can be observed in the Figure 5.20.

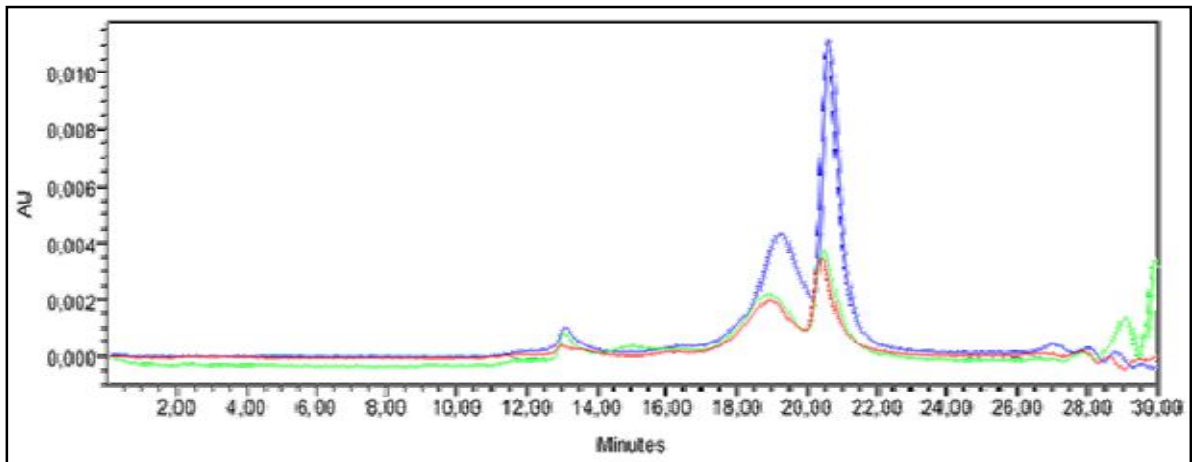


Figure 5.20 -Purification of BSA from bovine serum by HPLC size exclusion chromatography. The samples were loaded onto a SEC column and eluted with 0.1 M phosphate buffer, 0.05% M sodimazide, pH 6.7, at 0.30 mL/min.(—) resin (—) monolith (—) membrane.

From the chromatograms is evident that all affinity supports studied are able to separated BSA from bovine serum. These show that the CB affinity supports have a particular selectivity for albumin, as they allows to obtain samples of BSA with a certain purity, using a single step process.

## Conclusions

Affinity chromatography with dye, as a ligand, has a significant role in separation, purification and recovery of proteins and the choice of a suitable medium has a fundamental importance.

During my research a comparison among the performance of different chromatographic supports, resin, membranes and monoliths, was done using the same affinity system. BSA and Cibacron Blue F3GA were used as a model system.

The basic principle of the separation process exploits the affinity interaction between BSA and complementary substance, called ligand, chemically bound to the supports.

Since CB affinity beads are commercially available, this work was focused on the immobilization of CB in membranes and monoliths and characterization of the affinity supports obtained.

The ligand, CB, was covalently immobilized in membranes and monoliths.

CB-RC, CB-SartoE and CB-SartoA membranes were studied in terms of adsorption capacity with pure BSA solution. The aim of the experiments realized in batch system was primarily to verify the functioning of the separation system and, indirectly, the modification of the support, because it is not possible to directly verify the success of the chemical reaction between the ligand and matrix. Tests were realized with different initial concentration of protein in solution, enabling the construction of adsorption isotherms for the membranes with different activation. The interpolating model chosen was Langmuir model, thus determining the characteristic parameters. Different eluents were studied in order to identify the one with better efficiency. The eluent selected was 0.05 M Tris-HCl containing 0.05M NaCl and 0.5 M NaSCN pH 8.0. It was also performed a series of adsorption tests in flow. According to the



experiments, CB-RC membranes were chosen for the comparison with the resin (HiTrap Blue HP).

The performance of CB modified monoliths for albumin separation was studied. For immobilization of CB on monoliths, a specially system was constructed and this process was performed by recirculation. CB-monoliths were initially characterized in batch with pure protein solutions at different concentrations from 0.25 to 1.5 mg/mL. Batch experiments aimed to select the monolith which obtained better performance, but these tests showed no significant differences. In this way, flow tests were conducted in order to select the monolith that provide the best characteristics. Therefore, the CB-Epoxy affinity monoliths were chosen based on the experiments realized for comparison with the CB-RC membranes and the commercial resin (HiTrap Blue HP).

A comparison among membranes and monolith with commercial resin HiTrap Blue HP was performed in terms of binding capacity at saturation ( $DBC_{100\%}$ ) and dynamic binding capacity at 10% breakthrough ( $DBC_{10\%}$ ) using solutions of pure BSA.

In the experiments performed with solutions of pure BSA, the dynamic binding capacity until saturation of the resin and membranes resulted to be independent of the flow rate, while the  $DBC_{100\%}$  of the monolith decreased when the superficial velocity increased. In the experiments performed with solutions of pure BSA the dynamic binding capacity at 10% breakthrough of the membranes and monoliths resulted to be independent of the flow rate, while the  $DBC_{10\%}$  of the packed column decreased when the superficial velocity increased. This indicated that the affinity membranes and monolith were not affected by kinetic limitations in the range of superficial velocities investigated, while the column performance was heavily flawed by kinetic limitations.

Since the  $DBC_{10\%}$  of the new supports was independent of flow rate, the productivity, calculated with experiments in which the adsorption was

interrupted at 10% breakthrough, greatly increased with the flow rate. The column productivity increased too with the flow rate, but with higher superficial velocities.

On the other hand, tests carried out with bovine serum show that the supports have a particular selectivity with respect to albumin, as it allows to obtain samples of eluate with a certain purity, using a single step process.

The results obtained show that the CB-RC membranes and CB-Epoxy monoliths can be compared to commercial support, column HiTrap™ Blue HP, for the separation of albumin. These results encourage a further characterization of the new supports examined.

## References

- [1] R. Ghosh. Protein separation using membrane chromatography: opportunities and challenges. *Journal of Chromatography A*. 952 (2002) 13-27.
- [2] D. Josic, A. Buchacher. Review: Application of monoliths as supports for affinity chromatography and fast enzymatic conversion. *J. Biochem. Biophys. Methods*. 49 (2001) 153–174.
- [3] Denizli, E. Piskin. Review: Dye-ligand affinity systems. *J. Biochem. Biophys. Methods*. 49 (2001) 391–416.
- [4] A. Andaca, M. Andac, A. Denizli. Predicting the binding properties of cibacron blue F3GA in affinity separation systems. *International Journal of Biological Macromolecules*. 41 (2007) 430–438.
- [5] D. Voet, J. G. Voet, C. W. Pratt. *Fondamenti di Biochimica*, Zanichelli, Bologna (2001).
- [6] M. Sorci. Membrane di affinità per la separazione di biomolecole. Tesi di dottorato, Alma Mater Studiorum, Università di Bologna.
- [7] J. E. Kochan, Y. Wu , M. R. Etzel. Purification of bovine immunoglobulin G via protein G affinity membranes. *Industrial Engineering and Chemistry Research*. 35 (1996) 1150-1155.
- [8] F.H. Arnold, H. W. Blanch, C. R. Wilke, Analysis of affinity separations I: predicting the performance of affinity adsorbers. *The Chemical Engineering Journal*. 30 (1985) 9-23.
- [9] A. Tejada-Mansir, R. Montesinos, R. Guzmán. Mathematical analysis of frontal affinity chromatography in particle and membrane configurations, *Journal of Biochemical and Biophysical Methods*. 49 (2001) 1-28.

- [10] T. B. Tennikova, M. Bleha, F. Svek, T. V. Almazova, T. G. Belenki, *High performance membrane chromatography of proteins: a novel method of proteins separation*, Journal of Chromatography. 555 (1991) 97-107.
- [11] H. Zou, Q. Luo, Q. Zhou. Affinity membranre chromatography for the analysis and purification of proteins. J. Biochem. Biophys. Methods. 49 (2001) 199-240.
- [12] D. K. Roper, E. N. Lightfoot. Separation of biomolecules using adsorptive membranes. Journal of Chromatography A. 702 (1995) 3-26.
- [13] E. G. Vlakh, T. B. Tennikova. Preparation of methacrylate monoliths, J. Sep. Sci. 30 (2007) 2801-2813.
- [14] S. Xie, R. W. Allington, J. M. Frechet, F. Svec. Porous polymer monoliths: an alternative to classical beads. Adv. Biochem. Eng. Biotechnol. 76 (2002) 87.
- [15] M. Bedair, Z. E. Rassi. Affinity chromatography with monolithic capillary columns: I. Polymethacrylate monoliths with immobilized mannan for the separation of mannose-binding proteins by capillary electrochromatography and nano-scale liquid chromatography. Journal of Chromatography A. 1044 (2004) 177–186.
- [16] L. Uzun, H. Yavuz, R. Say, A. Ersoz, A. Denizli. Poly(ethylene dimethacrylate-glycidyl methacrylate) Monolith as a Stationary Phase in Dye-Affinity Chromatography. Ind. Eng. Chem. Res. 43 (2004) 6507-6513.
- [17] N. B. Afeyan, N. F. Gordon, I. Mazsaroff, L. Varady, S. P. Fulton, Y. B. Yang, F. E. Regnier. Flow-through particles for the high-performance liquid chromatographic separation of biomolecules: perfusion chromatography. J. Chromatogr. A. 519, 1, 19 (1990) 1–29.
- [18] A. Strancar, A. Podgornik, M. Barut, R. Necina. Short monolithic columns as stationary phases for biochromatography. Adv Biochem Eng Biotechnol. 76 (2002) 49-85.

- [19] G. Iberer, R. Hahn, A. Jungbauer. Monoliths As Stationary Phases for Separation of Biopolymers: The Fourth Generation of Chromatography Sorbents. *LC-GC Int.* 11 (1999) 998–1005.
- [20] A. Jungbauer. Chromatographic Media for Bioseparation. *J. Chromatogr. A* 1065 (2005) 3–12.
- [21] F. Svec, T. B. Tennikova, Z. Deyl. *Monolithic Material: Preparation, Properties and Applications*. Elsevier: Amsterdam, The Netherlands, 2003.
- [22] A. Podgornik, A. Strancar. Convective Interaction Media (CIM): Short Layer Monolithic Chromatographic Stationary Phases. *Biotechnol. Annu. Rev.* 11 (2005) 281– 333.
- [23] R. Hahna, M. Panzerb, E. Hansenc, J. Mollerupc, A. Jungbauerd. Mass Transfer Properties of Monoliths. *Sep. Sci. Technol.* 37, 7 (2002) 1545–1565.
- [24] S.Y. Suen, M. R. Etzel. A mathematical analysis of affinity membrane bioseparations. *Chem. Eng. Sci.* 47, 6 (1992) 1355–1364.
- [25] J. Urthaler, R. Schlegl, A. Podgornik, A. Strancar, A. Jungbauer, R. Necina. Application of Monoliths for Plasmid DNA Purification Development and Transfer to Production. *J. Chromatogr. A.* 1065 (2005) 93–106.
- [26] F. T. Sarfert, M. R. Etzel. Mass transfer limitations in protein separations using ion-exchange membranes. *J. Chromatogr. A.* 764 (1997) 3-20.
- [27] S. Dimartino. Studio sperimentale e modellazione della separazione di proteine con membrane di affinità, 2009, Tesi di dottorato, Alma Mater Studiorum, Università di Bologna.
- [28] R. A. Curvale. Buffer capacity of bovine serum albumin (BSA). *The Journal of the Argentine Chemical Society* Vol. 97 N 1, 174-180 (2009).].
- [29] [www.sigmaaldrich.com/etc/medialib/docs/Sigma/Product\\_Information\\_Sheet](http://www.sigmaaldrich.com/etc/medialib/docs/Sigma/Product_Information_Sheet), consulted on 5/24/2010.

- [30] J. F Foster. Binding properties of albumin. In *Albumin Structure, Function and Uses*. V. M. Rosenoer, M. Oratz, and M. A. Rothschild, editors. Pergamon Press, Oxford. (1977) 53–84.
- [31] M.L. Ferrer, R. Duchowicz, B. Carrasco, J. Garcia de la Torre, U. Acuña, The Conformation of Serum Albumin in Solution: A Combined Phosphorescence Depolarization-Hydrodynamic Modeling Study. *Biophysical Journal* 2001, 80, 2422.
- [32] W. J. Leonard, J.F. Foster. Changes in optical rotation in the acid transformations of plasma albumin: Evidence for the contribution of tertiary structure to rotator behavior. *J. Biol. Chem.* 236 (1961) 2662-2669.
- [33] J.N. De Wit. Nutritional and Functional Characteristics of Whey Proteins in Food Products. *Journal of Dairy Science.* 81, 3 (1998) 597–608.
- [34] N. El Kadi, N. Taulier, J. Y. Le Huérou, M. Gindre, W. Urbach, I. Nwigwe, P. C. Kahn, M. Waks. Unfolding and Refolding of Bovine Serum Albumin at Acid pH: Ultrasound and Structural Studies. *Biophysical Joun.* 91 (2006) 3397–3404.
- [35] A. Bujacz. Structures of bovine, equine and leporine serum albumin. *Journal: Acta Crystallogr.* 68 (2012) 1278-1289.
- [36] D. C. Carter, J. X. Ho. Structure of serum albumin. *Adv Protein Chem.* 45 (1994) 153-203.
- [37] A. Denizli, E. Piskin. Dye-ligand Affinity Systems, *Journal of Biochemical and Biophysical Methods.* 49, 1-3 (2001) 391-416.
- [38] J. C. Pearson, C. R. Lowe. Affinity chromatography on immobilized dyes. *Methods Enzymol.* 104 (1984) 97-112.
- [39] Gallant SR, Koppaka V, Zecherle N. Dye ligand chromatography. *Methods Mol Biol.* 2008;421:61-9.
- [40] R.K. Scopes. Strategies for enzyme isolation using dye-ligand and related adsorbents. *J. Chromatogr.* 376 (1986) 131.

- [41] Y. Kroviarski, S. Cochet, C. Vadon, A. Truskolaski, P. Boivin, O. Bertrand, *J. Chromatogr.* 449 (1988) 403.
- [42] L. Miribel, E. Gianazza, P. Arnaud, *J. Biochem. Biophys. Methods* 16 (1988) 1.
- [43] D.C. Nash, H.A. Chase. Modification of polystyrenic matrices for the purification of proteins. II. Effect of the degree of glutaraldehyde-poly(vinyl alcohol) crosslinking on various dye ligand chromatography systems. *J. Chromatogr. A.* 776 (1997) 55-63.
- [44] P.M. Boyer, J.T. Hsu, *Chem. Eng. J.* 47 (1992) 241.
- [45] X. Zeng, E. Ruckenstein. Supported chitosan-dye affinity membranes and their adsorption of protein. *J. Membr. Sci.* 117 (1996) 271
- [46] H. Yavuz, E. Duru, O. Genç, A. Denizli. Cibacron Blue F3GA incorporated poly(methylmethacrylate) beads for albumin adsorption in batch system. *Colloids and Surfaces A: Physicochem. Eng. Aspects* 223, 185-193, 2003.
- [47] K. Smith, K., Sundram, T. Kernick, T., Wilkinson, A., 1982, Purification of Bacterial Malate Dehydrogenases by Selective Elution from a Triazinyl Dye Column, *Biochimica et Biophysica Acta*, v. 708, n. 1, pp. 17-25.
- [48] R. K.Scopes. Dye-ligands and Multifunctional Adsorbents: an Empirical Approach to Affinity Chromatography. *Analytical Biochemistry.* 165, 2 (1987) 235-246.
- [49] C. Stead. The Use of Dyes in Protein Purification. *Bioseparation.* 2 (1991) 129-134.
- [50] N. Garg, I. Galaev, B. Mattiasson. Dye-affinity Techniques for Bioprocessing: Recent Developments, *Journal of Molecular Recognition.* 9, 4 (1996) 259-266.
- [51] L.-Z. He, Y.-R. Gan, Y. Sun. Adsorption-desorption of BSA to highly substituted dye-ligand adsorbent: quantitative study of the effect of ionic strength. *Bioprocess Engineering* 17 (1997) 301-305.

- [52] P. Boyer, J. Hsu. Adsorption Equilibrium of Proteins in a Dye-ligand Adsorbent. *Biotechnology Techniques*. 4 (1990) 61.
- [53] D. Müller-Schulte, S. Manjini, M. Vijayalakshmi. Comparative Affinity Chromatographic Studies Using Novel Grafted Polyamide and Poly(vinylalcohol) Media. *Journal of Chromatography*. 539, 2 (1991) 307-314.
- [54] A. Tuncel, A. Denizli, D. Purvis, C. Lowe. Cibacron Blue F3GA-attached Monosize Poly(vinylalcohol) Coated Polystyrene Microspheres for Specific Albumin Adsorption. *Journal of Chromatography*. 634, 2 (1993) 161-168.
- [55] S. Çamli, S. Senel, A. Tuncel. Cibacron Blue F3GA Attached Uniform and Macroporous Poly(styrene-co-divinylbenzene) Particles for Specific Albumin Adsorption. *Journal of Biomaterial Science Polymers*. 10, 8 (1999) 875-889.
- [56] A. Doğan, S. Özkara, M. M. Sarı, L. Uzun, A. Denizli. Evaluation of human interferon adsorption performance of Cibacron Blue F3GA attached cryogels and interferon purification by using FPLC system. *J Chromatogr B Analyt Technol Biomed Life Sci*. 893-894 (2012) 69-76.
- [57] H. L. Nie, L. M. Zhu. Adsorption of papain with Cibacron Blue F3GA carrying chitosan-coated nylon affinity membranes. *Intern. Journal of Biolog. Macromol*. 40 (2007) 261-267.
- [58] M. Y. Arica, A. Denizli, B. Salih, E. Piskin, V. Hasirci. Catalase Adsorption onto Cibacron Blue F3GA and Fe(III) Derivatized Poly(2-hydroxyethyl methacrylate) Membranes and Application to a Continuous System. *Journal of Membrane Science*. 129,1 (1997) 65-76.
- [59] S. Y Suen, R. Chen, Y. D. Tsai. Comparison of Lysozyme Adsorption to Immobilized Cibacron Blue F3GA Using Various Membrane Supports. *Journal of Liquid Chromatography & Related Technologies*. 23, 2 (2000) 223-239.



- [60] A. Kassab, H. Yavuz, M. Odabasi, A. Denizli. Human Serum Albumin Chromatography by Cibacron Blue F3GA-derived Microporous Polyamide Hollow-fiber Affinity Membranes. *Journal of Chromatography B*. 746, 2 (2000) 123-132.
- [61] B. Champluvier, M. Kula. Dye-ligand Membranes as Selective Adsorbents for Rapid Purification of Enzymes: a Case Study. *Biotechnology and Bioengineering*. 40 (1992) 33-40.
- [62] N. Demiryas, N. Tuzmen, I. Y. Galaev, ErhanPiskin and AdilDenizli. Poly(acrylamide-allylglycidyl ether) Cryogel as a Novel Stationary Phase in Dye-Affinity Chromatography. *Journal of Applied Polymer Science*. 105 (2007) 1808–1816.
- [63] A. Strancar, M. Barut, A. Podgornik, P. Koselj, D.J. Josic, A. Buchacher, *LC–GC* 11 (1998) 660.
- [64] A. Podgornik, M. Barut, S. Jaksa, J. Jancar, A. Strancar. *J. Chromatogr. Relat. Technol.* 25, 3099, 2002.
- [65] M. P. Deutscher. Protein Purification. *Methods Enzymol.* 182 (1990) 889-894.
- [66] C. M. Stoscheck. Quantitation of Protein. *Methods in Enzymology* 182 (1990) 50-69.
- [67] C.Y. Wu, S.Y. Suen, S.C. Chen, J.H. Tzeng. Analyses of protein adsorption on regenerated cellulose-based immobilized copper ion affinity membranes. *Journal of Chrom. A*. 996 (2003) 53-70.
- [68] A. Denizli, S. Senel, M. Y. Arica. Cibacron Blue F3GA and Cu (II) derived poly (2-hydroxyethylmethacrylate) membranes for lysozyme adsorption. *Colloids and Surfaces B: Biointerferences* 11 (1998) 113-122.
- [69] E. Ruckestein, X. Zeng. Albumin separation with Cibacron Blue carrying macroporous chitosan and chitin membranes. *Journal of Membrane Science*. 142(1998)13-26.

- [70] S. T. Thompson, E. S. Stellwagen. Binding of cibacron blue F3GA to proteins containing the dinucleotide fold. *Proc. Nat. Acad. Sci. USA* vol73, N. 2, 361-365, 1976.
- [71] S. Subramanian, B.T. Kaufman. Dihydrofolate Reductases from Chicken Liver and *Lactobacillus casei* bind Cibacron Blue F3GA in Different Modes and at Different Sites. *The Joun. Biolog. Chem.*, 255, 22, 10587-10590, 1980.
- [72] A. Denizli, G. Kokturk, H. Yavuz, E. Piskin. Albumin adsorption from aqueous solutions and human plasma in a packed-bed column with Cibacron Blue F3GA-Zn(II) attached poly(EGDMA-HEMA) microbeads. *Reactive & Functional Polymers* 40 (1999) 195-203.
- [73] A. Denizli, E. Piskin. Dye-ligand Affinity Systems, *Journal of Biochemical and Biophysical Methods*, v. 49, n. 1-3 (Oct), 2001, pp. 391-416.
- [74] S. Subramanian. Dye-ligand affinity chromatography: The interactions of Cibacron Blue F3GA with proteins and enzymes. *CRC Critical Reviews in Biochemistry*. Vol. 16, Issue 2, 169 – 205, 1984.
- [75] A. Denizli, G. Kokturk, H. Yavuz, E. Piskin. Albumin adsorption from aqueous solutions and human plasma in a packed-bed column with Cibacron Blue F3GA-Zn(II) attached poly(EGDMA-HEMA) microbeads. *Reactive & Functional Polymers* 40 (1999) 195–203.
- [76] Z. Ma, K. Masaya, S. Ramakrishna. Immobilization of Cibacron blue F3GA on electrospun polysulphone ultra-fine fiber surfaces towards developing an affinity membrane for albumin adsorption. *Journal of Membrane Science*. 282 (2006) 237–244
- [77] P. M. Boyer, J. T. Hsu. Protein purification by dye-ligand chromatography. *Adv Biochem Eng Biotechnol*. 49 (1993) 1-44.

- [78] F.J. Wolman, M. Grasselli, E.E. Smolko, O. Cascone Preparation and characterisation of Cibacron Blue F3G-A poly(ethylene) hollow-fibre affinity membranes. *Biotechnology Letters*. 22 (200) 1407–1411.
- [79] S Sanchez. Caratterizzazione di resine di affinità per la separazione di BSA. 2010. Tesi di laurea. Alma Matter Studiorum, Università di Bologna.

## Appendix I

### *Composition of the solutions used*

In this section we report the compositions of solutions used in this research and cited in previous chapters.

#### *1. CB leakage*

□ 0.05 M sodium acetate buffer pH 3.0 (100 mL)

2.89 g       $\text{CH}_3\text{COONa}$

0.89 mL      $\text{CH}_3\text{COOH}$

Titrated to pH 3.0

□ 0.05 M sodium phosphate buffer pH 7.0 (1 liter)

3.55 g       $\text{Na}_2\text{HPO}_4$

Titrated with 0.05 M  $\text{NaH}_2\text{PO}_4 \cdot \text{H}_2\text{O}$  to pH 7.0

To prepare 1 liter:

3.45 g       $\text{NaH}_2\text{PO}_4 \cdot \text{H}_2\text{O}$

□ 0.05 M sodium carbonate buffer pH 11.0 (1 liter)

1.59 g       $\text{Na}_2\text{CO}_3$

2.39 g       $\text{NaHCO}_3$

Titrated to pH 5.0

## 2. Resin

- 0.1 M Tris-HCl pH 8.0 (1 liter)

12.2 g          Tris Base

to pH 8.0 with 1 M HCl solution

bring to volume with deionized water

- 0.05 M  $\text{KH}_2\text{PO}_4$  containing 1.5 M KCl pH 7.0 (1 liter)

6.8 g           $\text{KH}_2\text{PO}_4$

11.83 g        KCl

To pH 7.0 with 1 M NaOH

bring to volume with deionized water

## 3. Membrane

- 0.05 M Tris-HCl containing 0.05M NaCl pH 8.0

6.057 g          Tris Base

2.922 g          NaCl

to pH 8.0 with 1 M HCl

bring to volume with deionized water

- 0.05 M Tris-HCl containing 0.05 M NaCl and 0.5 M NaSCN pH 8.0

6.057 g          Tris Base

2.922 g          NaCl

40.5352 g        NaSCN

to pH 8.0 with 1 M HCl

bring to volume with deionized water

#### 4. *Monolith*

□ 25 mM phosphate buffer containing 100 mM NaCl pH 7.4

3.55 g       $\text{Na}_2\text{HPO}_4$

5.843 g      $\text{NaCl}$

bring to volume with 25 mM  $\text{NaH}_2\text{PO}_4 \cdot \text{H}_2\text{O}$  containing 100 mM NaCl

To prepare 1 liter:

3.55 g       $\text{NaH}_2\text{PO}_4 \cdot \text{H}_2\text{O}$

5.843 g      $\text{NaCl}$

#### 5. *Electrophoresis*

□ Running buffer 5X (2 liters)

144 g      glycine

30 g        Tris Base

10 g        SDS

bring to volume with deionized water

□ CPB (Classic Buffer Solution) 5X

5 mL        glicerolo

1 g          SDS

2.31 mL    Tris-HCl pH 6.8

a pinch of Bromophenol Blue

Stock conditions: each Eppendorf with 372  $\mu\text{L}$  of the solution.

Work conditions: fill the Eppendorf with 128 mL of  $\beta$ -mercaptoethanol.

☐ Tris-HCl pH 6.8 (100 mL)

40 mL deionized water

6.5 g Tris base

0.4 g SDS

To pH 6.8 with 1 M HCl solution

bring to volume with deionized water

## 6. HPLC

☐ SEC buffer

Buffer A: 0.1 M sodium phosphate monobasic, 300 mM NaCl (1 liter)

13.8 g ± 0.1 g NaH<sub>2</sub>PO<sub>4</sub> · H<sub>2</sub>O

17.53 g ± 0.1 g NaCl

Dissolve all the components in approximately 800 mL of Milli-Q water. Stir until complete dissolution.

Buffer B: 0.1 M sodium phosphate dibasic, 300 mM NaCl

14.2 g ± 0.1 g Na<sub>2</sub>PO<sub>4</sub>

17.53 g ± 0.1 g NaCl

Dissolve all the components in approximately 800 mL of Milli-Q water. Stir until complete dissolution.

Add Buffer A to Buffer B until pH 6.7 is reached. Dissolve the 0.5 g of NaN<sub>3</sub> in 1 L of SEC Buffer. Filter through 0.22 μm filter.

## Appendix II

### *Calibration curves*

#### *1. Cibacron Blue calibration curves*

Calibration curve at 610 nm of CB solution in water

Spectrophotometer: Shimadzu 1601 UV/Vis

quartz cuvette with capacity of 1 ml

| Sample | Conc BSA (mg/ml) | A 610 nm (AU) |
|--------|------------------|---------------|
| 1      | 0.01             | 0.1602        |
| 2      | 0.025            | 0.3933        |
| 3      | 0.05             | 0.7791        |
| 4      | 0.075            | 1.1512        |
| 5      | 0.1              | 1.5247        |



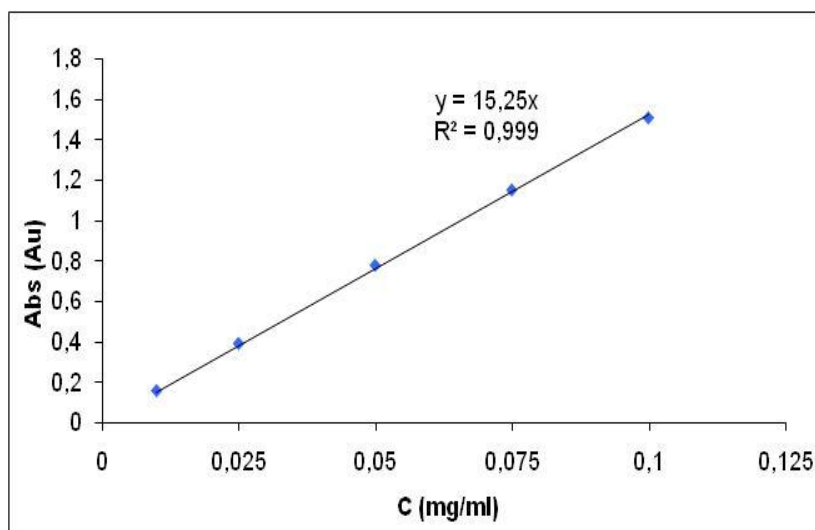


Figure A.II.1 – Cibacron Blue F3GA calibration curve performed in spectrophotometer with concentrations among 0.01 and 0.1 mg/mL .

Calibration curve at 610 nm of CB solution in water

Fast Protein Liquid Chromatography AKTA Purifier 100

| Sample | c <sub>BSA</sub> (mg/ml) | A 610 nm (AU) |
|--------|--------------------------|---------------|
| 1      | 0.01                     | 5.64          |
| 2      | 0.025                    | 20            |
| 3      | 0.05                     | 57.03         |
| 4      | 0.1                      | 102.92        |
| 5      | 1                        | 940.76        |

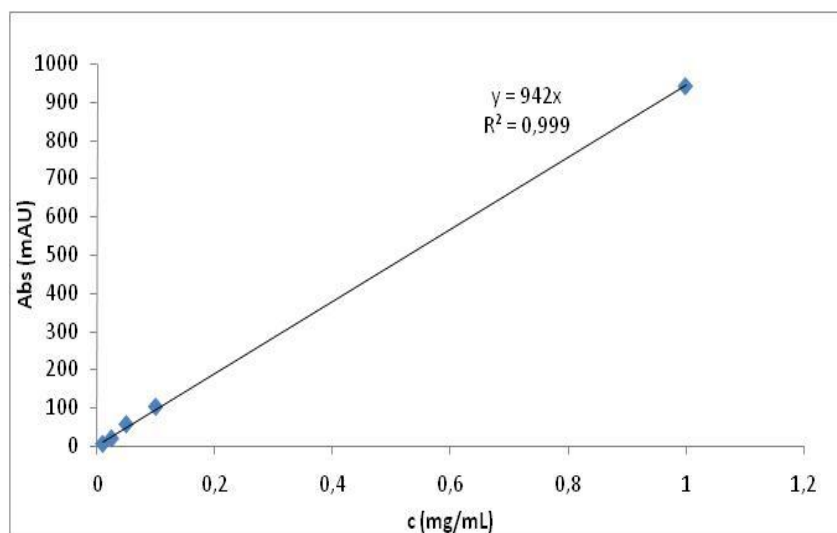


Figure A.II.2 - Cibacron Blue F3GA calibration curve performed in FPLC system with concentrations among 0.01 and 1 mg/mL.

## 2. BSA to BCA

Calibration curve at 562 nm with BSA in 0.05 M Tris-HCl pH 9 to BCA

BSA (Sigma Aldrich)

BCA Protein Assay (Pierce)

Spettrofotometro: Shimadzu 1601 UV/Vis

Cuvette: disposable, capacity 1 ml

| Sample | BSA (mg/ml) | A 562 nm (UA) |
|--------|-------------|---------------|
| 1      | 0.025       | 0.0508        |
| 2      | 0.125       | 0.1720        |
| 3      | 0.250       | 0.2939        |
| 4      | 0.500       | 0.4764        |
| 5      | 0.750       | 0.8745        |
| 6      | 1.000       | 1.1576        |
| 7      | 1.500       | 1.6941        |
| 8      | 2.000       | 2.0021        |

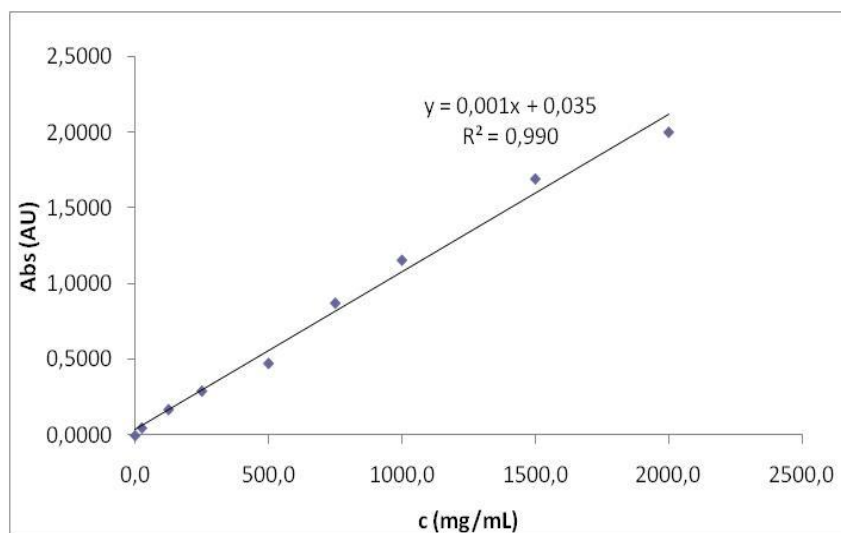


Figure A.II.3 - Calibration curve at 562 nm with BSA in 0.05 M Tris-HCl pH 8 to BCA.

### 3. BSA calibration curves

Calibration curve at 610 nm of CB solution in water

Spectrophotometer: Shimadzu 1601 UV/Vis

quartz cuvette with capacity of 0.7 ml

| sample | c (mg/ml) | Abs (Au) |
|--------|-----------|----------|
| 1      | 0.25      | 0.1504   |
| 2      | 0.5       | 0.2848   |
| 3      | 0.75      | 0.4485   |
| 4      | 1         | 0.5858   |
| 5      | 1.25      | 0.7687   |
| 6      | 1.5       | 0.8646   |
| 7      | 2         | 1.2085   |

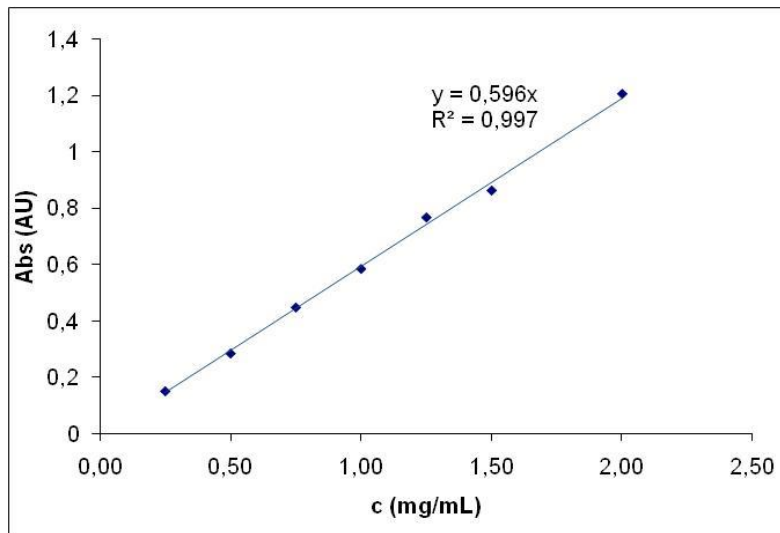


Figure A.II.4 – BSA calibration curve performed in spectrophotometer with concentrations among 0.25 and 2 mg/mL

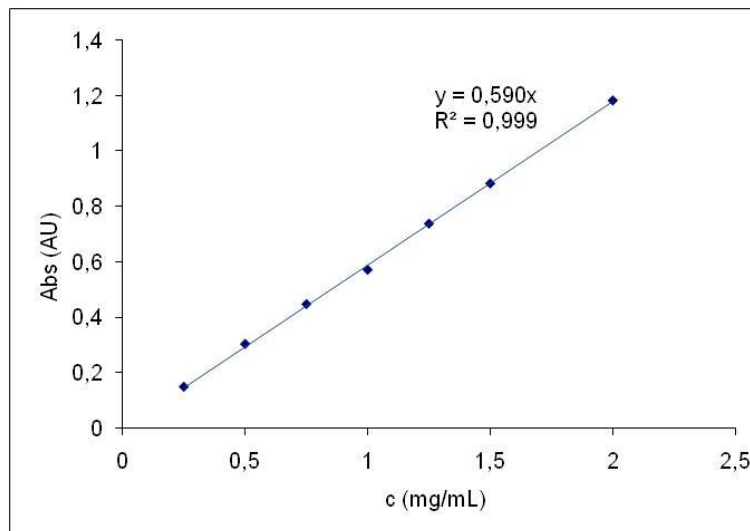


Figure A.II.5 - Calibration curve at 280 nm with BSA in 0.05 M Tris-HCl + 0.05 M NaCl + 0.5 M NaSCN pH 8.

Calibration curve at 280 nm of BSA solution in buffer

FPLC Äkta Purifier 100

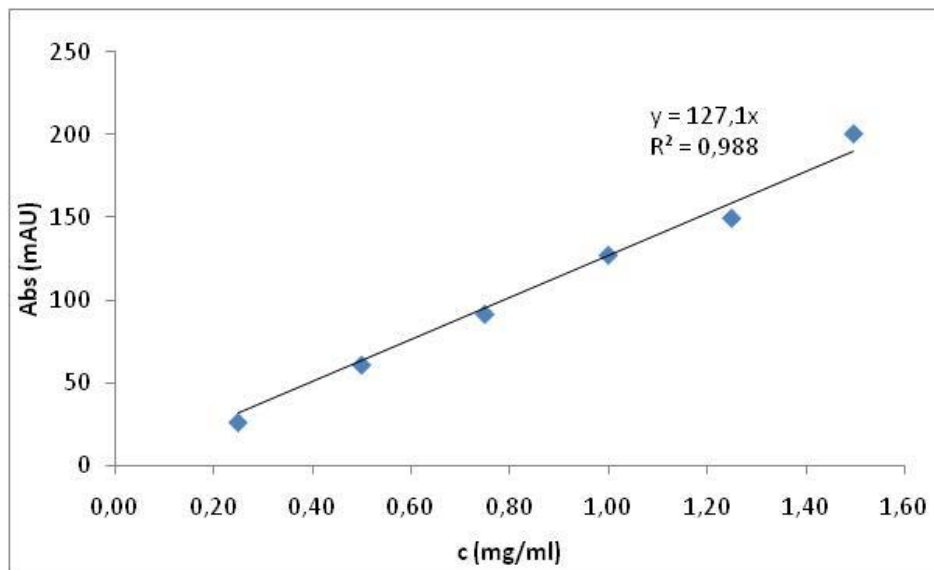


Figure A.II.6 – Calibration curve at 280 nm with BSA in 0.05 M Tris-HCl + 0.05 M NaCl pH 8.